UNIVERSITY OF CRETE

DEPARTMENT OF BIOLOGY

Ph.D. Thesis

Study of the *Tnfα* allele homologous pairing in murine macrophages

Kalliopi C. Stratigi

2013

Supervised by
Assistant Professor C. G. Spilianakis

ΠΕΡΙΛΗΨΗ

Αρκετά δια-αλληλικά φαινόμενα έχουν περιγραφεί στο παρελθόν, παρότι ο ρόλος τους στη ρύθμιση γονιδίων δεν έχει ακόμα αποσαφηνιστεί. Ένα τέτοιο σπάνιο φαινόμενο στα θηλαστικά είναι η σωματική ομόλογη αλληλεπίδραση. Μελετήσαμε την ομόλογη αλληλεπίδραση του γενετικού τόπου του *Tnfα* σε μακροφάγα ποντικού ενεργοποιημεένα με λιποπολυσακχαρίτη (LPS) και βρήκαμε ότι συμβαίνει νωρίς κατά την ενεργοποίηση και πριν την αλλαγή της έκφρασης του *Tnfα* γονιδίου από μόνο- σε δι-αλληλική. Ο προτεινόμενος ρυθμιστικός μηχανισμός περιλαμβάνει δύο συμπληρωματικά μεγάλα μη-κωδικά RNAs που μεταγράφονται από τον LT/TNF γενετικό τόπο, μια πρωτεϊνική κινάση με δυνατότητα ενεργοποίησης από απόσταση και μια πρωτεΐνη που θεωρείται να είναι το ομόλογο του παράγοντα GAGA της Δροσόφιλα, στα θηλαστικά. Πιστεύουμε ότι η ομόλογη αλληλεπίδραση, ως μέρος της γονιδιωματικής οργάνωσης των θηλαστικών θα έχει γενικότερο ενδιαφέρον και προτείνουμε ένα μηχανισμό για τη ρύθμιση της γονιδιακής έκφρασης από μόνο- σε δι-αλληλική.

CONTENTS

1. **Summary**
2. **Introduction**
   - 2.1 *Trans*-allelic phenomena
     - 2.1.1 Repeat-induced point mutation (RIP) process
     - 2.1.2 Paramutation
     - 2.1.3 Transvection
     - 2.1.4 Homologous pairing of oppositely imprinted loci
     - 2.1.5 X-chromosome inactivation
     - 2.1.6 DNA methylation during meiosis
     - 2.1.7 Intergenic transcription of the human β-globin locus
   - 2.2 Macrophages
   - 2.3 Tumor Necrosis Factor - alpha (TNFα)
     - 2.3.1 TNFα signaling pathway
     - 2.3.2 Transcription at the *Tnfα* locus
     - 2.3.3 Transcriptional control of the *Tnfα* gene
   - 2.4 Pyruvate kinase muscle isoform 2 (PKM2)
     - 2.4.1 PKM2 in the cytoplasm
     - 2.4.2 PKM2 in the nucleus
   - 2.5 T-helper-inducing POZ-Krüppel-like factor (ThPOK)
   - 2.6 Long non-coding RNAs (lncRNAs)
3. **Objectives**
4. **Materials and Methods**
   - 4.1 Cell culture and media
   - 4.2 Cell treatments
   - 4.3 Antibodies
   - 4.4 DH5α competent cells
   - 4.5 cDNA cloning
   - 4.6 Plasmid and BAC DNA extraction

4.7 Total RNA isolation
4.8 Reverse transcription - cDNA synthesis
4.9 DNA FISH
4.10 RNA-DNA FISH
4.10.1 Directly-labeled probe preparation
4.10.2 Indirectly-labeled probe preparation
4.10.3 Riboprobes
4.11 Immuno-DNA FISH
4.12 Whole cell and nuclear protein extracts
4.13 Electrophoretic Mobility Shift Assay (EMSA)
4.14 SouthWestern blotting (SW)
4.15 DNA affinity chromatography
4.16 Protein detection and Mass Spectrometry
4.17 Yeast One Hybrid Screening Library
4.18 Chromatin Immunoprecipitation assay (ChIP)
4.19 Co-Immunoprecipitation of proteins (Co-IP)
4.20 DNase I Hypersensitivity mapping
4.21 DNase I Footprinting
4.22 Luciferase assays
4.23 Rapid Amplification of cDNA Ends (RACE)

5. Results

5.1 Homologous association of the *Tnfα* alleles
5.2 Allelic expression of the *Tnfα* locus
5.3 LPS induction
5.4 Actin polymerization
5.5 Protein complexes
5.6 Long non-coding RNA transcripts
5.7 Potential mechanism for allelic expression regulation

6. Discussion

7. References

LIST OF FIGURES

Figure 1. Above: The *LT/TNF* locus. Below: Normalized distances (NDs) are calculated by dividing the absolute distances between the two *Tnfα* alleles by the diameter of each cell.

Figure 2. Time course of the homologous association of the *Tnfα* alleles.

Figure 3. Above: *Tnfα* allele distance distributions. Below left: Kolmogorov-Smirnov test for the randomness of distributions. Below right: Cumulative frequency curves of *Tnfα*, *E4f1*, *P2rx4* and *Arrb1*.

Figure 4. Frequency of co-localization of the *Tnfα* alleles in a time course of LPS-stimulated Raw 264.7 macrophages.

Figure 5. On-gel and quantitative RT-PCR analysis of the gene expression profile in the *LT/TNF* locus.

Figure 6. Above: Confocal microscopy images with representative images of the *Tnfα* alleles, along with the nascent mRNA transcripts in macrophage nuclei as seen expressing in a mono- or bi-allelic manner. Below: Percentage of expressing cells in a time course of LPS stimulation of Raw 264.7 macrophages.

Figure 7. Allelic pattern of *Tnfα* expression in Raw 264.7 macrophages after LPS stimulation.

Figure 8. The effect of TNFα stimulation on *Tnfα* homologous pairing in macrophages.

Figure 9. The effect of TNFα stimulation of macrophages on *Tnfα* allelic expression.

Figure 10. The effect of actin polymerization disruption on *Tnfα* homologous pairing and allelic expression.

Figure 11. LPS-induced GAGAG DNA binding activity in Raw 264.7 nuclear protein extracts.

Figure 12. Above: P11 phosphocellulose fractionation of 30min-LPS nuclear protein extracts. Below: stepwise elution of extracts and EMSA-analysis for the presence of DNA binding activity.

Figure 13. Mass Spectrometry identification of GA-binding proteins in nuclear protein extracts from LPS-stimulated Raw 264.7 macrophages.

Figure 14. Above: Immunostaining of PKM2 in the cytoplasm and nucleus of LPS-stimulated Raw 264.7 macrophages. Below: PKM2 is LPS-induced as confirmed by Western blotting of nuclear protein extracts from untreated and 30min-LPS stimulated Raw264.7 macrophages with a-PKM2 and a-NPM antibodies.

Figure 15. Quantitative RT-PCR of *Tnfα* mRNA before and after siRNA treatment of PKM2.

Figure 16. Immunostaining of PKM2 before and after siRNA-mediated knock down.

Figure 17. Left: ThPOK mRNA expression in untreated and LPS-stimulated macrophages assessed by quantitative RT-PCR. Right: Immunostaining of ThPOK protein in the nucleus of untreated and LPS-stimulated Raw 264.7 macrophages.

Figure 18. *Tnfα* expression before and after siRNA of PKM2 or ThPOK.

Figure 19. Quantitative RT-PCR of *Tnfα* mRNA before and after siRNA of ThPOK.

Figure 20. Left: The effect of PKM2 and ThPOK siRNA treatment on *Tnfα* homologous pairing. Right: The effect of PKM2 and ThPOK siRNA treatment on *Tnfα* bi-allelic expression.

Figure 21. Chromatin Immunoprecipitation experiments portray binding of ThPOK and PKM2 on the *Tnfα* promoter.

Figure 22. Co-immunoprecipitation of PKM2 and ThPOK from untreated and 30min-LPS stimulated Raw 264.7 nuclear extracts.

Figure 23. Long non-coding transcripts at the *LT/TNF* locus.

Figure 24. Cross-species conservation of DNA sequences on the 5' end of each lncRNA in the *Tnfα* locus, designated as #1 and #9.

Figure 25. Above: DNase I Hypersensitivity mapping on the conserved DNA sequences directly 5' of the long transcripts on the *LT/TNF* locus. Below: Luciferase assays with the two DNA sequences show that HSS-1 and HSS-9 have LPS-inducible transcription activation capabilities.

Figure 26. Above: RNA-DNA FISH representative images showing lncRNA#9 expressed in LPS-stimulated Raw 264.7 macrophages. Below: Expression of lncRNA#1 and lncRNA#9 in Raw 264.7 macrophages untreated or stimulated for 1h, 2h and 6h with LPS.

Figure 27. Effect of lncRNA#1 knock-down on *Tnfα* homologous pairing and bi-allelic gene expression.

Figure 28. Effect of lncRNA#9 knock-down on *Tnfα* homologous pairing and bi-allelic gene expression.

Figure 29. Potential mechanism for the *Tnfα* allelic expression regulation. Effect of TNFα stimulation, actin polymerization disruption, PKM2, ThPOK and lncRNA#9 knock down on *Tnfα* homologous pairing and allelic expression.

Figure 30. Potential mechanism for the *Tnfα* allelic expression regulation. Effect of lncRNA#1 knock down on *Tnfα* homologous pairing and allelic expression.

1. SUMMARY

Several *trans*-allelic phenomena have been described in the past although their mode of action on gene regulation lacks mechanistic insight. Such a rare phenomenon in mammals is somatic homologous pairing. We have investigated the homologous pairing of the *Tnfα* locus in LPS stimulated mouse macrophages and found that it occurs early upon activation prior to the *Tnfα* gene expression switch from monoallelic to biallelic. The proposed regulatory mechanism involves two complementary long non-coding RNAs transcribed from the *LT/TNF* locus, a protein kinase with transactivation potential and a protein considered to be the mammalian homolog of the *Drosophila* GAGA-factor involved in transvection. We believe that homologous pairing as a part of genome organization in mammals will be of general interest and propose a mechanism for the regulation of mono- to bi-allelic switch of gene expression.

2. INTRODUCTION

Regulation of gene expression has been demonstrated to be accomplished by several regulatory elements (promoters, enhancers, silencers, locus control regions, etc.), which are capable of mediating transcriptional and epigenetic events [1, 2, 3]. So far, evidence has suggested that these elements and the factors capable of transcriptional regulation act *in cis* on genes physically linked to them, on the same chromosome. Recently, chromatin *trans*-interactions have been shown to occur between regulatory elements located on a chromosome different than the one carrying the gene to be regulated.

In diploid organisms, the two alleles existing for each genetic locus do not always function independently. There are circumstances in which one "senses" the presence of the other *in trans* and alters accordingly the expression pattern [4]. These inter-chromosomal interactions have been studied extensively in several systems, pointing out that such a mechanism regulating gene expression *in trans* may be a general phenomenon. More specifically, methylation induced premeiotically (MIP) in *Ascobolus immersus* leads to irreversible gene silencing of inappropriately duplicated sequences [5, 6]; recombination induced premeiotically (RIP) in *Neurospora crassa* induces mutations in duplicated sequences causing their transcriptional repression [6, 7]; transvection in *Drosophila melanogaster* enables an enhancer on one chromosome to drive transcription on the homologous allele [8, 9]; sex chromosome dosage compensation in many organisms detects the number of X chromosomes in a cell and adjusts the levels of gene expression to balance males and females [10, 11, 12]; and paramutation in *Zea mays* enables one allele (paramutagenic) to silence its homolog (paramutable) [13, 14].

In mammals little is known about such phenomena [15]. So far some examples of interchromosomal interactions have been described between the *alpha* and *beta globin* loci which share transcription factories [16, 17], imprinted loci [18, 19, 20], the two homologous X chromosomes and the mutually exclusive silencing of all genes on one of the chromosomes [21, 22, 23, 24], the neuronal loci of olfactory receptors and the H enhancer located on a different

chromosome [25, 26] and the two mutually exclusive differentiation states of T helper cells, Th1 and Th2, which are defined by the interactions of chromosomes 10 (*Ifnγ*) and 11 (*Th2* locus) [27, 28]. Finally, in 2003, a public research consortium named ENCODE (the Encyclopedia of the DNA elements) was launched, in an attempt to identify all functional elements in the human genome [29]. Systematic integrated analysis of the genome-wide interchromosomal interactions, which emerged from the project's data [30, 31, 32], showed that these interactions seem to be much more common than previously thought. Moreover, it was displayed that spatially close regions tend to have similar chromatin and methylation state, similar patterns of histone modifications and expression levels [33].

Another significant parameter in understanding how the mammalian genome is organised and functions is the characterisation of factors capable of alleviating or enhancing the repressive nature of chromatin, which regulate such interactions between chromosomes. One factor that plays an important role in promoter architecture in *Drosophila* is the GAGA transcription factor. GAGA binds to GA-rich sequences, $(GA)_n$, found in numerous promoters in *Drosophila* genes and stimulates expression by opening chromatin [34] and maintaining the promoter in a conformation which allows further binding of other sequence-specific factors and RNA Polymerase II [35, 36, 37]. Being one of the key-players, along with Zeste protein, in the transvection phenomenon [9], the GAGA factor has been studied extensively, but, so far, no structural or functional homologs in mammals have been found.

Besides the unidentified mammalian GAGA homolog, it is suspected that, because of the mammalian genome's complexity and its constant evolution, other protein complexes, shall play a major role in such interactions. In addition, long non-coding RNAs (lncRNAs) have been implicated in gene regulation and coordinate gene silencing, *in cis* or *in trans* [38]. For example, the widely known and well-studied *Xist* is one of these functional lncRNAs. *Xist* functions *in cis*, resulting in transcriptional silencing of one of the two X chromosomes in female mammals, by coating the inactive one [12, 39, 40]. All these aspects of chromatin organization and the several levels of gene regulation will be discussed below, along the lines of *Tnfα* gene transcription in activated murine macrophages.

2.1 *Trans*-allelic phenomena

The pairing of homologous chromosomes is a process that all eukaryotes perform at meiosis. In most organisms, obvious pairing is restricted to pre-meiotic germ cells. However, in dipteran insects, somatic pairing is strikingly evident in numerous cell types, and extended pairing of sister chromatids and homologs is responsible for the precisely banded pattern of polytene chromosomes. The functional significance of somatic pairing in diploid nuclei has been the subject of debate: diploid pairing might be just a remnant of the pairing process that gives rise to polyteny, which is predominant in dipteran larvae. Whether or not pairing plays a functional role in somatic nuclei, our ignorance of the underlying homology-sensing mechanism precludes a full understanding of interphase chromosome behavior [41]. In addition, somatic pairing underlies several intriguing genetic and epigenetic phenomena involving both allelic and non-allelic interactions.

Phenotypic changes that depend upon somatic pairing have been intensively studied in *Drosophila*. In 1954 E.B. Lewis introduced the term transvection to describe cases in which homologous pairing influences gene expression. It is interesting enough that the number of loci that fall within the category of transvection is rapidly increasing. Most of these cases were described in *Drosophila melanogaster*, where homologs are synapsed together in somatic cells, and involve the action of enhancers *in trans*. However, several transvection-like phenomena have been described in other organisms as well, suggesting that homolog interactions are of general importance. Some of these phenomena are directional, in that the paired alleles are different from one another, whereas in other phenomena, identical alleles act reciprocally. Some interactions can be weakened by disrupting pairing (e.g. by chromosomal rearrangements) anywhere between the affected locus and the centromere and others cannot. Some interactions increase gene expression and others reduce expression [9]. To deal with this diversity, the term "*trans*-sensing effects" was introduced to encompass allelic pairing-dependent phenomena even though they might have different underlying mechanisms.

2.1.1 Repeat-induced point mutation (RIP) process

Fungi very often undergo chromosomal rearrangements via recombination events, which serve as a source of karyotype variability among the populations. All these frequent recombination events, either in mitosis or in meiosis, can result in sequence duplications but fungi have several mechanisms evolved specifically to limit the extent of such rearrangements. Two post-transcriptional gene-silencing defense mechanisms have been found in *Neurospora*: quelling and meiotic silencing by unpaired DNA [42]. During quelling, which is related to RNA interference (RNAi) in plants, nematodes and mammals, accidental or defective duplicated sequences are recognized and silenced during the fungus' vegetative growth. Meiotic silencing by unpaired DNA, which is so far unique to *N. crassa*, involves the recognition of unpaired DNA during meiosis, and the subsequent silencing of all genes encoded by that DNA. This mechanism results in an RNA-mediated silencing process that affects the expression not only of all the genes that are mapped within the unpaired region, but of all the homologous sequences as well [42, 43]. In addition, there is a third defense mechanism that exploits the homologous pairing of repetitive sequences to silence mutated DNA.

Repeat-induced point mutation (RIP) is a homology-based process that mutates repetitive DNA and frequently leads to epigenetic silencing of the mutated sequences through DNA methylation.

Long, similar sequences (longer than 400bp with more than 80% identity) are recognized during the pre-meiotic dikaryotic stage and are considered duplicated [44, 45]. In such sequences, more than 30% of C:G pairs are substituted with T:A within a single sexual cycle. It seems that there is a preference for mutation at CpA dinucleotides [44, 46], which permits the detection of sequences that have undergone repeat-induced point mutation, since it results in shifts in the distributions of dinucleotide frequencies. Evidently, the role of this process is to lead to gene inactivation, since such substitutions often result in nonsense codons and in a high probability of methylation of the mutated sequences.

Genetic evidence of such processes would come from the study of defects caused by the inheritance of recessive traits. The mechanism of RIP does not permit such research, because of the tissue it takes place in: firstly, the cells inherit whole nuclei from each parent

and, secondly, the tissue itself is microscopic and ascogenous, not allowing for biochemical approaches [7]. A candidate gene approach was used to identify a gene required for RIP. A gene encoding for a cytosine methyltransferase was identified (called RIP-defective -*rid*-), due to the observation that in homozygous mutant cells for *rid* RIP did not occur [47].

Methylation in *N. crassa* seemed to be closely interwined with RIP. Approximately 2% of cytosines in the *N. crassa* genome are methylated and, as with animals and plants, methylation has been shown to cause gene silencing in this fungus. Research results so far suggest that RIP-mutated sequences are *de novo* methylated when they are transformed back into the organism, a process most likely triggered by cooperative recognition in the minor groove of short A:T-rich tracts. Evidence for this *de novo* methylation process in *N. crassa* was provided by the failure of some methylated products of RIP to trigger *de novo* methylation [48, 49].

So far, another gene, apart from *rid* has been identified to take part in this protective methylation mechanism. The defective in methylation 2 (*dim-2*) gene, the only DNA methyltransferase gene evident in the *N. crassa* genome apart from *rid*, has been shown to be responsible for all known DNA methylation in this organism. Unlike RID, however, DIM-2 is not necessary for RIP [47].

2.1.2 Paramutation

Paramutation was first defined by Alexander Brink in the 1950s as "an interaction between alleles of genes that leads to heritable changes in gene expression" [50]. According to the initial observations, paramutation portrayed three characteristics: (1) alterations in the expression state are transmitted to subsequent mitotic or meiotic generations even though the allele or sequences originally encoding such alterations are not transmitted; (2) the alterations of the starting locus are established to homologous sequences; and (3) these alterations are not caused by sequence changes in the DNA *per se*, but the instructions transferred to the homologous sequences are mediated through epigenetic mechanisms.

This challenge of basic rules of inheritance raises questions as to how the homologous sequences communicate, how the alterations are maintained through subsequent mitotic and meiotic divisions in the absence of DNA sequence changes, what causes this memory

of information and what are the transferred molecules.

The most-studied example of paramutation is the *b1* locus in *Zea mays*. The *b1* locus encodes a transcription factor that promotes the biosynthesis of purple anthocyanin pigments and comes in two different possible alleles, *B-I* and *B′*.

Plants homozygous for the *B-I* allele have high expression of *b1* and are dark purple, whereas plants homozygous for the weakly transcribed *B′* allele are lightly pigmented. In contrast to what is expected by the differences in phenotype, the sequences of the *B-I* and *B′* alleles are identical. In addition, the mode of inheritance and dominance are also different between these and conventional genetic alleles.

The explanation for these differences came from heterozygous plants. In plants heterozygous for the two alleles, the *B-I* allele is converted (paramutated) to *B′*. This new *B′* allele (designated *B′**) is equally capable as the parental *B′* allele of paramutating *B-I* to *B′* in subsequent generations [51]. It has been found that the key sequences necessary for paramutation are tandem noncoding DNA repeats mapped to a 6-kb region located ~100 kb upstream of the *b1* transcription start site [52]. Although the *B-I* and *B′* alleles are identical in sequence, it was found that the "paramutagenic" ability is given by the different pattern of methylation of the DNA of *B-I,* as well as the fact that its chromatin is in a more open state relative to *B′* [52].

RNA in paramutation

Recent work in maize [53, 54, 55] has uncovered evidence for a prominent role of RNA in paramutation. It seems that an RNA-dependent mechanism is critical for paramutation in maize. Firstly, transcription occurs on both strands of the tandem repeats upstream of *b1* [53], which may lead to the production of double-stranded RNA (dsRNA). Also, an RNA-dependent RNA polymerase (RdRP) called *mediator of paramutation1* (*mop1)* [53, 55] is absolutely required for silencing of *B-I* by *B′* and for paramutation at several other maize genes [56]. Although transcription of the repeats may be necessary for paramutation, it is not sufficient – the number of repeats is also a critical factor. The tandem repeats are required for both paramutation and high expression of *B-I* [52]. In the current model for *b1* paramutation, RNA mediates the communication between the *B-I* and *B′* alleles to establish

distinct chromatin states within the repeats. RNA is then required to maintain those states to determine whether the *b1* gene is transcribed at the high (*B-I*) or low (*B′*) level.

An intriguing question is why the tandem repeats upstream of *b1* induce silencing, whereas a single copy does not [52]. Robert Martienssen proposed that multiple rounds of an RNA-dependent RNA polymerase and dicer-like activity with tandem repeats as templates would result in increased amounts of siRNA targeting the whole sequence [57]. On the other hand, starting with a single copy sequence, subsequent rounds of amplification would produce shorter and shorter dsRNAs. Another hypothesis is that a larger RNA synthesized from the repeats is responsible for silencing, which cannot be generated from a single copy sequence [13].

Paramutation in mice

Paramutation has also been reported in mice at the *Kit* locus [58]. A tyrosine kinase receptor that functions in melanogenesis, germ cell differentiation, and hematopoiesis is encoded by the *Kit* gene. Full knock-out mice lacking *Kit* die shortly after birth, heterozygotes, on the other hand, have white tail tips and white feet.

Remarkably, crosses between heterozygotes or between a heterozygote and a wild-type mouse, produce genetically wild-type progeny with white tail tips and feet and reduced levels of *Kit* mRNA similar to the heterozygous parent. Here, too, the results are explained with paramutation events. Progeny with this paramutant phenotype were designated *Kit**.

The transmission of this paramutant state is also considered to involve RNA. However, RNA in mice paramutation has a role very different from what was described for the *b1* locus in plants, with gene silencing occurring at the posttranscriptional rather than transcriptional level. Rassoulzadegan et al. propose that RNA molecules are transmitted through gametes and that these trigger degradation of *Kit* mRNA in the paramutant individuals [58].

2.1.3 Transvection

As mentioned earlier, the term transvection was introduced by E.B. Lewis in 1954 to describe cases in which gene activity is influenced by homologous pairing. He illustrated transvection by showing how complementation between two alleles of the *bithorax* gene complex can be antagonized by disruptions of somatic pairing. Since then, the number of loci exhibiting transvection effects in *Drosoph*ila has grown significantly to include, among others, *white, decapentaplegic, eyes absent, vestigial, and yellow*.

The mechanism of transvection may differ among loci, thus two representative models will be presented here.

Transvection at *Yellow*

Transvection at the *yellow* locus was first demonstrated for the y^2 allele, which had long been known to complement a number of other *y* alleles [59, 60]. y^2 entails a *gypsy* element inserted at -700 bp from the transcription start site separating the wing and the body enhancers from the *y* promoter. The *gypsy* element presents insulation capabilities, thus resulting in y^2 flies with yellow cuticle in the wing and body.

Geyer *et al.* identified several *y* alleles that complement y^2 thus reversing wing and body coloration. They subsequently found that they all deleted or damaged the *y* promoter, without altering the wing and body enhancers. For example, y^{59b} is a derivative of y^2 with a deletion that covers a part of the *gypsy* element, the whole promoter, and part of the coding region. Homozygotes either for y^2 or y^{59b} do not transcribe *y* in the pupal stage, it is restored, however, in y^2/ y^{59b} heterozygotes. The mRNA transcribed is of normal length, which means that transcription begins at the promoter of the y^2 allele. Complementation of y^2 and y^{59b} appears to be pairing-dependent since y^2 transgenes inserted at ectopic locations do not complement y^{59b} [59].

Another derivative of y^2, y^{88d}, removes the entire coding sequence of *y*, the promoter and part of the *gypsy* element, but leaves the enhancers intact. This also complements y^2, indicating that it is the wing and body enhancers that act *in trans* to drive transcription of the y^2 promoter in the wing and body cuticle.

A third y^2 derivative (y^{69}) also deletes part of *gypsy*, the *y* promoter, and the transcribed region of *y*. Surprisingly, however, y^{69} does not complement y^2, as do y^{88d} and y^{59b}. It seems that y^{69}does not delete the *gypsy* insulator region, whereas this is deleted in y^{59b} [9, 61]. Interestingly, in all these cases, transvection occurs by the enhancers of one allele acting *in trans* on the promoter of a paired allele.

In 1998, a second mechanism by which transvection can occur at *y* was discovered [62]. Looking for derivatives of y^1 (causes a missense change in the initiating ATG of the *y* coding region) that can complement y^2, an allele (y^{3c3}) was recovered that deletes the body enhancer, the promoter, and the first exon of the gene, but not the wing enhancer [62, 63].

Remarkably, y^{3c3} complements y^2 for both body and wing color, implying that this allele allows the body enhancer of y^2 to bypass the insulating *gypsy* element. An appealing model to explain this mechanism is that this bypass occurs because the *gypsy* element loops out when y^{3c3} associates with y^2 and the wing and body enhancers of the y^2 allele are brought into close proximity with the promoter [59].

Transvection at *White*

Transvection is also involved in the interaction of the *zeste*^{1} (z^1) mutation and the *white* gene [65, 66]. The *white* gene is important for the red pigmentation of the eyes in the fly. In a mutant z^1 background the pairing alleles of the *white* gene are repressed resulting in yellow eyes. On the other hand, an unpaired *white* gene escaped repression, leading to the suggestion that the mutant z^1 protein binds on the *white* gene, aggregating so extensively that becomes repressive, which is more efficient when the *white* alleles are paired. We now know that Zeste is a DNA-binding transcription factor, with the ability to homopolymerize and a role in expression of many genes in Drosophila. Zeste protein has been proposed to act generally, holding DNA segments together either intramolecularly, during looping, or intermolecularly, during transvection [67].

GAGA factor

The GAGA factor (GAF) in *Drosophila melanogaster* is a transcription factor that can regulate gene expression at multiple levels. It is encoded by the *Trithorax-like* (*Trl*) gene and has the ability to bind alternating (GA)*n* or (CT)*n* sequences. It was first described as an *in vitro* activator of the *Ultrabithorax* (*Ubx*) and *engrailed* (*En*) genes, and was later shown to bind to GAGA elements (GAGA or CTCT stretches) in multiple promoters and enhancers of Drosophila genes, including *hsp70*, *hsp26*, histones *H3/H4*, *Krüppel*, *actin-5C*, *1-tubulin*, *etc* [68, 69, 70, 71, 72]. It has also been found to bind to polycomb response elements (PREs) and a large array of euchromatic genes, which suggests a role in maintaining chromatin open and transcriptionally active [73, 74].

The GAGA factor (GAF) consists of a single zinc finger DNA-binding domain (DBD) , a BTB/POZ domain, a protein–protein interaction motif [75], and a polyglutamine-rich or Q domain, whose function is not yet fully elucidated [36, 76].

GAF interacts with its natural binding site(s) through contact between the DNA major groove and the DBD zinc finger and when multiple GAF binding sites are clustered, the binding appears to be cooperative [77].

Besides its obvious ability to bind DNA (single, double, and triple stranded), the GAF's protein interaction domains provide multiple anchors for a number of cofactors that together form a functional complex. In addition it has also the ability to homopolymerize through the BTB/POZ domain which may play a significant role in enhancing DNA binding to multiple GA or CT stretches [78].

The GAGA factor displays both activator and repressor activities, depending on its target genomic location. In addition, the GAF-mediated regulation of expression appears to be intimately linked with modifications of the chromatin structure. It seems to be able to associate with highly compacted heterochromatin, contributing to gene repression, or participate in nucleosome remodeling to activate specific genes [79, 80].

2.1.4 Homologous pairing of oppositely imprinted loci

There has been evidence for low, but significant, levels of somatic homologous pairing in mice but also in humans. For example, cytological studies have revealed centromeric pairing of human chromosomes 1 and 17 in normal brain tissues [81, 82] as well as homologous pairing of the pericentric regions in human lymphocytes [83].

Of particular interest are reports of chromosomal proximity in the region associated with the imprinted Prader-Willi and Angelman syndromes, the latter of which may be, in some cases, phenotypically and genetically related to autism and Rett syndrome [84, 85]. Homologous association of 15q11–13 domains has been observed during the late S-phase in lymphocytes as well as in neurons and brain tissue. There is evidence for increased homologous pairing of 15q11–13 domains during normal postnatal brain development in human brain. The protein MeCP2 (methyl CpG-binding protein 2) that binds to methylated CpG sites within nuclear heterochromatin, has been implicated in the mechanism of homologous pairing. Specific blocking of its binding to endogenous chromatin resulted in a significant reduction in homologous pairing of 15q11–13 domains in cultured neuroblastoma cells [85]. Furthermore, altered levels of MeCP2 in human cells have been correlated with changes in the tendency of the Prader-Willi and Angelman Syndrome regions to become aligned in the nucleus [85].

2.1.5 X-chromosome inactivation

In mammals, the X-chromosome is is the only chromosome with the potential of complete inactivation. Complete X inactivation evolved to compensate for gene dosage differences between females with two X chromosomes and males with one. The two X chromosomes start out as epigenetically equivalent, but the cell treats the two identical X chromosomes in completely different ways: one X chromosome remains transcriptionally active while the other becomes repressed. In the embryos of eutherian mammals, the choice to inactivate the maternal or paternal X chromosome is random [86, 87]. Moreover, the fact that the Xs always adopt opposite and mutually exclusive fates gave evidence for the existence of a *trans*-sensing mechanism that ensures the silencing of only one X

chromosome.

The X-chromosome inactivation (XCI) process starts with the counting of the number of X chromosomes present in a nucleus, and the process of inactivation continues only if this number exceeds one per genome [89, 90]. Transcriptional silencing of a single female X chromosome is controlled *in cis* by *Xist*, whose RNA product coats the inactive X chromosome (Xi), and the X-inactivation centre (Xic) [91]. A transgenic study limited the Xic to 450 kb including *Xist*, and demonstrated that it is sufficient to initiate X inactivation [92]. On the future inactive X, *Xist* becomes upregulated and *Tsix* (its antisense unit) is down-regulated.

The accumulation of the *Xist* transcript on the X chromosome chosen to be inactivated (Xi) triggers the initiation of X-chromosome inactivation.

In order to ensure mutually exclusive silencing, the two Xs are also regulated *in trans*. Interchromosomal pairing mediates this control [93], which occurs transiently at the onset of X inactivation (sensing) and is specific to the X-inactivation center (Xic) [21].

Deleting *Xite* and *Tsix* disturbs the pairing and counting/choice processes, whereas their ectopic autosomal insertion induces de novo pairing between the X and the autosome, suggesting that they counting and exclusive silencing is regulated through pairing [24].

2.1.6 DNA methylation during meiosis

Studies in *Cre-LoxP* recombination in pachytene spermatocytes revealed extensive methylation of *LoxP* sites that spreads progressively *in cis.* When a normal homolog is made heterozygous with a methylated *LoxP* homolog, it acquires the ability to cause extensive methylation of naïve *LoxP* homologs in subsequent generations. This ability does not depend upon the continued presence of *Cre* therefore the spreading of this epigenetic mark appears to result from a cellular mechanism [58].

2.1.7 Intergenic transcription of the human β-globin locus

Expression of a number of genes is regulated by a locus control region (LCR), an

element that exerts a dominant transcriptional activation function over a chromatin domain.

The human *β-globin* locus covers a stretch of 70 kb of DNA and consists of an LCR and five erythroid-specific genes, ε-^{G}γ-^{A}γ-δ-β, arranged in the order of their developmental expression [94]. The *β-globin* LCR contains five erythroid-specific, developmentally stable DNase I hypersensitive sites, HS1–HS5, situated upstream of the *ε-globin* gene [95]. Surprisingly, transcription analysis at the *β-globin* locus after transfection into non-erythroid cells reveals that intergenic transcription is induced from the chromosomal *β-globin* locus. Insight into the mechanism of transinduction came from plasmid-transfected HeLa cells, which revealed that the plasmid colocalized with the chromosomal *β-globin* locus [96].

2.2 Macrophages

Macrophages are phagocytic cells involved in the clearance of cellular debris generated during tissue remodeling, wound healing and necrosis after pathogenic infection. They display remarkable plasticity and, in response to several environmental cues, change their physiological properties, migrate and give rise to different cell populations with distinct functions [97]. They are present in virtually all tissues and differentiate from circulating peripheral blood mononuclear cells (PBMCs), which migrate into the tissue in the steady state or in response to inflammation. During monocyte development, myeloid progenitor cells give rise to monoblasts, pro-monocytes and finally monocytes, which are released from the bone marrow into the bloodstream. Monocytes then migrate from the blood into the tissue to form osteoclasts (bone), alveoli (respiratory tract), microglial cells (central nervous system), histiocytes (connective tissue), Küpffer cells (liver) and others [97, 98].

Macrophages can respond to endogenous stimuli that are rapidly generated following injury or infection, to signals that are produced by antigen-specific immune cells or to signals produced by other activated macrophages. Following activation, they undergo a reprogramming which leads to the emergence of a spectrum of distinct functional phenotypes. Mirroring the Th1/Th2 nomenclature for the differentiation of T helper cells, macrophages are classified as M1 for the classically activated macrophages and M2 for

the alternatively activated.

In general, M1 cells have an IL-12^{high}, IL-23^{high}, IL-10^{low} phenotype, are efficient producers of effector molecules (reactive oxygen and nitrogen intermediates) and inflammatory cytokines (IL-1β, TNFα, IL-6), participate as inducers and effector cells in polarized Th1 responses and mediate resistance against intracellular parasites and tumors.

Classically activated M1 macrophages have long been known to be induced by IFNγ alone or in concert with microbial stimuli (e.g. LPS) or cytokines (e.g. TNFα and GM-CSF). Typically, a TLR ligand acting in a MyD88-dependent manner will induce transcription of the *Tnfα* gene, which can then cooperate with IFNγ. Some TLR ligands can also activate TIR-domain-containing adaptor protein inducing IFNβ (TRIF)-dependent pathways, independent of MyD88, which signal through IFN-regulatory factor 3 (IRF3) and result in IFNβ production, replacing the NK- or T cell- produced IFNγ in activation [97, 99].

The recognition of conserved non-self molecules expressed by microorganisms is mediated by the so- called pattern recognition receptors, many of which belong to the Toll-like receptor family. The most studied of these receptors is Toll-like receptor 4 (TLR4), which mediates signals generated by lipopolysaccharide (LPS), a major component of the cell walls of gram-negative microorganisms. Stimulation of macrophages with exogenous TNFα or with a TLR ligand, such as lipopolysaccharide (LPS), can also result in the complete clearance of the parasite. In response to LPS, mouse macrophages undergo a major change in gene expression, inducing the expression and release of numerous biologically active cytokines that orchestrate the inflammatory response.

The LPS response in mouse macrophages has been analyzed on a number of different approaches and such profiling reveals a cascade of gene regulation and several LPS-induced genes. However, it has not yet been possible to provide a reliable detailed map of the underlying regulatory transcriptional architecture [101, 102].

The role of classically activated macrophages in host defense to intracellular pathogens has been well documented. Indeed, mice lacking IFNγ expression are more susceptible to various bacterial, protozoan or viral infections, as are humans with genetic

mutations in these signaling pathways. Although they are vital components of host defense, their activation must be tightly controlled because the cytokines and mediators that they produce can also lead to host-tissue damage. Indeed, classically activated macrophages are key mediators of the immunopathology that occurs during several autoimmune diseases, including rheumatoid arthritis and inflammatory bowel disease [97].

The M2 designation has expanded to include all other types of activated macrophages. In general, M2 cells take part in polarized Th2 cell responses, parasite clearance, the dampening of inflammation, the promotion of tissue remodeling, angiogenesis, tumor progression and immunoregulation.

Wound-healing macrophages can develop in response to innate or adaptive signals released during tissue injury. Basophils and mast cells are the major sources of the early IL-4 production [103], a cytokine which rapidly programs resident macrophages to promote wound healing, via the production of extracellular matrix [104]. Similarly to the uncontrollable activity of classically activated macrophages in autoimmunity, wound-healing macrophages can also become destructive when their matrix-producing activity is deregulated, resulting in tissue fibrosis or asthma [105, 106, 107, 108].

Another alternatively activated population of macrophages arises through stress responses [109]. Adrenal cells release glucocorticoids in response to stress which inhibit macrophage-mediated host defense and inflammatory functions. This is achieved mainly by inhibition of transcription of pro-inflammatory cytokine genes and a decrease in mRNA stability, giving rise to a population of regulatory macrophages. During the later stages of adaptive immune responses, regulatory macrophages also have the primary role to dampen the immune response and limit inflammation, mainly by producing high levels of the immunosuppressive cytokine IL-10, in contrast to classically activated macrophages [102, 110, 111, 112].

It is now known that many other cytokines can govern M2 polarization. IL-33 is a cytokine of the IL-1 family associated with Th2 and M2 polarization. It amplifies IL-13-induced polarization of alveolar macrophages to an M2 phenotype, which is marked by the up-regulation of chemokines like YM1, CCL24 and CCL17. IL-21, a Th2-associated cytokine, as well as colony-stimulating factors, have also been shown to activate macrophages and drive M2 polarization.

Lastly, tumor-associated macrophages (TAMs) have been described to infiltrate most tumors and to provide the link between inflammation and cancer. In the tumor, macrophages can express both pro-, as well as anti-tumor functions, based on distinct signals they receive from the particular microenvironment in which they reside, independent of the location of the tumor. TAMs generally display an M2-like phenotype which is able to promote tumor growth, remodel tissues in order to promote angiogenesis and suppress the host's adaptive immune responses [97, 113].

In summary, macrophage plasticity gives them the ability to adapt their physiology to both innate and adaptive signals, and alter their phenotype allowing them to participate in homeostatic processes, such as tissue remodeling and wound healing, as well as in host defense. However, each of these alterations can have potentially dangerous consequences if not appropriately regulated.

2.3 Tumor Necrosis Factor - alpha (TNFα)

Tumor necrosis factor (TNF) -α is a pleiotropic, pro-inflammatory cytokine, which was initially described as a necrotic factor in peripheral inflammation, that induced cell death in tumor cell lines *in vitro* and transplanted tumors *in vivo* [114]. It was first described by Carswell *et al.* in 1975 in an attempt to identify tumor (sarcoma 37) regression activity induced in the serum of mice treated with *Serratia marcescens* polysaccharide [115]. Since then, it has been implicated in a wide range of inflammatory, autoimmune and malignant conditions.

TNFα is produced in response to bacterial, inflammatory and other stimuli, primarily by cells of the immune system, such as macrophages, T and B lymphocytes, but also by additional cell types, including endothelial cells, mast cells and neuronal tissues [116]. It is expressed as a 212 amino-acid long type II trans-membrane form (26 kDa protein), which is cleaved by the metalloprotease TNF-α-converting enzyme (TACE or ADAM17) at its extracellular domain to produce a 17-kDa active protein [117]. The secreted monomers that are generated form biologically active homotrimers. Both the soluble (sTNF) and the membrane-integrated forms of TNF are active in their trimeric forms [117].

2.3.1 TNFα signaling pathway

TNFα can activate a pathway that leads to the induction of NF-κB and further pro-inflammatory cytokine expression. It has, thus, the ability to upregulate cell adhesion molecules, necessary for the migration and recruitment of leukocytes and it stimulates the release of other cytokines, such as IL-1 and IL-6 [118]. These functions are achieved through the binding of TNFα to its TNF receptor. Two receptors, TNFR1 (TNF receptor type 1; CD120a; p55/60) and TNFR2 (TNF receptor type 2; CD120b; p75/80), can bind TNFα [119]. TNFR1 is expressed in most tissues and can be fully activated by both the membrane-bound and soluble trimeric forms of TNFα, whereas TNFR2 is found preferentially in hematopoietic cells and is more efficiently activated by the transmembrane form of the TNFα homotrimer [120, 121].

The TNF-TNFR binding causes a conformational change in the receptor, leading to the dissociation of the inhibitory protein SODD (Silencer of Death Domain) from its intracellular death domain. This dissociation allows the binding of the adaptor protein TRADD (Tumor necrosis factor receptor type 1-associated death domain protein) to the receptor's death domain, serving as a platform for subsequent protein binding and signaling activation. TRADD can recruit TRAF2 (TNF receptor-associated factor 2) and the death domain kinase RIP (receptor interacting protein) and lead to the nuclear translocation of NF-κB and the transcription of proteins involved in cell proliferation and survival [122, 123]. The pro-inflammatory effect of TNFα is mediated through NF-κB–regulated proteins, such as IL-6, IL-8, IL-18, chemokines, inducible nitric oxide synthase (iNOS), cyclooxygenase-2 (COX-2) and 5-lipoxygenase (5-LOX).

Alternatively, TRAF2 can activate the JNK-inducing kinases of MEKK1 (or MAP3K1 Mitogen-activated protein kinase kinase kinase 1) and ASK1 (Apoptosis signal-regulating kinase 1, or MAP3K5). These two kinases then phosphorylate MKK7 (Mitogen-activated protein kinase kinase, or MAP2K), which then activates JNK (c-Jun N-terminal kinase) to translocate to the nucleus and activate transcription factors such as c-Jun and ATF2. The JNK pathway is involved in cell differentiation and is generally pro-apoptotic [125, 126, 127, 128, 129, 130].

As a third alternative, TRADD binds FADD (Fas-associated protein with death

domain), which then recruits the cysteine protease caspase-8 to form the death-inducing signaling complex (DISC). A high concentration of caspase-8 in the DISC induces its autoproteolytic activation and subsequent cleavage of effector caspases, leading to cell apoptosis [130, 131, 132].

In turn, TNFR2 lacks the intracellular death domain, present in TNFR1, and appears to mediate signals promoting cellular activation, proliferation and migration.

2.3.2 Transcription at the *Tnfα* locus

The lymphotoxin/tumor necrosis factor (*LT/TNF*) locus comprises of the tandemly arranged genes coding for TNFα (also known as cachectin), Lymphotoxin alpha (*Ltα*) and Lymphotoxin beta (*Ltβ*) and is mapped within the class III region of the major histocompatibility complex (MHC). Their coding regions occupy ~12 kb of genomic DNA on human chromosome 6 and mouse chromosome 17. The *Tnfα* and *Ltα* genes are in the same transcriptional orientation while *Ltβ* is transcribed in the opposite orientation.

The *LT/TNF* locus contains intergenic sequences that are not generally conserved, but there are also regions with highly conserved noncoding sequences. The *TNF* promoter is among these conserved sequences, presenting almost complete conservation among primates especially in the proximal region which is critical for transcriptional regulation [134, 135, 136, 137].

TNFα and the soluble lymphotoxin α are cytokines with similar biological activities. Ltα when expressed by activated T cells forms a heterotrimer with Ltβ which is a membrane- anchored ligand that binds specifically to the Ltβ receptor (LtβR). The LtβR is implicated as a critical element in controlling lymph node development and cellular immune responses.

Transcription of the *Tnfα* gene is regulated in a cell type- and stimulus- specific fashion via the recruitment of specific sets of transcription factors and co-activators to the promoter region (~200bp), forming distinct nucleoprotein complexes known as enhanceosomes [139, 140, 141, 142]. Among the stimuli are calcium signaling [143], pathogens, like bacteria and viruses, mitogens, like phorbol esters, chemical stress and radiation. Furthermore,

Tnfα transcription is induced by several receptor signaling pathways, such as the T cell receptor, pattern recognition receptors (TLRs) and cytokine receptors, such as TNFR1/R2.

Specifically, there are multiple mechanisms implicated in the lipopolysaccharide (LPS)-stimulated TNFα production in macrophages. LPS, released by invading bacteria, can trigger the expression of TNFα via two different receptors, the macrophage-specific surface receptor CD14 and the membrane protein Toll-like receptor 4 (TLR4) and through two respective signaling pathways.

In the first case, LPS-binding protein (LBP) facilitates LPS binding to the macrophage receptor CD14. LPS-LBP-CD14 interaction provokes rapid activation of protein tyrosine kinase (PTK) causing tyrosine phosphorylation of several intracellular protein kinases. PTK activates a pathway involving Ras/Raf-1/MEK/MAPKs/NFkB. Ras is an early target of the activated PTK and is able to interact directly with Raf-1. Raf-1/MEK appears to activate members of the MAPK family of protein kinases; of these the p38 MAPK appears to play a pivotal role in the cascade leading to *Tnfα* gene induction. The protein kinase cascade leads to NF-κB activation, its translocation to the nucleus and TNFα production [118, 121, 144, 145].

In the case of TLR4, signaling originates from its conserved cytoplasmic Toll/IL-1 receptor (TIR) domain. Downstream of the TIR domain, a TIR domain-containing adaptor, MyD88, is recruited. This MyD88-dependent pathway leads to the recruitment of the IL-1 receptor-associated kinase (IRAK) to TLRs through the interaction of their death domains. IRAK is phosphorylated and active to associate with TRAF6. The IRAK-1/TRAF6 complex dissociated from the receptor to bind to TGF-β-activated kinase 1 (TAK1) and TAK1-binding proteins, TABs. This signaling pathway leads to the activation of NF-κB and the production of inflammatory cytokines [101, 145].

There is also a MyD88-independent pathway in TLR signaling. In the absence of MyD88, LPS stimulation leads to the activation of the transcription factor IRF-3, and thereby induces IFNβ. IFNβ, in turn, activates STAT1, leading to the induction of several IFN-inducible genes. The TRIF-TRAM module that is activated in this pathway can also recruit RIP1 and TRAF6, but the induction of NF-κB in this case only leads to the induction of IFN-inducible genes and not *Tnfα*[146, 147].

The *Tnfα* gene is transcribed much more heavily than *lymphotoxin-α* in T

lymphocytes, even though the *Lt*α mRNA is more abundant. Resting T cells and macrophages, which do not accumulate any *Tnf*α mRNA, nevertheless transcribe the *Tnf*α gene actively and, notably, within minutes of activation. On the other hand, the *Lt*α gene is transcriptionally silent in macrophages.

2.3.3 Transcriptional control of the *Tnf*α gene

Tight control of *Tnf*α expression in specific cell types and after specific stimuli is essential for cellular homeostasis and normal physiology. This is evidenced by the fact that deregulated TNFα levels are associated with multiple disease states. While TNFα deficiency has been linked to differential susceptibility to infections, resulting in complete lack of B cell follicles or causing tuberculosis, prolonged high concentrations of TNFα can result in severe tissue damage, asthma, rheumatoid arthritis, cardiovascular diseases, inflammatory bowel disease, type II diabetes, systemic lupus erythematosus, psoriasis, septic shock and cancer [127, 130, 148, 149]. It is thus evident that a tightly regulated balance of TNFα levels is of critical importance.

*Tnf*α transcriptional control is mediated at several levels. Apart from the understanding that each cell type requires a different stimulus to activate *Tnf*α transcription, and that specific transcription factors within the *Tnf*α enhanceosome, are themselves cell-type specific, *Tnf*α transcription is also regulated by cell type-specific regulatory DNA elements within, or flanking the *Tnf*α promoter.

The 5'-UTR of the *Tnf*α gene spans a 200-nucleotide conserved proximal promoter, which is sufficient to drive transcription in response to several stimuli. The promoter is compact and modular, with distinct spacing between DNA motifs some of which can be recognized by more than one class of transcription factors, depending on the cell type, stimulus and factor concentration. These DNA motifs, which include, among others, a TATA-box, six nuclear factor of activated T cells (NFAT) binding sites, four Ets/Elk, a cyclic AMP response element (CRE) and two Sp1 binding sites, give the promoter remarkable flexibility to respond to every stimulus specifically.

Moreover, the 5'-region flanking the proximal *Tnf*α promoter contains several NF-κB binding sites, both in humans (κ1, κ2, κ3, κB1, κB2 and ζ) and in mice (κB1, κB2, κB2α, κB3

and κB4) [151, 152, 153]. These sequences were first studied due to their similarity with the NF-κB binding sites and were shown to be involved in *Tnfα* gene regulation [151, 154]. However, subsequent studies have proven this connection to be indirect and experiments with deletions or mutations of the sequences have shown that they are not typical NF-κB sites, have low affinity for NF-κB and are not indispensable for LPS-induced *Tnfα* transcription [155]. In addition, deletion of the genes encoding the NF-κB proteins p50, c-Rel, p52 and RelB had little or no effect upon expression of *Tnfα* mRNA or protein. Lastly, inhibition of NF-κB revealed that induction of *Tnfα* expression was NF-κB-independent, while expression at late time points after LPS or virus stimulation was not. This confers a post-induction role to NF-κB, partially confirming its role in LPS tolerance, the state of repressed or inhibited transcription, following prolonged exposure to LPS [156].

Gene transcription does not only involve the assembly of transcription factors on promoters but the accessibility of chromatin as well. To this end, covalent modifications of both histones and DNA mark transcriptionally active genes, promoting the formation of "open" areas of chromatin, by altering the net charge of nucleosomes. Acetylation of histones H3 and H4 at the *Tnfα* promoter has been correlated, in multiple studies, with increased *Tnfα* transcription and mono-, di- and tri-methylation of lysine 4 of histone H3 (H3K4), typically associated with gene derepression, has been observed at the *Tnfα* promoter after LPS induction. Accordingly, cells that do not express TNFα, including LPS-tolerant cells, display lower levels of methylation at H3K4 and phosphorylation at H3S10 and higher levels of di- or tri-methylation at H3K9, which generally marks repressed genes, recruits heterochromatin protein 1 (HP1), which in turn promotes gene silencing. Moreover, the *Tnfα* gene and its proximal promoter are unmethylated in cells expressing TNFα, including monocytes and lymphocytes, whereas DNA is found highly methylated in non-expressing cells, like HeLa [157, 158, 159].

Accessibility of chromatin is also represented by hypersensitivity to DNase I. Numerous DNase I hypersensitive sites (HSSs) have been identified in the *LT/TNF* locus, with the most representative being the *Tnfα* proximal promoter itself. Constitutive HSSs have been detected in both the *Tnfα* and *Ltα* promoters in human stimulated macrophages and monocytes, two inducible ~3kb downstream of the *Tnfα* transcription start site in rat astrocytes, a constitutive HSS in *Tnfα* intron 3 in Jurkat T cells, constitutive HSSs in the 3'

UTR of *Tnfα* and many more.

Apart from the transcription factor-DNA interactions and the epigenetic regulation, regulation of gene expression in eukaryotic cells also requires a tight spatial regulation, which is provided by long-range intra- and/or inter-chromosomal interactions. Higher order chromatin configurations that arise from such interactions bring, otherwise separated regulatory elements, into close proximity with gene promoters. It has been shown that, upon activation of T cells, intrachromosomal interactions occur between the *Tnfα* gene promoter, HSS+3 (~3kb downstream of the *Tnfα* transcription start site) and HSS-9 (~9kb upstream of the *Tnfα* gene). These interactions facilitate the proximity of distal enhancers and the promoter and the recycling of transcription machinery, for the rapid expression of TNFα high levels in T cells. At the same time, these interactions, besides establishing easier and faster *Tnfα* transcription, also sequester the *Ltα* gene into inactive chromatin, by placing it into a loop away from the enhancers gathered near the *Tnfα* promoter [159, 160, 161].

2.4 Pyruvate kinase muscle isoform 2 (PKM2)

Pyruvate kinase isoform type M2 (PKM2) is one of four isoenzymes implicated in the glycolysis pathway, with widely different kinetic and regulatory characteristics [162, 163, 164]. The three other isoforms are type M1, type L and type R. PKM2 arises from alternate splicing of *Pkm* (formerly known *Pkm2*) pre-mRNA leading to the inclusion of exon 10 (PKM2) and the exclusion of exon 9 (PKM1) mediated by polypyrimidine-tract binding protein (PTB) and hnRNPA1/2 splicing factors. Isoforms L and R are encoded by the *Pkl/r* gene and are the isoforms found in liver and kidney respectively [165, 166].

PKM2 is expressed in differentiated tissues, such as lung, fat tissue, retina, pancreas, as well as in all cells with a high proliferation rate, including normal proliferating cells, embryonic and adult stem cells and tumor cells.

2.4.1 PKM2 in the cytoplasm

PKM2 is an enzyme that catalyzes the conversion of phosphoenolpyruvate (PEP) to pyruvate in the glycolysis pathway. It has been demonstrated that PKM2 interacts with

tyrosine phosphopeptides and this interaction affects the pyruvate kinase activity of PKM2 [164, 168].

PKM2 occurs in a tetrameric as wells as a dimeric form. The tetramer has a high affinity to PEP and thus, favors the degradation of glucose and lactate with regeneration of energy. The dimeric form is characterized by a low PEP affinity and is nearly inactive, leading to an increase in phosphometabolites and a channeling of glucose towards the synthesis of DNA, phospholipids, and amino acids. Tumor cells have been found to contain high levels of the dimeric form (termed tumor PKM2) which is essential for the Warburg effect. It was found that replacing PKM2 with the more active PKM1 isozyme in human lung cancer cells fails to support the Warburg effect and inhibits tumor formation. However, the mechanisms underlying the distinct role of PKM2 and PKM1 in the Warburg effect remain unclear [162, 169, 170].

2.4.2 PKM2 in the nucleus

In addition to its well-established role in aerobic glycolysis, PKM2 directly regulates gene transcription [171, 172]. However, until now, there is little evidence for the mechanism that underlies this function. Both proliferative and pro-apoptotic signals have been described to induce the translocation of PKM2 in the nucleus.

Among these, IL-3-induced nuclear translocation stimulated cell proliferation, whereas TT-232, H_2O_2 or UV radiation resulted in caspase-independent programmed cell death [174, 175, 176, 177].

Within the nucleus, PKM2 has been found to play several different roles. It interacts directly with the HIF-1a subunit to promote transactivation of HIF-1 targets and it binds OCT4, facilitating the transcription factor [178, 179]. In addition, it has been described to bind β-catenin and act as a transcription co-activator, upon phosphorylation by EGFR-activated ERK2 [180].

Interestingly, PKM2 has been found to participate in the phosphorylation of histone H1 by direct phosphate transfer from PEP [181] and phosphorylate histone H3 at T11 upon EGF receptor activation, which results in HDAC3 dissociation from the *cyclin d1* (*Ccnd1*)

and the *c-myc* promoters [173]. The role of PKM2 as a protein kinase, besides histone modification, is also portrayed by the finding that nuclear PKM2, using PEP as a phosphate donor, catalyzes the tyrosine phosphorylation of the STAT3 transcription factor, leading to expression of STAT3 target genes, such as *Mek5* [171].

2.5 T-helper-inducing POZ-Krüppel-like factor (ThPOK)

During T cell development, $CD4^+CD8^+$ double-positive (DP) thymocytes give rise to two cell subsets with distinct functionalities, helper and cytotoxic T cells. The mechanism underlying the lineage decision still remains a major issue in immunology. The process of lineage decision involves several steps and results in loss of cell plasticity and commitment to one cell subset.

It has been shown that ThPOK has an antagonistic role compared to Runx transcription factor complexes and plays an essential role in the decision process of alternate fates.

ThPOK has been described to bind and repress the *CD4* silencer, permitting CD4 expression. At the same time, it binds the silencer on its own locus, stabilizing its own expression in a positive feedforward loop [182, 183, 184].

Recently, Matharu *et al.* reported the identification of ThPOK (also known as c-Krox) as the vertebrate homolog of the Drosophila GAGA factor, on the basis of sequence similarity and comparative structural analysis.

Their *in silico* analysis of ThPOK's DNA binding domain showed preferential interaction of ThPOK with GAGA sequences, also confirmed *in vivo* and a high conservation and similarity with Drosophila GAF [185].

2.6 Long non-coding RNAs (lncRNAs)

Much of the non-coding genome of complex organisms is now known to produce RNA molecules in varying sizes and functions. An abundance of these are long transcripts (>200 nt) and serve a wide range of roles in developmental and disease processes, from gene

regulation to pluripotency and cancer. Besides the sensory, guiding and allosteric capacities, they have been also reported to have epigenetic and scaffolding roles, in combination with chromatin-modifying proteins or transcription factors [186, 187].

Examples of such roles include the *Xist*, *HOTAIR* and *ANRIL* lncRNAs, which target members of the polycomb repressive complexes (PRC1 and PRC2), epigenetic factors and DNA methyltransferases, thus acting as scaffolds [188, 189]. Due to their length and sequence specificity, lncRNAs are suited to act allele-specifically *in cis* or *in trans*, as guides for protein factors to their expressing loci. This is also facilitated by the RNA-DNA hybrids with chromatin that are formed during their expression. In the case of the *cis*-acting *HOTTIP* RNA, it was found that the transcript can act as a bridge between the MLL complex and the promoters at the *HOXA* cluster [190, 191], while *NRON* ncRNA regulates the nuclear trafficking of NFAT [192]. *NEAT1* (*MEN3/b* in mouse), on the other hand, is an abundant polyadenylated ncRNA that is an integral component of nuclear paraspeckles, which besides acting as structural element, seems to also govern the nuclear export of mRNAs [193, 194].

Taking into consideration the wide variety of examples of function, their functional potential, along with the abundance of lncRNAs, it is evident that lncRNAs play a major role in gene regulation and the regulation of epigenetic events.

3. OBJECTIVES

In correspondence to the model of transvection, an epigenetic phenomenon which involves interaction events between enhancers or silencers on one allele with a promoter on the homologous allele, we investigated the existence of somatic homologous pairing in mammals. Although somatic homologous pairing is common in Drosophila it is not generally observed in mammalian cells. However, a number of regions have recently been shown to come into close proximity with their homologous allele, and it has been proposed that pairing might be involved in the establishment or maintenance of allelic expression.

Here, we focus on the identification of factors – proteins or RNA molecules – capable of mediating such phenomena, in order to ultimately uncover a mechanism for the regulation of gene expression that could be used in the future to study and possibly resolve the deregulation of gene expression in disease models. Specifically, we studied the sub-nuclear interacting events that mediate *Tnfα* gene regulation in murine macrophages and we investigated the mechanisms involved in the maintenance of *Tnfα* mRNA levels. We further examined the allelic pattern of *Tnfα* expression and the molecules – protein and RNA – that mediate/regulate the allelic interaction and expression.

4. MATERIALS AND METHODS

4.1 Cell culture and media

The murine monocyte-derived macrophage cell line, Raw 264.7, was cultured under 5% CO_2 at 37°C, in Dulbecco's Modified Eagle's Medium (ATCC, Cat No.30-2002 or GIBCO, Cat.No.41966) supplemented with 10% fetal bovine serum (Biosera, FB1001/500), penicillin and streptomycin (Sigma, P4333 or Biosera LM, A4118) at 5μg/mL each.
The mouse embryonic stem cell line, CGR8, was cultured under 5% CO_2 at 37°C, in Dulbecco's Modified Eagle's Medium supplemented with 10% fetal bovine serum, penicillin and streptomycin at 5μg/mL each.
The human acute monocytic leukemia cell line, THP-1, was cultured under 5% CO_2 at 37°C, in Dulbecco's Modified Eagle's Medium supplemented with 10% fetal bovine serum, penicillin and streptomycin at 5μg/mL each.

4.2 Cell treatments

Cell line macrophages were stimulated with 50ng/ml LPS (EB Ultrapure, Invivogen, O111:B4), or 10ng/ml TNFα (r.mTNFα, R&D Systems, Cat No.410-MT), for 0h (untreated), 10min, 20min, 30min, 1h, 2h, 3h, 6h, 12h and 24h.

THP-1 monocytes were differentiated into macrophages with phorbol 12-myristate 13-acetate (PMA, Sigma, P1585) at a concentration of 50ng/ml for 24h, and then washed with 1xPBS and stimulated with 50ng/ml LPS for 0h (untreated), 10min, 20min, 30min, 1h, 2h, 3h, 6h, 12h and 24h.

Actin polymerization was blocked with pretreatment of the cells with 10μM Latrunculin A

(LTA, Sigma, L5163) for 1h before LPS stimulation.

PKM2 and ThPOK mRNAs were knocked down with the use of 5nM siRNAs (*Silencer*® Select siRNAs, Ambion, Applied Biosystems), which were incubated firstly with siPORT *NeoFX* Transfection Agent (Ambion, Applied Biosystems, AM4510) in OPTI-MEM medium (GIBCO Cat No.31985-062) for 10min to create lipid-based complexes and then introduced to the cells ($3x10^4$ cells/24-well) for 48h (for mRNA detection) or 72h (for protein detection experiments) at 37ºC.
The siRNAs used were: PKM2 – s71680
ThPOK – s76338
Scrambled oligo – *Silencer*® Select Negative control #1 Cat. No. 4390843

Knock-down of the *LT/TNF* locus long transcripts was achieved with the use of two Locked Nucleic Acid (LNA) oligos (HPLC, Exiqon, Product No. 500150):
LNA oligo #1: 5'-GTCTTTATGCTTCCTGTTG-3'
LNA oligo #9: 5'-ATGTATTGAGGTGGGTGGA-3'
Negative control: 5'-GTGTAACACGTCTATACGCCCA-3' (5-FAM/ miRCURY LNA Inhibitor Control, Exiqon, Product No. 199004-04)
The transfection of Raw 264.7 macrophages was performed with Lipofectamine 2000 (Invitrogen, 11668-019).

4.3 Antibodies

Rabbit anti-mouse ThPOK: Abcam, ab20985
Rabbit anti-mouse PKM2 (D78A4) XP: Cell Signaling, Cat.No.4053
Mouse anti-mouse NPM (FC82291) monoclonal: Abcam, ab10530
Goat anti-mouse IgG, HRP-conjugated: Jackson IR Laboratories, Cat.No.115-035-146
Goat anti-rabbit IgG, HRP-conjugated: Jackson IR Laboratories, Cat.No.111-035-003
Goat anti-rabbit IgG, 488: Alexa Fluor, Molecular probes, A11008
Goat anti-rabbit IgG, 594: Alexa Fluor, Molecular probes, A11012

Goat anti-rabbit IgG, 647: Alexa Fluor, Molecular probes, A21244
Donkey anti-mouse IgG, 488: Alexa Fluor, Molecular probes, A21202
Goat anti-mouse IgG, 594: Alexa Fluor, Molecular probes, A11005
Goat anti-mouse IgG, 647: Alexa Fluor, Molecular probes, A21235
Streptavidin-conjugate, 488: Alexa Fluor, Molecular probes, S11223
Streptavidin-conjugate, 594: Alexa Fluor, Molecular probes, S11227

4.4 DH5α competent cells

DH5α cells were grown in Psi broth (LB medium - 1% Bacto tryptone, 0,5% yeast extract, 1% NaCl, 4mM $MgSO_4$, 10mM KCl) at 37^{o}C until an OD_{550}=0.4-0.5. They were then centrifuged at 2000rpm for 10min and the pellet was resuspended in TFB-I solution (30mM potassium acetate, 100mM RbCl, 10mM $CaCl_2$, 50mM $MnCl_2$, 15% glycerol, pH5.8). After a 5min incubation on ice, they were centrifuged and resuspended in TFB-II solution (10mM MOPS, 75mM $CaCl_2$, 10mM RbCl, 15% glycerol, pH6.5) for 15min on ice. Cells were then aliquoted, fast frozen and kept at -80^{o}C, ready for transformation.

4.5 cDNA cloning

DNA digestion was performed with restriction endonucleases provided by Minotech *biotechnology* at conditions described in their catalog depending on the enzyme.
The pCR® 2.1 plasmid vector (TA cloning® kit, Invitrogen, K2020-20) was used, according to the manufacturer's instructions. Ligations were performed using T4 DNA ligase (Minotech *biotechnology*) at 16^{o}C for 2h.
Sequencing reactions were performed using the T7 promoter primer on pCR® 2.1, by the Microchemistry Laboratory of IMBB-FORTH.

DH5α competent cells were transformed by incubating them with half the ligation reaction for 30min on ice, heat-shocked at 42^{o}C for 90sec and moved straight back on ice. After a recovery period of 1h at 37^{o}C with LB medium, the cells were plated on Petri dishes with LB/agar media (LB medium plus 1.5% agar) supplemented with the appropriate antibiotic

and incubated for at least 16h at 37^{o}C.

4.6 Plasmid and BAC DNA extraction

Bacterial cells containing either plasmid vectors or Bacterial Artificial Chromosomes (BACs) were grown overnight at 37^{o}C. The cells were then pelleted at 3000rpm for 15min at 4^{o}C and resuspended by vortexing in Solution 1 (50mM glucose, 10mM EDTA, 25mM Tris, pH8.0) supplemented with 100-400μg/ml RNase A (Qiagen, Cat. No. 19101). An equal volume of Solution 2 (0.2N NaOH, 1% SDS) was then added to lyse the cells for <5min and it was subsequently neutralized with Solution 3 (3M KOAc, pH6.0) for 5min on ice. After centrifugation at 3000rpm for 30min at 4^{o}C the mix was filtered over Whatman filter paper and the DNA was precipitated with 0.7 volumes of isopropanol and subsequent centrifugation at 3000rpm for 45min, at 4^{o}C.
If high quality DNA was needed, an extra step of P-PCI-C (Phenol – Phenol:Chloroform:Isoamyl Alcohol/25:24:1 – Chloroform) purification was used. DNA was precipitated with 1/10V sodium acetate and 2V ethanol.

4.7 Total RNA isolation

Cells were seeded in 6well plates and left overnight to settle. Then they were rinsed and stimulated with LPS before harvesting.
The cell monolayer was rinsed with 1xPBS and 1ml TRIzol Reagent (Ambion, Cat.No.15596-026) per 10cm^{2} of cultured dish area was used to lyse them. The cell lysate was scraped from the dish and incubated at room temperature for 5min. Then, 0.2ml chloroform was added, the lysate was vortexed and centrifuged at 14000rpm for 15min at 4^{o}C. The RNA-containing supernatant was isolated and the RNA was precipitated with the use of 0.5ml of isopropyl alcohol per 1 ml of TRIzol Reagent used for the initial homogenization. After centrifugation at 14000rpm for 20min at 4^{o}C, the RNA precipitate was dissolved in DEPC-treated water (Ambion, AM9916). Sample concentration and purity was determined with spectrophotometric analysis, measuring the OD at 260nm in a Spectrophotometer (ND-1000, NanoDrop), taking into account that 1 OD at 260nm equals

40μg /ml RNA.

4.8 Reverse transcription - cDNA synthesis

2μg of total RNA was incubated with Oligo-dT primers in a 20μl reaction volume. After 5min at 70^{o}C for the denaturation of secondary structures, 2μl of 10x M-MuLV buffer, 1μl of 10mM dNTPs, 0.5μl M-MuLV Reverse Trascriptase (Finnzymes, Thermo, F572S) and 1μl of RNase inhibitor (Human placental ribonuclease inhibitor, HT biotechnology Ltd, RI01a) were added and incubated at 42^{o}C for 90min. The samples were kept at -20^{o}C until use.

For quantitative mRNA expression analysis, 10% of the synthesized cDNA was used, in a 20μl PCR reaction, using the SYBR Green PCR Master mix (Applied Biosystems, Cat.No.4309155) according to the manufacturer's instructions. qPCR was performed in an Opticon 2 DNA Engine (MJ Research) using a standard curve and the results were normalized over *Hprt1* mRNA expression.

The data analysis was performed with the use of the Opticon Monitor software.

The primers used for mRNA quantitation were:

TNFα.F: 5'-GAAGAGCGTGGTGGCCC-3'

TNFα.R: 5'-CTCCAGGCGGTGCCTATGT-3'

HPRT1.F: 5'-GTCCCAGCGTCGTGATTAGC-3'

HPRT1.R: 5'-TTCCAAATCCTCGGCATAATG-3'

PKM2.F: 5'-TGGACGATGGGCTCATCTCACTGC-3'

PKM2.R: 5'-TTCTTGCTGCCCAAGGAGCCAC-3'

ThPOK.F: 5'-CCTGTGAGGTCTGCGGCGTCC-3'

ThPOK.R: 5'-GGGCGTTCTCCTGTGTGCTTCC-3'

4.9 DNA FISH

Murine Bacterial Artificial Chromosome clones (BACs, BACPAC Resources Centre, CHORI)

LT/TNF locus (chr.17): RP23-446-C22

E4f1 (chr.17): RP24-162018

P2rx4 (chr.5): RP24-228I1

Arrb1 (chr.7): RP23-102I6

Probe preparation

DNA FISH probes were constructed with the use of the Nick Translation kit (Roche, Applied Science, Cat.No.11 745 808 910) supplemented with Spectrum Orange/Green dUTP (Abbott Molecular, 02N33-050/02N32-050), or Far Red dCTP (Chromatide AlexaFluor 647-12-OBEA-dCTP, Molecular Probes, C21559). The reaction was prepared with 1-3μg BAC DNA in a final volume of 20μl according to the manufacturers' instructions. The DNase I/DNA Polymerase I reaction was stopped when the DNA size was within the 300-700bp range.

The probe was then purified through a QIAquick PCR purification column (QIAGEN, Cat.No.28104 or Invitrogen, Purelink PCR purification kit, K31001) following the manual's procedure. Briefly, the appropriate binding buffer with isopropanol was mixed with the DNA, it was loaded on the column, provided by the kit and centrifuged at 10000xg for 1 min. The flow-through was discarded and the column was washed with a wash buffer containing ethanol. After two steps of centrifugation at 10000xg for 1 and 2min respectively, the dry column was incubated with H_2O for 1min at RT, the DNA (probe) was then eluted with centrifugation at 10000xg for 2min, in a dark-colored eppendorf tube and stored at -20^{o}C.

Cell preparation

Cells were seeded on sterile glass coverslips (300-400x10^3cells/coverslip depending on cell size), were allowed to adhere for at least 2h and were then stimulated with LPS (50ng/ml) or TNFα (10ng/ml) in a time course.

Cells were then washed with ice-cold 1x PBS and fixed with 4% PFA (paraformaldehyde 16% aqueous solution, EM Grade, Electron Microscopy Sciences, Cat.No.30525-89-4) in 1x PBS for 12min. After 3x5min washes with 1x PBS, the cells were permeabilized with 0.5% Triton X-100 in 1x PBS for 10min and incubated in 20% glycerol in 1x PBS. After

three freeze-thaw cycles in liquid nitrogen, the cells were washed in 1xPBS and incubated in freshly prepared 0,1N HCl for 5min. The cells were finally rinsed in 2xSSC (for 20xSSC: 3M $NaCl_2$, 0,3M Sodium citrate) and stored in 70% ethanol at 4^{o}C.

Hybridization

Probe: 100ng from each probe and 1μg mouse COT-1 DNA (Invitrogen, Cat.No.18440-016) were placed in a dark-colored eppendorf tube and lyophilized under vacuum. The pellet was resuspended in 5μl pre-warmed de-ionized formamide (Ambion, AM9342) and reconstituted for 30min at 37^{o}C. DNA was then denatured for 10min at 95^{o}C and the probes were kept on ice until used for hybridization. 5μl 2x hybridization buffer (4xSSC, 20% Dextran sulfate, 50mM Sodium Phosphate) were added in the probe mix.

Cells: The cells were dehydrated with 4 consecutive washes of increasing ethanol concentration (70%, 80%, 95%, 100% - 3min each). The coverslips were dried on a heating block and then placed in a plate with fresh denaturation buffer (70% de-ionized formamide, 2xSSC, pH7, pre-warmed at 73^{o}C) and incubated at 73^{o}C for 5min. The cells were then incubated in ice-cold 70% ethanol for 3min on ice and washed again in 80%, 95% and 100% ethanol for 3min.

The probe was placed on a glass microscope slide and the coverslip with the cells was flipped on top and sealed with rubber cement. When the paper cement dried (15-30min at room temperature) the slide was placed on a block heated at 73^{o}C for 5min and then incubated at 37^{o}C in a humidified hybridization chamber.

After 12-16h, the coverslips were washed with 2xSSC and, when needed, the nucleus was counterstained with ToPro3 in 1:8000 dilution in 2xSSC (ToPro3 Iodide 642/661, Molecular Probes, T3605) for 1,5min at room temperature. The coverslips were rinsed in 1xPBS, allowed to air-dry and mounted in ProLong Gold antifade reagent supplemented with DAPI (Invitrogen, Molecular Probes, P-36931), for 5-10h before they were visualized with the use of a Zeiss confocal microscope.

4.10 RNA-DNA FISH

4.10.1 Directly-labeled probe preparation

RNA FISH probes were constructed following the same procedure as for DNA FISH probes with the use of the cDNA from the desired gene cloned in the pCR® 2.1 plasmid vector.

Cell preparation

For RNA-DNA FISH, after the cells were washed with ice-cold 1xPBS they were incubated in Cytoskeletal buffer (CSK buffer: 100mM NaCl, 300mM Sucrose, 3mM $MgCl_2$, 10mM PIPES, 0.5% Triton X-100, 1mM EGTA, 2mM Vanadyl Ribonucleoside Complex) for 5min on ice. Then they were fixed with 4% PFA/1x PBS for 10min, washed 3x5min with 70% ethanol and stored at -20ºC.

For RNase A treatment the cells were incubated with 100μg/ml RNase A for 30min.

Hybridization

Probe: 100ng from each cDNA probe and 1μg mouse COT-1 DNA along with 20μg yeast tRNA (Ribonucleic acid, transfer from baker's yeast, SIGMA, R5636) were placed in a dark-colored eppendorf tube and lyophilized. The pellet was resuspended in 5μl pre-warmed de-ionized formamide and reconstituted for 20min at 37ºC. DNA was then denatured for 10min at 95ºC and 5μl 2x fresh hybridization mix (4xSSC, 2mg/ml BSA, 20mM Vanadyl Ribonucleoside Complex, 20% Dextran sulphate) were added. The probes were kept on ice until hybridization.

Cells: The cells were dehydrated with 4 consecutive washes of increasing ethanol concentration (70%, 80%, 95%, 100% - 3min each).

The probe was then placed on a glass microscope slide and the coverslip with the cells was put on top and sealed with rubber cement. When the paper cement dried (15-30min at room temperature) the slide was placed on a block heated at 73ºC for 5min and then incubated at 37ºC for 16h (overnight) in a humidified hybridization chamber.

Next day the coverslips were washed with 2xSSC and when needed, the nucleus was counterstained with ToPro3 (1:8000 dilution from 1mM stock, in 2xSSC) for 1min at room temperature. The coverslips were allowed to air-dry and were mounted in ProLong Gold antifade reagent with DAPI (Invitrogen).

4.10.2 Indirectly-labeled probe preparation

Biotinylated probes were generated using the Biotin-Nick Translation mix (Roche, Applied Science, Cat.No. 11 745 824 910) according to the manufacturer's instructions.
The cells were prepared as for the direct RNA-DNA FISH assays and hybridized with biotinylated cDNA probes. The Tyramide Signal Amplification System (TSA^{TM} Biotin System, Perkin Elmer, NEL700A001KT) was used to amplify the RNA signals and streptavidin-conjugated fluorophores were used for detection.
Briefly, after hybridization, the coverslips were washed with 2xSSC in 50% formamide, 2xSSC, 1xSSC and 4xSSC, then blocked with TNB buffer (0.1M Tris pH7.5, 0.15M NaCl, 0.5% blocking reagent) for 30min and incubated with Streptavidin-HRP (1/200 in TNB) for 30min at RT. After 3 washes with TNT buffer (0.1M Tris pH7.5, 0.15M NaCl, 0.05% Tween-20), the coverslips were incubated with biotinyl-tyramide (1/50 in amplification buffer) for 10min, washed with TNT buffer and stained with Streptavidin-488 in TNB for 30min. If needed, the cells were then counter-stained with ToPro3 dilluted in TNT buffer and mounted in ProLong Gold antifade reagent with DAPI.

4.10.3 Riboprobes

RNA probes were used for the allele-specific hybridization experiments of the LT/TNF locus long RNA transcripts. Probes were prepared with *in vitro* transcription of PCR products spanning the T7 promoter on the 5'end. The PCR products specific for each long RNA transcript were amplified with the following primers:
lncRNA#1.F: 5'-GAGAGCCACCAACAAAGTTTAC-3'
lncRNA#1.R: 5'-TCTCCATCATCCCCTTATGCACC'3'
lncRNA#9.F: 5'-TATTGGTGTTGGGATCAAATC-3'
lncRNA#9.R: 5'-GCTCTGCCTTTCGGTCAC-3'

The lncRNA#1 and #9 riboprobes (920 and 340bp respectively) were prepared with the Biotin RNA labeling mix (Roche, Cat. No. 11685597910) and were then precipitated with LiCl.

The cells were prepared as for the direct RNA-DNA FISH experiments and hybridized with the riboprobes. The Tyramide Signal Amplification System (TSA^{TM} Biotin System, Perkin Elmer, NEL700A001KT) was used to amplify the RNA signals.
Briefly, after hybridization, the coverslips were washed with 2xSSC in 50% formamide, 2xSSC, 1xSSC, 0.5xSSC, 0.2xSSC and 0.1xSSC, the blocked with TNB buffer for 30min and incubated with Streptavidin-HRP (1/200 in TNB) for 30min at RT. After 3 washes with TNT buffer, the coverslips were incubated with biotinyl-tyramide (1/50 in amplification buffer) for 8min, washed with TNT and stained with Streptavidin-488 (1/400 in TNB) for 30min. The cells were then counter-stained with ToPro3 diluted in TNT and mounted in ProLong Gold antifade reagent with DAPI.

4.11 Immuno-DNA FISH

The probes were prepared as for the DNA FISH assay and the cells as for the RNA-DNA FISH assays. The hybridization was performed as for the RNA FISH protocol.
After hybridization, the coverslips were washed consecutively with 2xSSC for 5min, 2xSSC pre-warmed at 42^{o}C for 5min and 2xSSC for 5min at room temperature. The cells were then incubated in blocking buffer (4xSSC, 0.1% Tween-20, 4mg/ml BSA) for 30min in a humidified hybridization chamber pre-warmed at 37^{o}C. Incubation with the primary antibody (1:500 in detection buffer: 4xSSC, 0.1% Tween, 1mg/ml BSA) followed, in a humidified hybridization chamber and after 1h the cells were washed 3x2min with 0.1% Tween-20 in 4xSSC, pre-warmed at 37^{o}C. After incubation with the secondary fluorescent antibody (diluted 1:500 in detection buffer) for 30min in a humidified hybridization chamber, the cells were washed again 2x2min with 0.1% Tween-20 in 4xSSC, pre-warmed at 37^{o}C, counterstained with ToPro3 in 2xSSC for 1min and finally washed in 2xSSC for 3min. The coverslips were rinsed in 1xPBS, allowed to air-dry and mounted in ProLong Gold anti-fade reagent with DAPI.

4.12 Whole cell and nuclear protein extracts

LPS-stimulated macrophages were washed in ice-cold 1xPBS and harvested by scraping and centrifuged at 1200rpm for 5min.

Whole cell extracts were prepared by incubating the cell pellet with EBC buffer (150mM NaCl, 50mM Tris pH7.5, 5% glycerol, 1% NP-40, 1mM $MgCl_2$, 10mM NaF, 1mM sodium orthovanadate) for 30min on ice. The lysate was centrifuged at 14000rpm for 10min and protein concentration was measured with the Bradford assay.

For nuclear extracts the pellet was resuspended in 5 pellet-volumes Buffer A (10mM Hepes pH7.9, 1.5mM $MgCl_2$, 10mM KCl, 5mM NaF, 1mM DTT, 1mM PMSF) and incubated on ice for 10min. 0.1% NP-40 was added and after <5min on ice, the cells were vortexed for no more than 10sec and centrifuged at 4000rpm, for 1,5min at 4^{o}C. The pellet (nuclei) was washed twice with Buffer A and after gentle resuspension by hand, Buffer C (20mM Hepes pH7.9, 25% glycerol, 420mM NaCl, 1.5mM $MgCl_2$, 0.2mM EDTA, 1mM DTT, 1mM PMSF and 5mM NaF) was added while flicking. The extracted nuclei were incubated on ice for 30min and then centrifuged at 14000rpm for 15min at 4^{o}C.

For DNA affinity chromatography, the extracts were also dialyzed twice against at least 50 volumes of the DNA binding buffer with stirring for 2h at 4^{o}C. The samples were snap frozen in liquid nitrogen and kept at -80^{o}C until use.

4.13 Electrophoretic Mobility Shift Assay (EMSA)

The oligonucleotide sequences that were used to create double stranded oligonucleotides were as follows:

GA repeat: 5'-GAGAGAGAGAGAGAGAGAGAGAGAG-3'

GA single: 5'- GGTGGTGCATGAGAGGCCCACAGTC-3'

GA mutant: 5'- GGTGGTGCATACACAGCCCACAGTC -3'

200ng of double-stranded oligonucleotides (Microchemistry laboratory, IMBB, FORTH) were end-labeled with T4 polynucleotide kinase (New England Biolabs) and [γ-^{32}P] ATP for 45min at 37^{o}C and then purified with a G-50 column.

The binding reactions were carried out in a binding buffer (80mM KCl, 10mM Hepes pH7.9, 5mM $MgCl_2$, 10% glycerol, 0.1% NP-40, 50μM $ZnCl_2$, 1mM DTT, 1mM PMSF) containing 3μg macrophage nuclear extracts and radio-labeled oligonucleotides (60-100x10^3cpm). After 20min incubation on ice the reactions were analyzed in a 6% polyacrylamide gel (39:1) and electrophoresed at 120-150V. The gel was dried for 1h at 72^{o}C under vacuum and exposed either on a film or on a PhosphoImager screen.

4.14 SouthWestern blotting (SW)

Protein samples were separated on a 10% SDS-PAGE acrylamide gel and transferred on a nitrocellulose membrane (Protran, Whatman) overnight (~16h) at 50mA (21-25V) or 1.5h at 200-300mA at 4^{o}C. The membrane was placed in a glass box with 25ml Blocking/Renaturation buffer (25mM Hepes pH7.5, 50mM KCl, 6.25mM $MgCl_2$, 10% glycerol, 0.1% NP-40, 1mM DTT and 1mM PMSF) with rocking for 10min at room temperature and then another 25ml Blocking/Renaturation buffer were added, this time with 3% non-fat milk and was left rocking for ~8h (the buffer was replaced every 2h). The membrane was then washed with 25ml Binding/Wash buffer (12.5mM Hepes pH7.5, 50mM KCl, 6.25mM $MgCl_2$, 10% glycerol, 0.05% NP-40, 1mM DTT and 1mM PMSF) for 5min and stored at 4^{o}C until hybridization.

The membrane was sealed in a plastic bag with hybridization buffer containing ~20x10^6 cpm radio-labeled oligonucleotide and 60μg Salmon Sperm DNA in 3ml Binding/Wash buffer and left rotating 16h at room temperature. The next day the membrane was washed 3-4 times with Binding/Wash buffer for 15min each and exposed on a film.

4.15 DNA affinity chromatography

Binding of biotinylated oligonucleotide on beads:

A 30bp biotinylated oligonucleotide was bound on washed beads (200ng/sample biotinylated oligonucleotide with 20μl/sample beads in 1x Beads-Binding buffer) for >10min according to the manufacturer's protocol (Dynabeads M-280 Streptavidin, Invitrogen, Cat.No.112.05D).

Pre-clearing of Nuclear Extracts (NEs) with beads:

100μg/sample of NEs were incubated with 100ng/μl poly(dI:dC) in 1x Biotin-Binding buffer (80mM KCl, 10mM Hepes pH7.9, 5mM $MgCl_2$, 10% Glycerol, 50μM $ZnCl_2$, 0.05% NP-40, 1mM DTT, 1mM PMSF, 5mM NaF) for 10min on ice. 20μl beads were added per sample and left rotating for 1h at 4ºC.

Binding of NEs to biotinylated-oligonucleotides:

Either beads-bound to oligonucleotide or beads only were added to the extracts and incubated under rotation for 20min at room temperature. The beads were washed (Wash buffer: 80mM KCl, 20mM Hepes pH7.9, 5mM $MgCl_2$, 50μM $ZnCl_2$, 0.05% NP-40, 1mM DTT, 1mM PMSF, 5mM NaF) for 3x3min at room temperature, with the first wash containing 100ng/μl poly(dI:dC).

The samples were then denatured in 1x Protein loading buffer for 10min at 95ºC, loaded on a 10% SDS-PAGE gel and electrophoresed at 100V. The gel was visualized with silver staining.

For the isolation of DNA binding proteins for subsequent Mass Spectrometric analysis, the Yaneva and Tempst protocol for "Isolation and Mass Spectrometry of Specific DNA Binding Proteins" was followed [195].

Untreated and stimulated (50ng/ml LPS for 30min) Raw 264.7 murine macrophages ($2x10^9$ cells/condition), were lysed in 10mM Tris-HCl pH8.0, 10mM NaCl, 8mM $MgCl_2$, homogenized with a Dounce pestle B in hypotonic buffer (20mM Tris-HCl pH7.5, 20mM KCl, 1.5mM $MgCl_2$, 0.2mM EDTA, 25% glycerol) and nuclear extracts were prepared in a high salt buffer (20mM Tris-HCl pH7.5, 1.2M KCl, 1.5mM $MgCl_2$, 0.2mM EDTA, 25% glycerol) and dialyzed against 20mM HEPES-KOH pH7.9, 0.2 mM EDTA, 0.5 mM DTT, 0.01% NP-40, 10% glycerol, 0.75-1M NaCl.

P11 fractionation

To avoid binding of non-specific DNA binding proteins to "specific" DNA beads the extracts were fractionated in a P11 phosphocellulose column with 0.1M, 0.3M, 0.5M and

0.85M NaCl stepwise elution and the presence of the desired DNA binding activity was analysed by EMSA as described above.

Concatamerization of DNA bait oligonucleotides

Multimers of DNA binding sites were generated by a self-priming PCR method using two direct repeats of complementary single-stranded oligonucleotides. The oligonucleotides used were the biotinylated 30nt GA repeat (see EMSA) and its complementary 30nt CT repeat. 460ng of each oligonucleotide were used in a PCR reaction, which produced double-stranded GA/CT repeat concatamers of 5-10kb in length.

The nuclear extracts were then incubated with 1mg concatamerized DNA bound to magnetic M280 streptavidin beads, in the presence of the competitor DNA oligo(dI:dC) and poly(dI:dC) at 0.1 mg/mL each.

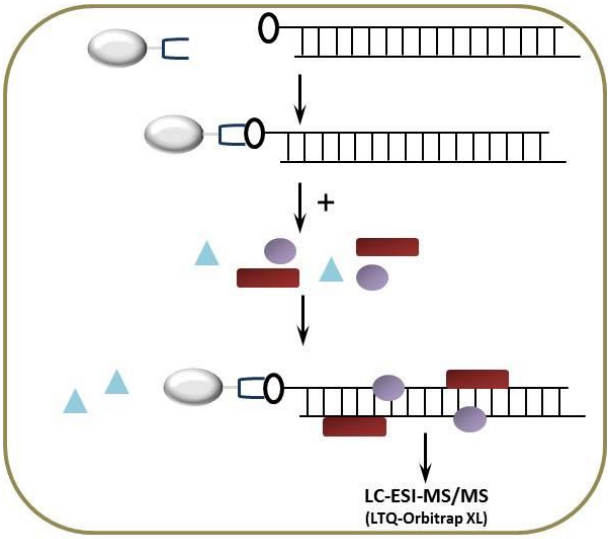

4.16 Protein detection and Mass Spectrometry

Protein samples were separated on 8-10% polyacrylamide gels and either stained by Coomassie G250 Colloidal blue (Fluka, Cat No.27815) or transferred to nitrocellulose membranes, silver stained or blotted with specific antibodies.

For the Coomassie staining the gel was fixed in 30% methanol, 10% acetic acid for 30min,

washed with distilled water and incubated in 0.12% dye, 10% ammonium sulphate, 10% phosphoric acid, 20% methanol.

For the silver staining, the membrane was fixed in 50% methanol, 5% acetic acid for 20min, washed with 50% methanol for 10min, sensitized with 0.02% sodium thiosulfate and stained with 0.1% silver nitrate for 20min at 4^{o}C. The nitrate was then developed in 0.04% formalin, 2% sodium carbonate with intensive shaking and terminated with 5% acetic acid.

For Western blotting, membranes were blocked for 30min with 5% non-fat milk in 1xTBS-Tween20, incubated with a protein-specific antibody in 1% non-fat milk in 1xTBS-Tween20 for 1h, washed 3 times with 1xTBS-Tween20 and incubated with an HRP-conjugated antibody in 1% non-fat milk in 1xTBS-Tween20 for 45min. Pierce ECL Western Blotting Substrate (Thermo Scientific, Cat.No.32106) was used to detect the antibodies either by exposing on film or with the use of the LAS-3000 Imaging System.

For protein identification and characterization, Coomassie-stained gel bands were destained, reduced, alkylated and digested with trypsin (Proteomics grade, Sigma, T6567). Eluted protein peptides were analysed with an LC-ESI-MS/MS method (LTQ-Orbitrap XL, Thermo Scientific).

4.17 Yeast One Hybrid Screening Library

The Matchmaker One-Hybrid System (Clontech laboratories, Inc, Cat.No.630304) was used according to the manufacturer's protocol. Briefly, a GA-repeat DNA sequence was cloned upstream of the His3 reporter in pHIS2.1 and a high-complexity cDNA library, which expressed fusions of nuclear proteins from Raw 264.7 upon LPS-induction, with the Gal4 AD. After co-transformation of competent yeast cells with the cDNA library, as well as the pHIS-GA plasmid, expression from the HIS3 reporter was detected only in colonies that were able to grow on minimal medium that lacks histidine and is supplemented with 3-AT.
PCR and DNA sequencing analysis were used to identify and confirm the positive clones.

The library was constructed twice and the results were repeated and verified by PCR and DNA sequencing.

4.18 Chromatin Immunoprecipitation assay (ChIP)

A monolayer of Raw 264.7 macrophage cells were fixed with 1% formaldehyde for 10min at room temperature and the reaction was quenched with the use of glycine at a final concentration of 0.125M, for 5min. The cells were then washed, harvested and counted and then resuspended in 10ml Cell lysis buffer (5mM PIPES pH8, 85mM KCl, 0.5% NP-40, 1mM PMSF) and incubated on ice for 10min. Nuclei were pelleted and subsequently resuspended in SDS lysis buffer (1% SDS, 10mM EDTA, 50mM Tris-HCl pH8.1, 1mM PMSF, protease inhibitors – $3x10^6$/100μl buffer) and incubated for 10min on ice. The nuclei suspension was sonicated (LabsonicM Ultrasonic homogenizer, Sartorius) for 12 times of 30sec. The shearing efficiency was tested by taking 30μl of the sample, reversing the cross-linking with 200mM NaCl in SDS lysis buffer, for 4h at 65ºC. After phenol/chloroform extraction, the DNA was precipitated and electrophoresed on a 1.5% agarose gel. The soluble chromatin solution was cleared by spinning at 13000rpm for 10min, aliquoted and stored at -80ºC.

Chromatin aliquots of 100μl (about 20μg) were diluted with 900μl ChIP dilution buffer (0.01% SDS, 1.1% Triton-X100, 1.2mM EDTA, 16.7mM Tris-HCl pH8.1, 167mM NaCl supplemented with protease inhibitors) and incubated with 5μg of the desired antibody overnight at 4ºC. Protein G-coupled magnetic beads (Dynabeads Protein G, Invitrogen, Cat.No.100.03D) were used according to the manufacturer's instructions and were incubated with the Ab-chromatin complexes for 2h, with rotation at 4ºC. The immunoprecipitated complexes were washed twice with 1ml of 20mM Tris-HCl pH8.1, 1mM EDTA, 1% Triton-X100, 0.1% SDS, 0.1% Na-Deoxycholate, 0.5% PMSF (the first with 150mM NaCl and the second with 500mM NaCl) and once with 1ml of 20mM Tris-HCl pH8.1, 250mM LiCl, 1mM EDTA, 0.5% NP-40, 0.5% Na-Deoxycholate, 0.5mM PMSF. The chromatin complexes were then washed and resuspended in 1ml TE, eluted in 500μl 1% SDS with 100mM $NaHCO_3$ for 30min at room temperature and the crosslinking

was reversed by incubating the complexes with 20μl 5M NaCl overnight at 65ºC.
DNA was finally purified twice in Phenol/chloroform/isoamyl alcohol and once in chloroform and ethanol precipitated in the presence of 50μL 3M Na-acetate and 10μg glycogen as a carrier. The samples were analyzed by quantitative PCR.
The primers that were used were:
HSS-9.F: 5'-ATGGAATGTCTTCACCTTTGGT-3'
HSS-9.R: 5'-CACTGGGGTGACCTAGATAGTG-3'
HSS-1.F: 5'-TGATGACTAGGAGTCTTGTGCA-3'
HSS-1.R: 5'-AACTTGGGTAAAATCTGAGGCT-3'
TNFprom1.F: 5'-TTTATAGCCCTTGGGGAAGAGG-3'
TNFprom1.R: 5'-CCTCCACATGAGATCATGGTTT-3'
TNFprom2.F: 5'-GCTTGAGAGTTGGGAAGTGTG-3'
TNFprom2.R: 5'-AGGAGAAGGCTTGTGAGGTC-3'
HSS-8.F: 5'-CCCCAGGGCAAAGGTAATTAG-3'
HSS-8.R: 5'-CCCTACGGGTCATTGAGAGAAA-3'
P4.F: 5'-CAGAGCATTGGAAGATGATTTGG-3'
P4.R: 5'-CAGGTCTGGAAGATGATTTGG-3'
E4F1.F: 5'-GGTAACGAGCCTACCGAAGCCT-3'
E4F1.R: 5'-TGCATCTGGCCCAACGGGTTA-3'

4.19 Co-Immunoprecipitation of proteins (Co-IP)

Protein G-coupled magnetic beads (Dynabeads Protein G, Invitrogen, Cat.No.100.03D) were used according to the manufacturer's instructions and were incubated with 5μg anti-ThPOK antibody overnight at 4ºC in Binding buffer (150mM NaCl, 20mM Tris pH7.5, 1% NP-40). The beads were then washed twice with Binding buffer and once in Conjugation buffer (20mM sodium phosphate ph7.8, 150mM NaCl) and incubated with 5mM BS^3 crosslinker (Thermo Scientific, Cat.No.21585) for 30min at room temperature. The reaction was quenched with 12.5μl 1M Tris pH7.5 for 15min at room temperature with rotation.

The Ab-beads complex was washed 3 times with IP buffer and 2mg whole cell extracts, prepared from Raw 264.7 stimulated with 50ng/ml LPS for 0h and 30min, were added and left rotating for 2h at 4^{o}C. After the incubation, the samples were washed 4 times with IP buffer, denatured for 10min at 95^{o}C in 2x protein sample buffer and separated in two identical 10% polyacrylamide gels. Anti-ThPOK and anti-PKM2 were used to confirm the immunoprecipitation of ThPOK by the beads-Ab and the co-immunoprecipitation of PKM2, respectively.

4.20 DNase I Hypersensitivity mapping

Raw 264.7 murine macrophages (100x10^6 cells) were stimulated with 50ng/ml LPS for 0h and 30min, were then harvested and incubated in Lysis buffer (50mM Tris pH7.9, 50% glycerol, 100mM KCL, 5mM $MgCl_2$, 0.05% saponin, 200mM β-mercaptoethanol) for 10min on ice. After a 15min-centrifugation at 1300g at 4^{o}C, the resulting nuclei were washed once with 1,5ml buffer A and finally resuspended in 4ml Buffer A (50mM Tris pH7.9, 100mM NaCl, 3mM $MgCl_2$, 1mM DTT and 0.2mM PMSF).

Aliquots of 180μl nuclei were dispensed in a series of DNase I dilutions (initial dilution 1 kunitz unit/μl, SIGMA D5052), incubated for 20min at 37^{o}C and the reactions were terminated by adding 16.6μl 0,5M EDTA and vortexing for three cycles. Samples were then treated with 12μl RNase A (QIAGEN Cat.No.1007885) (10mg/ml in TE) for 30min at 37^{o}C and 40μl Proteinase K (MERCK Cat.No.1.24568.0100) (0.2mg/ml in 50mM Tris/100mM NaCl) were added, as well as 100μl SDS buffer (20mM Tris pH7.9, 70mM EDTA pH8, 100mM NaCl, 2% SDS) and incubated for 16h at 50^{o}C.

DNA was extracted with 3 cycles of phenol/chloroform and precipitated with ice-cold ethanol for 30min on ice and centrifugation at 1200g. Samples were resuspended in 200μl TE buffer at 55^{o}C overnight, were digested with the restriction enzyme *PstI* and then separated on a 0.8% agarose gel. DNase I hypersensitive sites were detected on Southern blots (Amersham Hybond N nylon membrane, GE Healthcare, Life Sciences) using radio-labeled probes, prepared with random priming-PCR amplification of the template with [α-

^{32}P] dCTP (Stratagene, Prime-it II Random Primer Labeling kit, Agilent Technologies, Cat.No.300385).

4.21 DNase I Footprinting

Polynucleotide Kinase T4 (PNK) was used to end-label 10pmol of primers with [γ-^{32}P] ATP in a 20μl reaction, for 45-60min at 37^{o}C. The radio-labeled oligonucleotides were purified with a G-50 column and used in a PCR reaction to produce a radio-labeled probe. The probe was then loaded on a native polyacrylamide gel (30%, acrylamide:bis-acrylamide, 29:1), which ran at 200V for 2h. The resulting band containing the radiolabeled probe was sliced and DNA was eluted overnight in a buffer containing 0.5M ammonium acetate, 0.1% SDS, 10mM magnesium acetate, purified using phenol/chloroform, ethanol precipitated and dissolved in 50μl TE buffer.

Nuclear extracts prepared from Raw 264.7 macrophages, stimulated with 50ng/ml LPS for 0h and 1h, were dialyzed over Buffer D (20mM Hepes pH7.9, 20% glycerol, 0.2mM EDTA, 0.1M KCl, 1mM DTT, 1mM PMSF, 0.1% NP-40) and used in DNase I reactions (1000-10000cpm probe, 20ng poly(dI:dC), 10μg BSA, 70mM β-mercaptoethanol, 15μg NEs/ per reaction). After incubating for 30min on ice, sequential dilutions of DNase I (initial dilution 1 kunitz unit/μl, SIGMA D5052) were added for 1-3min at RT and the reactions were terminated with 100μl Stop solution (400mM sodium acetate, 10mM EDTA, 0.2% SDS, 50μg/ml yeast tRNA). Proteinase K (10μg) and the samples were subsequently incubated at 55^{o}C for 15min. The DNA was then phenol/chloroform extracted, precipitated with ethanol and resuspended in formamide/dye mix (80% formamide, 10mM EDTA, 1mg/ml Bromophenol blue, 1mg/ml Xylene cyanol). After a 2min denaturation at 95^{o}C, the samples were loaded on a denaturing polyacrylamide gel (30%, acrylamide:bis-acrylamide, 29:1, 7M urea), along with a DNA sequencing reaction. The gel ran at 50-70W for 2h and was dried under vacuum at 80^{o}C for 1h before exposure to a film.

HSS1.F: 5’-CAGACGAAGGAAGGGTAAGC-3’

HSS1.R: 5’-GACTACTGTCAGTTCAGCCTGG-3’

HSS9.F: 5’-GATTGTGTCCGAGGAGGAGG-3’

HSS9.R: 5’-CAGTGGGCTCTTTGTTGGTTG-3’

4.22 Luciferase assays

Raw 264.7 cells were co-transfected with the pCMV-LacZ vector as well as with either the pGL3-basic vector, pGL3-basic/HSS-1 or pGL3-basic/HSS-9 constructs, using lipofectamine 2000 (Invitrogen, Cat.No.11668-019), according to the manufacturer’s instructions. The cells were stimulated with 50ng/ml LPS 24h upon plasmid transfection, they were washed, harvested and resuspended in 200μl 0.25M Tris pH7.8. After 3 sonication pulses, 20μl of the cell suspension was supplemented with 20μl luciferin (PROMEGA, E1601) and luciferase activity was measured in a Luminometer (TD-20/20, Turner Designs).

The transfection efficiency was measured by using the β-galactosidase gene expression as an internal control. The cell suspension was supplemented with *o*-nitrophenyl-β-D-galactopyranoside (ONPG, SIGMA, N1127) in lacZ buffer and β-galactosidase activity was measured at 420nm in a Photometer (DigiScan 400, ASYS HITECH GMBH).

Cloned promoter sequences were generated using the following primers:

HSS1.F-HSS1.R (see section 4.21)

HSS9.F-HSS9.R (see section 4.21)

4.23 Rapid Amplification of cDNA Ends (RACE)

The FirstChoice RLM-RACE kit (Invitrogen, AM1700M) was used to identify the 5’- and 3’-ends of specific capped mRNA molecules from Raw 264.7 macrophages treated with 50ng/ml LPS for 1hour.

Briefly, according to the manufacturer’s instructions, total RNA was treated with Calf Intestine Alkaline Phosphatase to remove free 5’-phosphate groups from the non-capped molecules. The sample was then treated with Tobacco Acid Pyrophosphatase to uncap the mRNA molecules which were then ligated to a 45nt RNA adapter with the use of T4 RNA ligase. A random-primed reverse transcription reaction followed and nested PCR amplified the 5’-end of the specific transcript, using an adapter-specific and a gene-specific nested

primer.

For the 3’ RACE, an oligo(dT)-adapter was used to synthesize the first cDNA strand from total RNA and then the gene of interest was amplified by PCR using an adapter-specific and a gene-specific primer.

5’-Race was performed using the following primers:

lncRNA#1:	#1.F: 5’-GAGAGCCACCAACAAAGTTTAC-3’
	#1Nested.F: 5’-AAAGACCCACTTACACGTTAATG-3’
lncRNA#9:	#9.R: 5’-TCACCCTCTCACCCCACTG-3’
	#9Nested.R: 5’-GTCCAAAGCACATAAGGAGTG

3’-Race was performed using the following primers:

lncRNA#1:	#9.R: 5’-TCACCCTCTCACCCCACTG-3’
	#9Nested.R: 5’-GTCCAAAGCACATAAGGAGTG-3’
	HSS2A.R: 5’-TCCTTGTGACTTTGGCTATCCAC -3’
	#2.R: 5’-AAGGCAAGCCATCGAAACTG-3’
	NP1.R: 5’-GCCAAGGTCATGAAACTCGATCA-3’
lncRNA#9:	#1.F: 5’-GAGAGCCACCAACAAAGTTTAC-3’
	#1Nested.F: 5’-AAAGACCCACTTACACGTTAATG-3’

5. RESULTS

5.1 Homologous association of the *Tnfα* alleles

In order to study the subnuclear localization of the *Tnfα* alleles, we performed DNA fluorescence *in situ* hybridization (DNA FISH) experiments in LPS-stimulated Raw 264.7 monocyte-derived, murine macrophage-like cells. Fluorescently-labeled DNA probes encompassing the *LT/TNF* locus (**Fig. 1**) were hybridized to the endogenous *LT/TNF* locus. The method used enabled us to study the allele localization in the nucleus in relation to space and to each other, in the axis of LPS-stimulation time, since it permitted the maintenance of the three-dimensional structure of the cells.

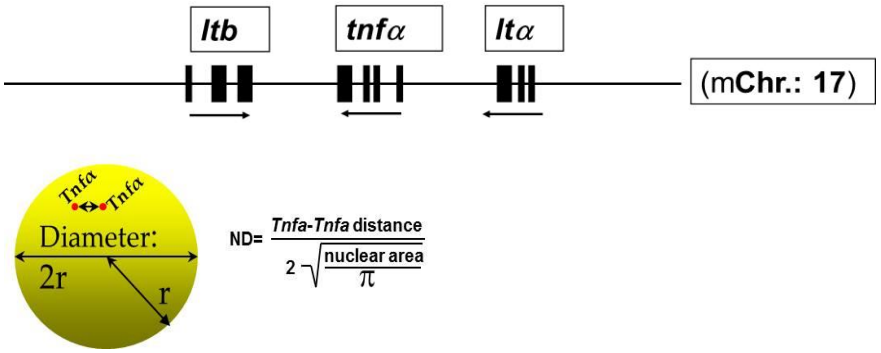

Figure 1. Above: The *LT/TNF* locus. Below: Normalized distances (NDs) are calculated by dividing the absolute distance between the two *Tnfα* alleles by the diameter of each cell.

The distances between the two *Tnfα* alleles were measured and normalized to the diameter of the cell nucleus, since nuclei diameters (ranging between 6-7μm) and volumes did not significantly differ between LPS-stimulation time points. We call this number "Normalized Distance" (ND), it ranges from 0 to 1 and it represents the proximity of the two *Tnfα* alleles – the smaller the ND the closer the two alleles are (**Fig. 1**). We consider that two alleles are co-localized when the distance between them is equal or less than 0.6μm, which equals with an ND equal or smaller than 0.1 for a macrophage diameter of

6μm. The *Tnfα* interallelic distances were measured in more than 10 independent experiments, for at least 100 cells each. The NDs were then clustered in 10 categories (0-0.1, 0.1-0.2, 0.2-0.3, 0.3-0.4, 0.4-0.5, 0.5-0.6, 0.6-0.7, 0.7-0.8, 0.8-0.9 and 0.9-1) and the frequencies of cells that fall within these clusters were calculated.

We found a considerable decrease of the *Tnfα* allele mean ND upon 30min of LPS stimulation and a subsequent increase upon 1h of LPS induction (**Fig. 2**). This represents shorter *Tnfα* allele distances in average, which means that upon 30min of LPS stimulation, the two *Tnfα* alleles come in close proximity and subsequently move away from each other 1h upon stimulation.

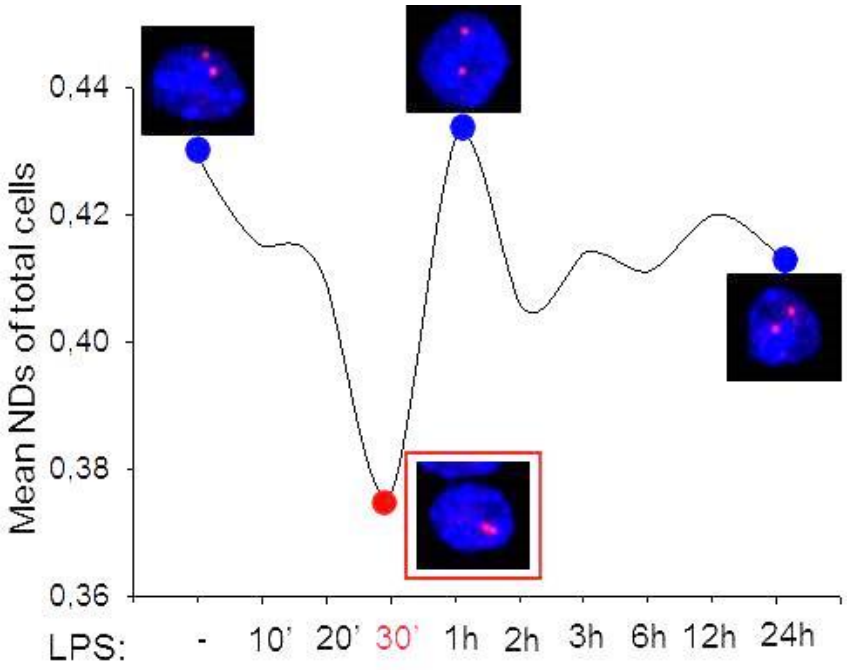

Figure 2. Time course of the homologous association of the *Tnfα* alleles. Mean Normalized Distances (NDs) of the total number of cells analyzed for each time-point in relation to time of LPS stimulation are presented in the graph, with a representative image of a cell with the *Tnfα* alleles in the respective distance from each other. The shortest distance of the two *Tnfα* alleles was found at 30min upon LPS stimulation of macrophages, when the two alleles come into close proximity and the longest 1h after macrophage activation, where the two alleles move the furthest away from each other.

This observation was corroborated by statistical analysis for the randomness of the distance distributions (Kolmogorov-Smirnov test, $P<0.001$), portraying a normal

distribution for interallelic distances in untreated cells but not for the 30min-LPS-stimulated macrophages (**Fig. 3**).

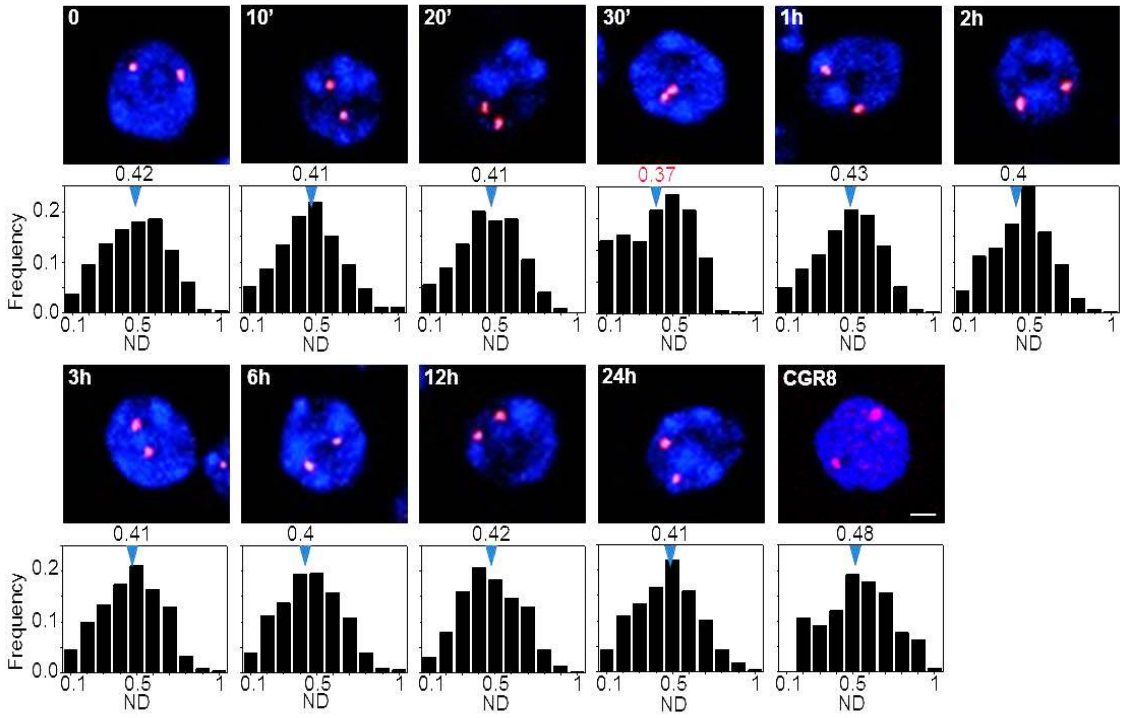

Kolmogorov-Smirnov test, P

	TNFα	P2RX4	Arrb1	E4F1
10'	0.092	0.090	0.564	0.884
20'	0.285	0.479	0.523	0.783
30'	<0.001	0.301	0.912	0.107
1h	0.046	0.327	0.106	0.758
2h	0.001	0.400	0.320	0.143
3h	0.374	0.839	0.034	0.512
6h	0.080	0.868	0.358	0.076
12h	0.589	0.673	0.404	0.009
24h	0.316	0.966	0.700	0.002
CGR8	0.010			

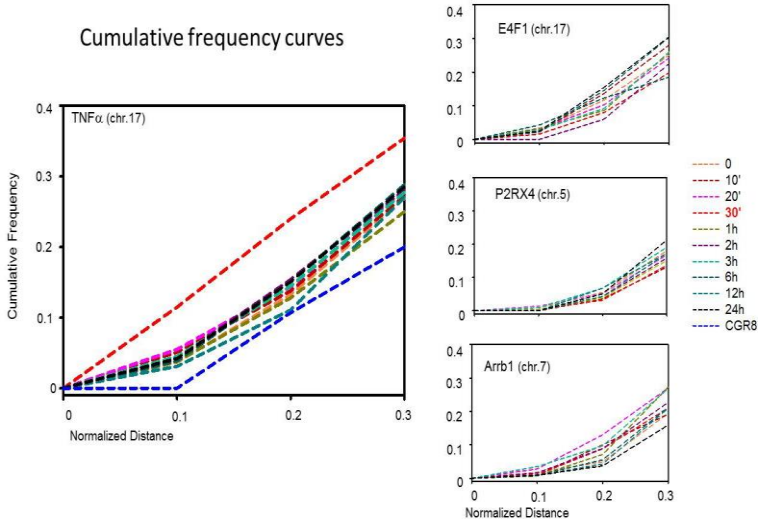

Figure 3. Above: *Tnfα* allele distance distributions. NDs are measured and they are plotted in 10 clusters from 0 to 1, for each time point of LPS stimulation, in Raw 264.7 macrophages and CGR8 Stem cells. Mean ND is shown with an arrow over the distributions. Below left: Kolmogorov-Smirnov test for the randomness of distributions. Below right: Cumulative frequency curves of *Tnfα*, *E4f1*, *P2rx4* and *Arrb1*.

In addition, cumulative frequency curves displayed that the 30min LPS stimulation time point was clearly differentiated from the other time points, as well as untreated cells, in co-localized *Tnfα* signals (**Fig. 3**).

In order to demonstrate that regions flanking the *LT/TNF* locus were not also brought together by the homologous pairing of the *Tnfα* alleles, we performed DNA FISH in LPS-induced Raw 264.7 macrophages using a BAC probe spanning the *E4f1* locus, which is mapped 10,7Mb upstream of the *Tnfα* gene on mouse chromosome 17. NDs and cumulative frequency curves of the *E4f1* gene locus showed that proximal regions were not affected by the interacting *Tnfα* locus and that the pairing was specific to *Tnfα*. This was also evidenced by DNA FISH experiments performed for two other gene loci, *P2rx4* and *Arrb1*, in LPS-stimulated macrophages. The NDs measured for these two loci were also clustered together in the cumulative frequency curves, displaying random distributions within the cell populations (**Fig. 3**).

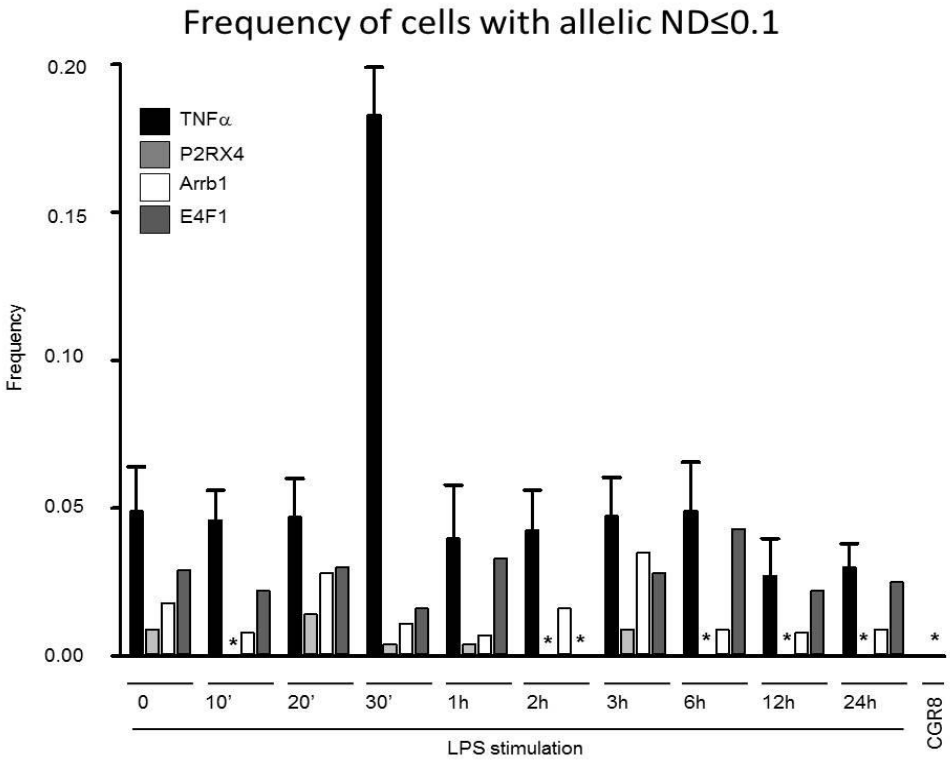

Figure 4. Frequency of co-localization of the *Tnfα* alleles in a time-course of LPS-stimulated Raw 264.7 macrophages. The frequency of cells with ND≤0.1 is plotted over time, for the *Tnfα*, *E4f1*, *P2rx4* and *Arrb1* alleles in Raw 264.7 macrophages and of *Tnfα* alleles in CGR8 embryonic Stem cells.

This close proximity of the *Tnfα* alleles upon 30min of LPS stimulation, taken together with the known rarity of somatic homologous pairing, suggested that the homologous association of the *Tnfα* alleles would be temporally transient. By taking a closer look, within the ND clusters of the cell frequencies, we found that *Tnfα* alleles co-localized (ND≤0.1, distance equal or shorter than 0.6μm) in about 18% of the cells upon 30min of LPS stimulation, compared to less than 5% of untreated macrophages (**Fig. 4**). These frequencies of cells within the 0-0.1 ND cluster explain the smaller mean ND that we calculated for the time point of 30min LPS stimulation. They portrayed a co-localization event (homologous pairing) between the *Tnfα* alleles 30min upon LPS stimulation. The Kolmogorov-Smirnov test confirmed the statistical significance of this finding and the lack of randomness in distance distribution between the samples of untreated and 30min-LPS-stimulated macrophage cells.

It is evident by the experiments performed for the other three loci (*P2rx4*, *Arrb1* and *E4f1*), as well as *Tnfα* interallelic distances measured in an embryonic stem cell line (CGR8), that the phenomenon of homologous pairing is specific to the *Tnfα* locus within the specific context of LPS-stimulated macrophages (**Fig. 4**).

In summary, our data highlight a homologous pairing phenomenon between the *Tnfα* alleles in LPS-stimulated mouse macrophages. This interallelic association occurs as early as 30min upon LPS stimulation, rapidly ceases 1 hour upon stimulation and it is specific of the *Tnfα* locus.

5.2 Allelic expression of the *Tnfα* gene

Next, we investigated whether this transient homologous pairing of the *Tnfα* alleles might have any functional effect on the gene's expression kinetics. Quantitative RT-PCR analysis was used to quantitate the *Tnfα* mRNA levels in Raw 264.7 murine macrophage cells, after 50ng/ml LPS stimulation in a time-course. Total RNA was extracted after stimulation of the cells with LPS for 10min, 20min, 30min, 1h, 2h, 3h, 6h, 12h and 24h. The choice of 50ng/ml LPS for the stimulation of macrophages was made after a dose-dependent experiment that enabled us to decide which concentration would resemble the normal inflammation levels.

Quantitative RT-PCR-based analysis of the gene expression profile in the *LT/TNF* locus indicated that *Tnfα* transcription initiates upon minutes of LPS stimulation, it reaches maximal mRNA levels after 1 hour and steadily declines until it reaches basal levels at 24 hours upon stimulation (**Fig. 5**).

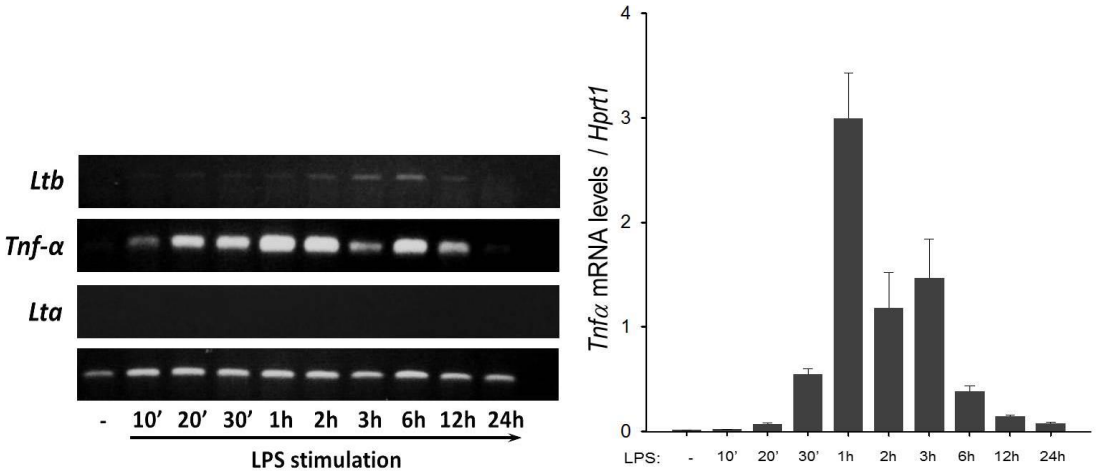

Figure 5. On-gel and quantitative RT-PCR analysis of the gene expression profile in the *LT/TNF* locus. *Tnfα* mRNA levels were normalized over *Hprt1* mRNA levels upon LPS stimulation of Raw 264.7 macrophages.

We also analyzed the pattern of *Tnfα* expression at the single-cell level, with the simultaneous detection of both the newly-synthesized mRNA transcript and the DNA of the two alleles. The RNA-DNA FISH experiments we performed to visualize the nascent mRNA transcripts confirmed the qRT-PCR results placing the highest levels of expressing cells (~80%) and maximal *Tnfα* mRNA transcript levels at 1 hour upon LPS stimulation of the cells (**Fig. 6**). In order to confirm that the RNA fluorescent signals visualized were indeed due to the hybridization of the cDNA probe to the nascent mRNA, and not hybridized to genomic DNA, we pretreated the cells with RNase A prior to hybridization, which cleaved the nascent RNA. Lack of RNA signals in the RNase A-treated cells confirmed that the signals from the non-treated cells were indeed due to the presence of nascent mRNA (**Fig. 6**).

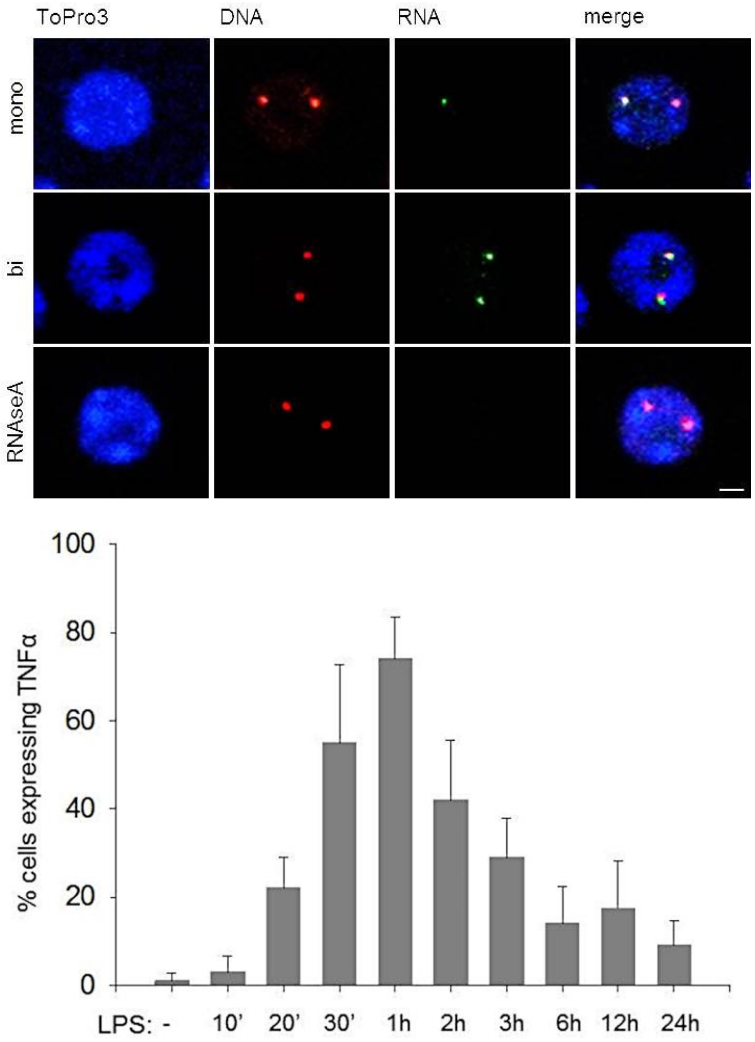

Figure 6. Above: Confocal microscopy images with representative images of the *Tnfα* alleles, along with the nascent mRNA transcripts in macrophage nuclei as seen expressing in a mono- or bi-allelic manner. ToPro3 staining of the nucleus (blue) represents the presence of DNA, *LT/TNF* probe labeled with Spectrum Orange was hybridized on the two *Tnfα* alleles (red) and *Tnfα* mRNA transcripts were hybridized with Spectrum Green - labeled *Tnfα* cDNA probes (green). Below: Percentage of expressing cells in a time course of LPS stimulation of Raw 264.7 macrophages.

Interestingly, close examination of *Tnfα* gene transcription at the single-cell level, uncovered a unique allelic pattern of expression (**Fig. 7**). Analysis of gene expression using RNA-DNA fluorescence in situ hybridization (RNA-DNA FISH) revealed that, during the first minutes upon LPS stimulation, *Tnfα* is expressed mono-allelically. One hour upon stimulation however, about 55% of the expressing cells displayed a bi-allelic pattern of transcription.

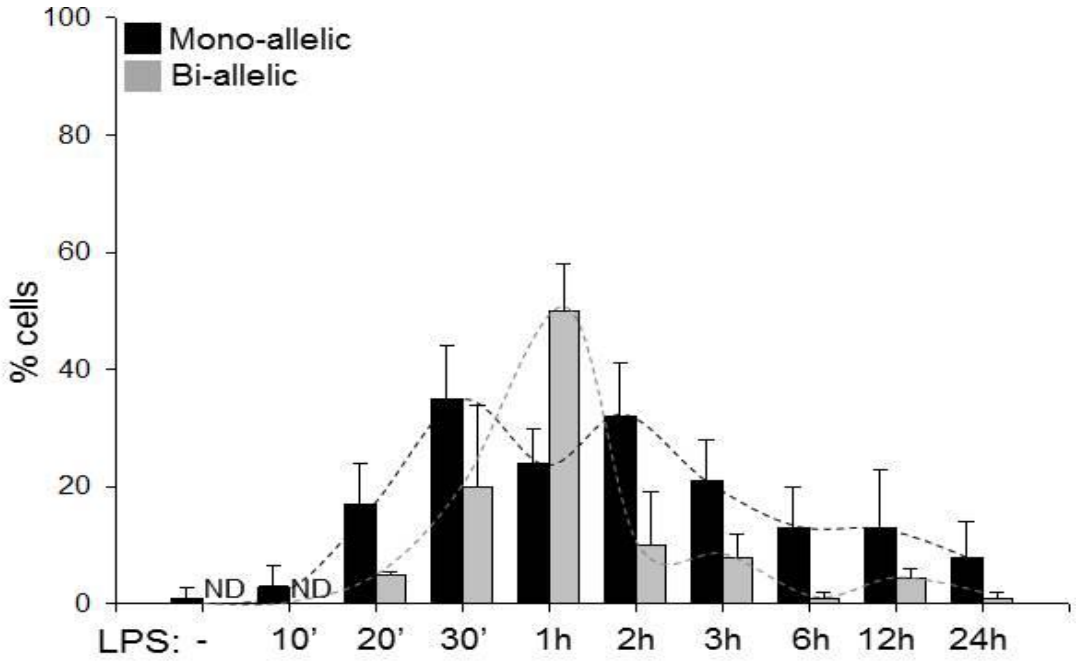

Figure 7. Allelic pattern of *Tnfα* expression in Raw 264.7 macrophages after LPS stimulation. The examination of the allelic expression pattern showed a mono-allelic pattern of expression, during the first minutes of stimulation, a switch to bi-allelic expression 1 hour upon stimulation. After the 1h-LPS bi-allelic switch, a rapid transition back to mono-allelic expression occurred and expression progressively diminished.

This switch to bi-allelic *Tnfα* expression is in agreement with the quantitative QRT-PCR results of maximal transcript levels at the 1h LPS time point. After the 1h-LPS bi-allelic switch, a rapid transition back to mono-allelic expression occurred and expression progressively diminished, portrayed both by *Tnfα* expressing cell numbers and transcript levels (**Fig. 6** and **7**).

If we follow these two events along the axis of time, we see that upon stimulation of macrophages, the *Tnfα* alleles come in close proximity in as fast as 30min upon activation, and within 30min after this co-localization event, a switch into the allelic expression profile occurs, rendering the *Tnfα* transcription bi-allelic. These rapid events are also transient and the expression turns back to mono-allelic within minutes.

5.3 LPS induction

To further explore the homologous pairing of the *Tnfα* alleles, as well as its role in mediating the subsequent bi-allelic switch in expression, we questioned whether an alternative stimulus of the *Tnfα* expression pathway would succeed in inducing the same phenomena. We thus treated macrophages with mouse recombinant TNFα protein which according to the literature would activate the TNFR1/R2 signaling pathways, leading to nuclear translocation of NF-κB, in simulation of the TNFα autocrine and paracrine signaling.

We showed that, in contrast to LPS stimulation, treatment of Raw 264.7 macrophages with mouse recombinant TNFα failed to activate the pairing of the two *Tnfα* alleles. The percentage of cells with homologous pairing (ND≤0.1) was decreased by 76% in cell samples stimulated with TNFα compared to samples stimulated with LPS (**Fig. 8**).

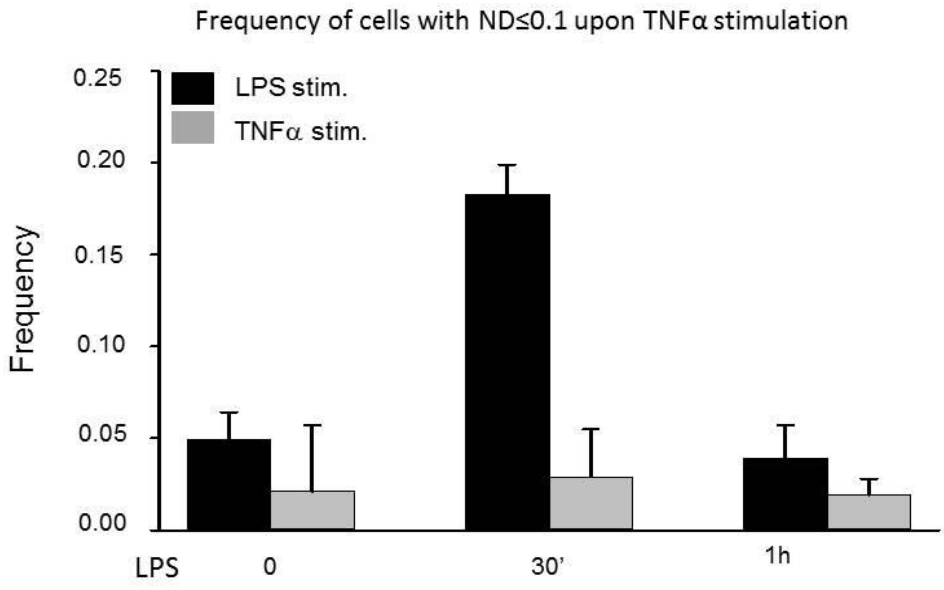

Figure 8. The effect of TNFα stimulation of macrophages on *Tnfα* alleles homologous pairing. Frequency of co-localization of the *Tnfα* alleles is plotted in a time course of LPS stimulation of Raw 264.7 macrophages.

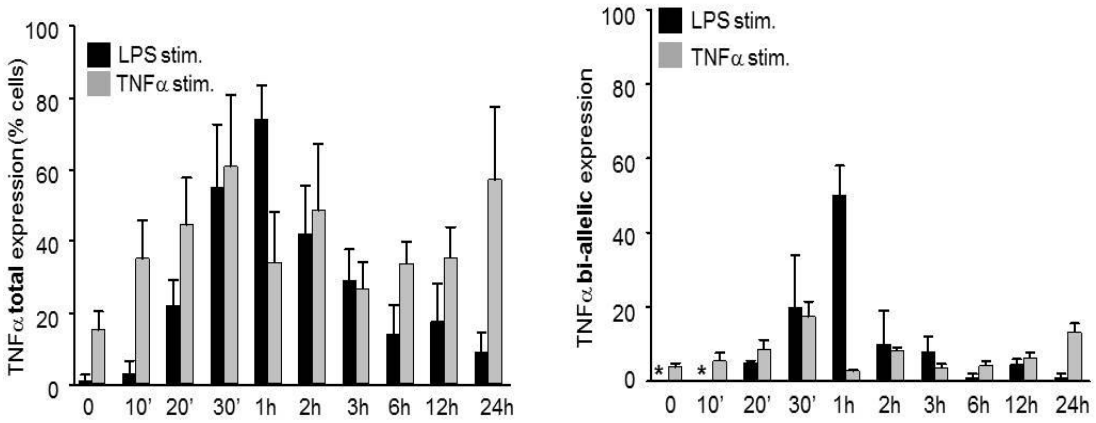

Figure 9. The effect of TNFα stimulation of macrophages on *Tnfα* allelic expression. Left: Frequency of total expressing cells in respect to time in TNFα-stimulated compared to LPS-stimulated Raw 264.7 macrophages. Right: Frequency of bi-allelic expression on macrophages upon TNFα or LPS stimulation.

Surprisingly, *Tnfα* bi-allelic expression was also impaired upon TNFR activation and *Tnfα* expression was restricted to one allele (**Fig. 9**). Although LPS stimulation leads to TNFα expression and secretion from the cells which activates TNF receptors in the same (activated) or neighbouring cells, these results show that the direct activation of TNF receptors does not have the same results on *Tnfα* transcription. It is evident that *Tnfα* homologous pairing is strictly LPS-induced and TNFα itself is not capable of activating the phenomenon. LPS induction is necessary for the switch of TNFα allelic expression, without which *Tnfα* transcription is solely mono-allelic.

5.4 Actin polymerization

If indeed there is a rapid relocalization of the *Tnfα* alleles within a short time frame upon LPS stimulation of macrophages, one would expect that motor proteins are involved in regulating these dynamic changes. Indeed, *Tnfα* homologous pairing was shown to be actin-dependent and necessary for the bi-allelic switch in expression, upon LPS stimulation. We blocked actin polymerization in the cell nucleus with the use of the drug Latrunculin A (LTA) and found that the movement of the locus was impeded and pairing of the *Tnfα* alleles was disrupted. We performed DNA FISH experiments on LTA

pretreated macrophages and subsequently stimulated with LPS. We found that impaired movement within the nucleus did not allow the co-localization of the *Tnfα* alleles (**Fig. 10**). We measured an 85% decrease in the percentage of cells with co-localized *Tnfα* alleles 30min upon LPS stimulation, and notably the percentage of cells with homologous pairing after LTA treatment dropped below the background levels calculated for the untreated cells.

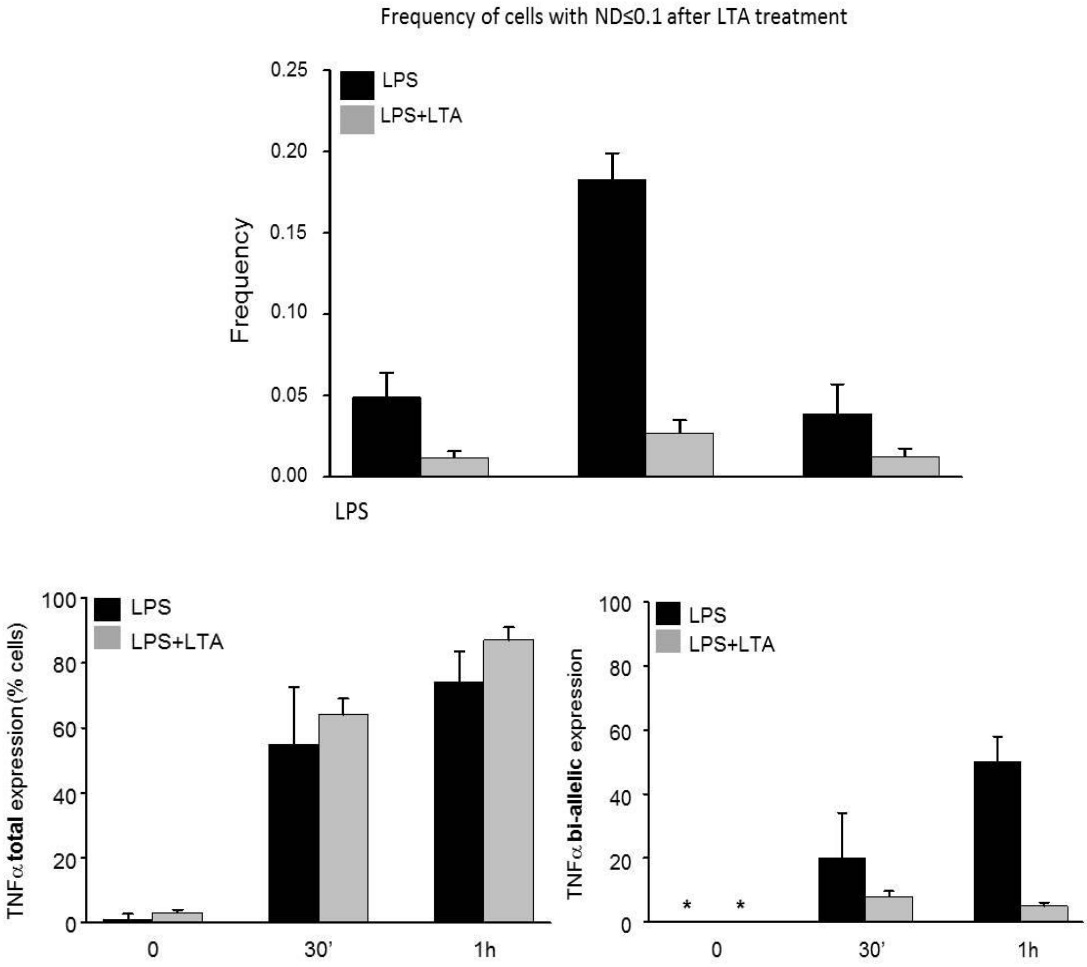

Figure 10. The effect of actin polymerization disruption on *Tnfα* homologous pairing and allelic expression. Above: Frequency of co-localization of the *Tnfα* alleles in respect to time in untreated or LTA-pretreated and LPS-stimulated Raw 264.7 macrophages. Below left: Percentage of *Tnfα* expressing cells in LTA-pretreated compared to untreated LPS-stimulated Raw 264.7 macrophages. Below right: Percentage of biallelically *Tnfα* expressing macrophages upon LTA treatment.

RNA-DNA FISH experiments performed on LPS-stimulated macrophages pretreated with LTA showed that the monoallelic *Tnfα* expression was not affected by treatment with LTA. More importantly, the switch from mono- to bi-allelic expression 1 hour upon LPS stimulation was not evident after the LTA pretreatment rendering *Tnfα* expression mono-allelic (**Fig. 10**). We found that the percentage of the *Tnfα* expressing cells remained the same even after the pre-treatment with LTA. Although the total number of *Tnfα* expressing cells remained the same, these cells transcribe *Tnfα* only from one allele.

We conclude that the constraint of movement within the nucleus disrupted the homologous association of the *Tnfα* alleles, but more importantly, blocked the switch from mono- to bi-allelic *Tnfα* expression. This suggests that the bi-allelic expression of *Tnfα* depends on the homologous pairing of its two alleles that occurs prior to the allelic switch.

5.5 Protein complexes

To unravel the functional mechanism behind the regulation of homologous association of alleles and its effect in the regulation of the allelic expression profile of the *Tnfα* gene we have chosen to purify and characterize protein complexes that mediate such a phenomenon. We resorted to the protein factors that play a major role in mediating transvection in Drosophila. In accordance with this, GAGA factor (GAF), a protein encoded by the *Trithorax-like* (*Trl*) gene, is a transcription factor with DNA-binding and transactivation properties that binds to GA motifs and locally remodels chromatin to enable such enhancer-promoter interactions. We checked if there were any $(GA)_n$ repeats within the *LT/TNF* locus. We selected these specific stretches to synthesize 25bp oligonucleotides which were P^{32} end-labeled with T4 polynucleotide kinase. We used these repetitive GA DNA oligonucleotides to perform Electrophoretic Mobility Shift Assays with nuclear extracts from LPS-stimulated Raw 264.7 macrophages, which showed that there is indeed at least one GA-specific binding factor. In addition we found that this factor's DNA binding activity is LPS-induced (**Fig. 11**). More specifically, we observed a DNA-bound protein complex that was induced by LPS over time and the band shift was increased at the time when the homologous association occurs (20-30min upon LPS stimulation). The gel shift was increased with the "GA-repeat"

oligonucleotide, which contained multiple binding sites, it became sharper with the "single GA" binding site and disappeared with the mutated "mutant single GA" binding site.

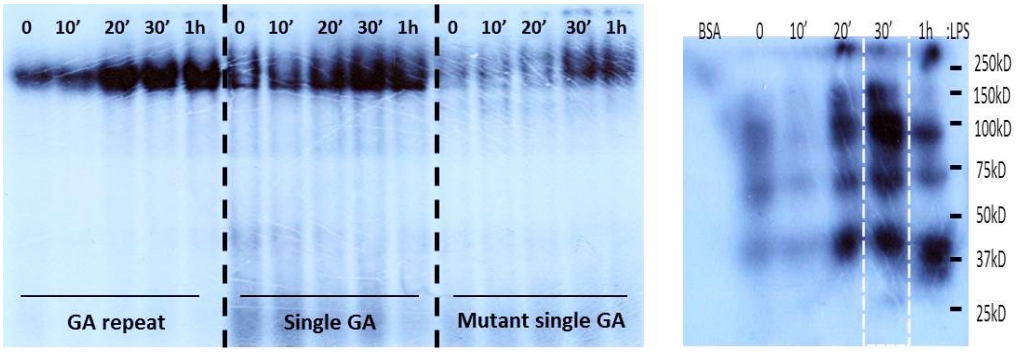

Figure 11. LPS-induced GAGAG DNA binding activity in Raw 264.7 nuclear protein extracts. Left: EMSA of P^{32}-labeled oligonucleotides and Raw 264.7 nuclear extracts before, 10min, 20min, 30min and 1h after LPS stimulation. First column: GA repeat 25bp oligonucleotide, second column: single GA binding site (GAGAG) chosen from within the *Tnfα* promoter, third column: same sequence as "single GA" with the GAGAG site mutated to ACACA. Right: SouthWestern blot of Raw 264.7 nuclear protein extracts, hybridized with the "GA-repeat" 25bp oligonucleotide.

The gel shift assays performed here can only inform us about the existence of a certain factor with specific DNA binding activity and only about its relative quantity between samples. The accurate molecular weight was deduced with a SouthWestern assay which separated the nuclear proteins by size in a polyacrylamide gel and then upon the hybridization with a radiolabeled DNA probe on a nitrocellulose membrane permitted the visualization of GA-binding proteins (**Fig. 11**). The same LPS stimulation time-course was used for the preparation of nuclear protein extracts as for the EMSA assays and the hybridization was performed with the multiple binding site "GA-repeat" 25bp oligonucleotide.

The multiple bands visible can be accounted for by either multiple GA binding proteins, or by slight degradation of the sample. In any case, we can distinguish several bands, which were induced at 20-30min upon LPS stimulation and diminished at 1h upon stimulation. We hypothesized that this protein-binding pattern could correspond to a factor that was induced to mediate the $Tnf\alpha$ homologous association phenomenon (at 30min upon LPS stimulation) and would be removed/degraded after the completion

of the pairing (1h upon LPS stimulation).

It is clear, however, that, for the complete identification of any factor, we would need to incorporate mass spectrometric data in the analysis. To this end, nuclear protein extracts from Raw 264.7 macrophages stimulated with LPS were used for DNA affinity chromatography coupled to Mass Spectrometry.

For the DNA affinity chromatography experiments we utilized concatamerized 30bp synthetic biotinylated DNA oligonucleotides which were immobilized on magnetic streptavidin beads and used to isolate proteins from LPS-stimulated macrophages.

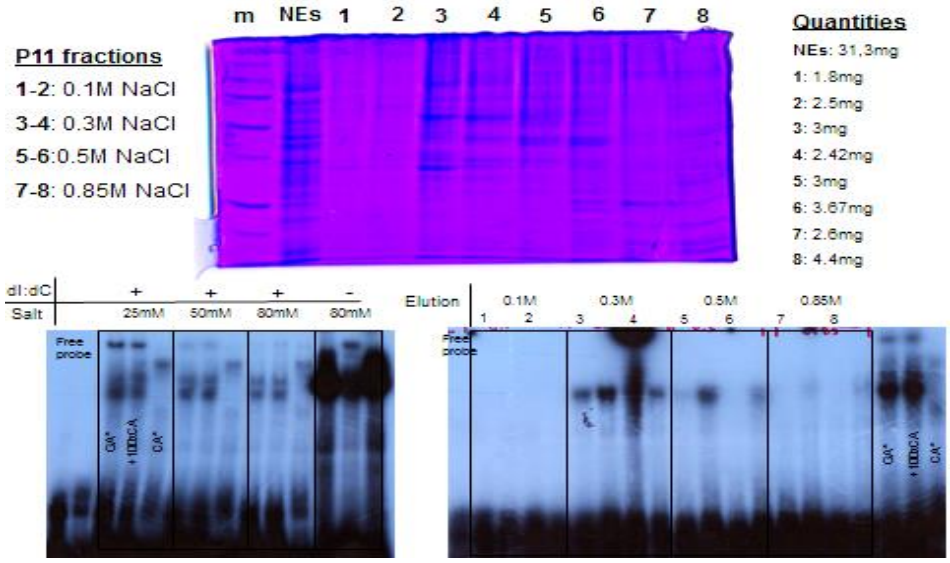

Figure 12. Above: P11 phosphocellulose fractionation of 30min-LPS nuclear protein extracts. Below: stepwise elution of extracts and EMSA-analysis of the presence of the DNA binding activity.

More specifically, nuclear protein extracts from untreated and 30min LPS-stimulated Raw 264.7 macrophage cells were prepared. We selected the 30min LPS stimulation of cells for the preparation of nuclear extracts, since it was the time when the homologous pairing was detected. The extracts were initially pre-cleared with the use of a CA-repeat oligonucleotide which bound all the non-specific DNA binding proteins and then fractionated on a P11 phosphocellulose column (**Fig. 12**). EMSA was used to identify the fraction with the DNA binding activity and then, binding reactions were carried out between the extracts and concatamerized bead-immobilized biotinylated oligonucleotides (GA-repeat sequence). The bound proteins were denatured and

separated on a 10% poly-acrylamide gel. Isolated gel bands were digested with trypsin and eluted protein peptides were analyzed with an LC-ESI-MS/MS method (**Fig. 12** and **13**).

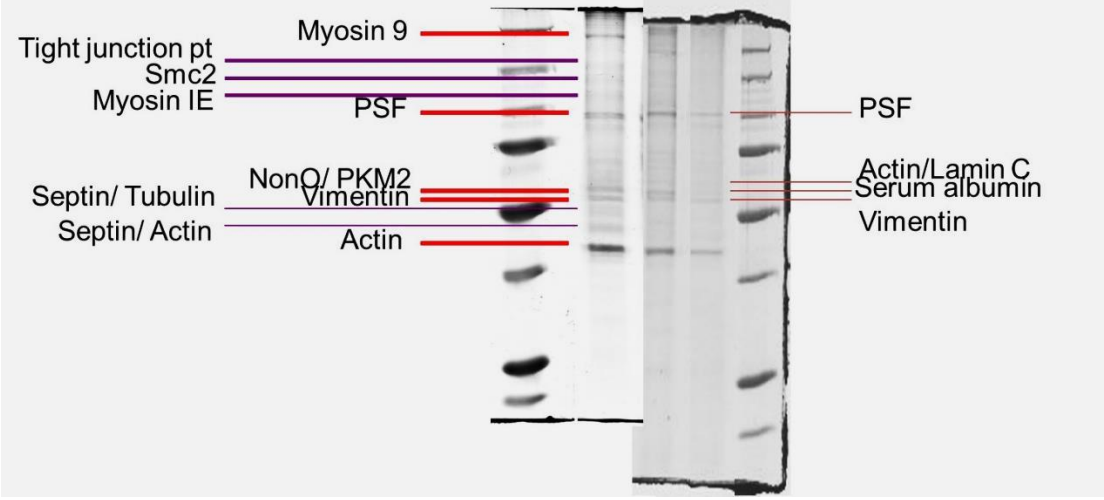

N	Accession #	#AAs	MW [Da]	Description	1A	1B	2A	2B	3A	3B	4A	4B	5A	5B
1	IPI:IPI00407130.4	531	57808.0045	Isoform M2 of Pyruvate kinase isozymes M1/M2		180.33	109.98	752.8	57.93	412.07		56.61		
2	IPI:IPI00222228.5	538	58188.22219	Putative uncharacterized protein				57.48	71.49		64.38	38.27		56.71
3	IPI:IPI00347110.2	539	58874.69617	Keratin, type II cytoskeletal 73				55.87	77.09		38.54		57.03	51.96
4	IPI:IPI00330480.1	324	35143.57587	35 kDa protein	46.73	46.94	71.501	52.02						
5	IPI:IPI00404881.1	394	44317.51679	Putative uncharacterized protein				47.29						
6	IPI:IPI00756624.1	190	21521.18522	Putative uncharacterized protein Gltp				38.39						
7	IPI:IPI00458514.2	98	10932.7886	HIG1 domain family member 1B			37.66	33.35						
8	IPI:IPI00886213.1	105	11177.71267	11 kDa protein				32.09						
9	IPI:IPI00330649.4	1107	126738.028	myosin IE	84.42									
10	IPI:IPI00131695.3	608	68647.71097	Serum albumin	62.145	51.93	40.51			36.84				

Figure 13. Mass Spectrometric identification of GA-binding proteins in nuclear protein extracts from LPS-stimulated Raw 264.7 macrophages.

Another approach that was used in parallel as an *in vivo* assay to verify the results was a Yeast One Hybrid Screening. A 30bp tandem GA-repeat DNA oligonucleotide was cloned in a plasmid vector which was used to transform a macrophage-derived cDNA expression library under stringent growth conditions. A clone was considered positive if it had the ability to express three selection markers, one of which comes from the successful interaction of an expressed protein with the DNA element cloned.

A protein that we were able to identify by both strategies was mouse Pyruvate Kinase Muscle isoform 2 (PKM2) (**Fig. 13**), as a protein with the ability to bind GA repeats in the *Tnfα* promoter. PKM2, a protein formerly known to have a role in glycolysis, was

recently shown to also translocate into the nucleus and directly regulate transcription as a protein kinase.

Immunostaining and Western blotting confirmed PKM2 expression in Raw 264.7 macrophages, its nuclear localization and its LPS induction (**Fig. 14**).

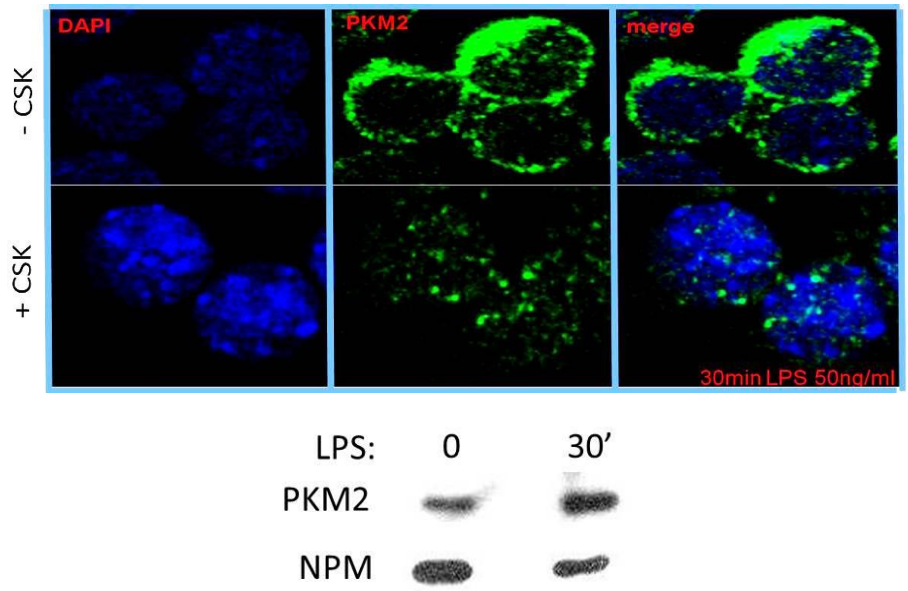

Figure 14. Above: Immunostaining of PKM2 in the cytoplasm and nucleus of LPS-stimulated Raw 264.7 macrophages. Below: PKM2 is LPS-induced as confirmed by Western blotting of nuclear protein extracts from untreated and 30min-LPS stimulated Raw 264.7 macrophages with a-PKM2 and a-NPM antibodies.

We then investigated whether siRNA-mediated knock-down of PKM2 affected the homologous pairing of *Tnfα* alleles. Knock-down of PKM2 decreased the levels of *Tnfα* expression, as portrayed by quantitative RT-PCR of mRNA, extracted from untreated and siRNA-PKM2-treated stimulated macrophage cells (**Fig. 15**).

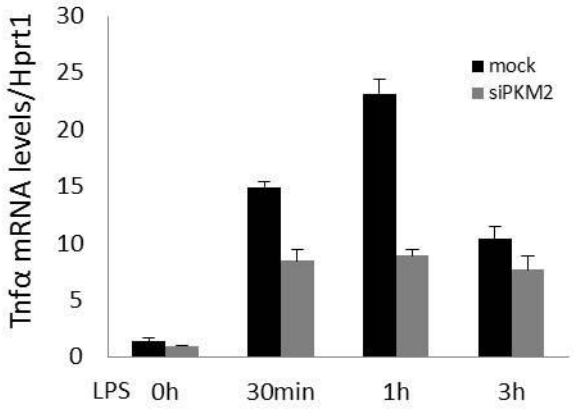

Figure 15. Quantitative RT-PCR of *Tnfα* mRNA before and after siRNA treatment of PKM2.

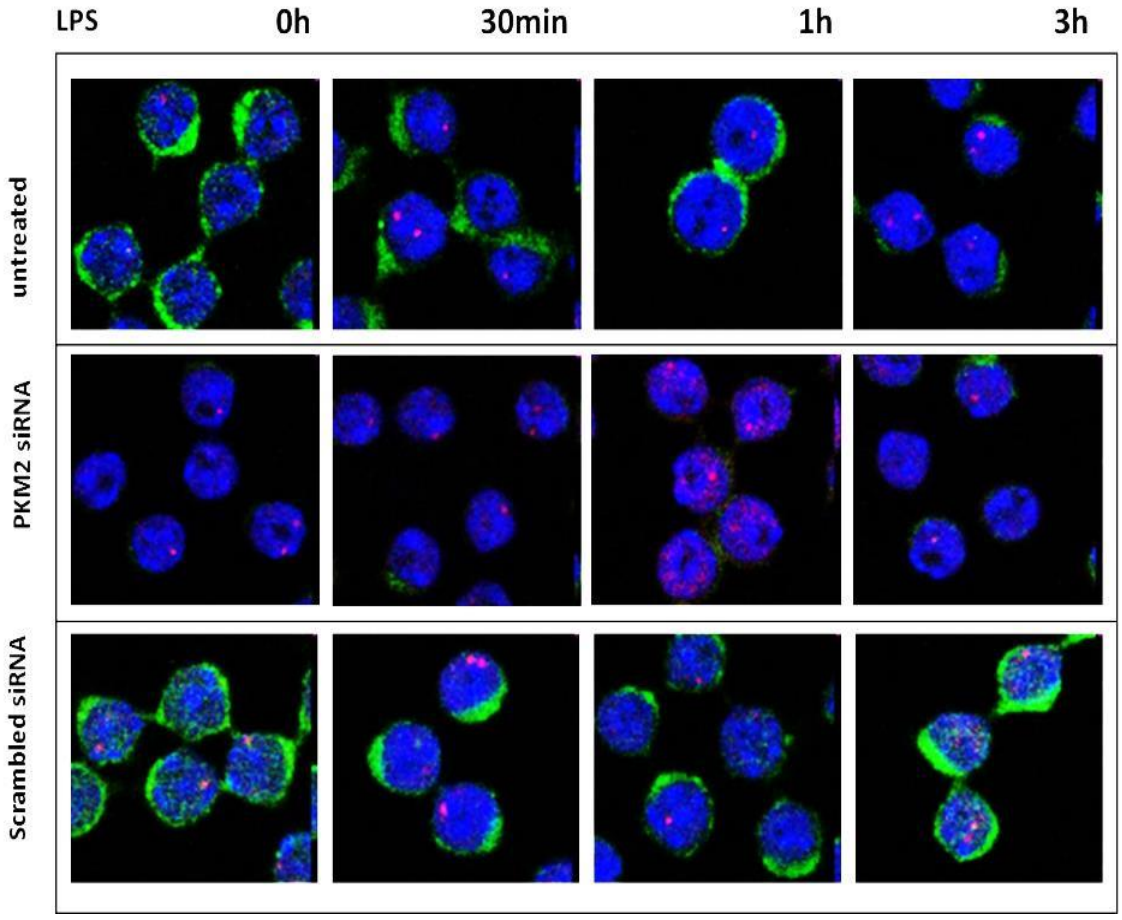

Figure 16. Immunostaining of PKM2 protein before and after siRNA-mediated knock down.

Moreover, RNA-DNA FISH experiments showed that PKM2 knock-down in Raw 264.7 macrophage cells disrupted homologous pairing of the *Tnfα* alleles upon LPS stimulation and, as expected, also blocked the switch to bi-allelic transcription, in contrast to scrambled control siRNA sequences (**Fig. 16**, **18** and **20**).

T-helper-inducing POZ-Krüppel-like factor (ThPOK, encoded by the *Zbtb7b* gene) was recently *in silico* predicted to be the vertebrate homolog of *Drosophila* GAGA factor, due to its structural and sequence similarity. Thus we also tested this protein factor for its role in *Tnfα* homologous pairing. Quantitative RT-PCR was used to evaluate the expression kinetics of ThPOK in LPS-stimulated macrophages and immunostaining experiments showed ThPOK's speckled pattern of localization in the nucleus of the cells (**Fig. 17**).

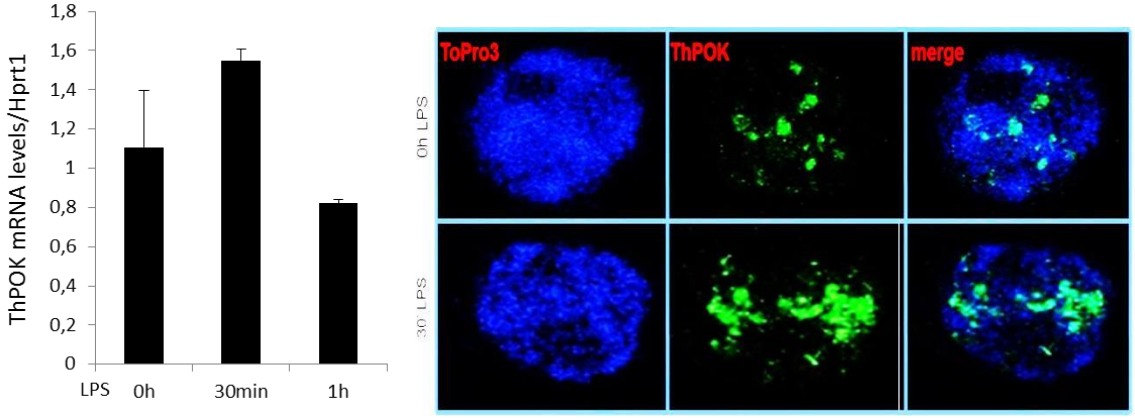

Figure 17. Left: ThPOK mRNA expression in untreated and LPS-stimulated macrophages assessed by quantitative RT-PCR. Right: Immunostaining of ThPOK protein (green) in the nucleus of untreated and LPS-stimulated Raw 264.7 macrophages.

We also used RNA-DNA FISH to assess the effects of siRNA targeting of ThPOK mRNA on *Tnfα* homologous pairing and expression in untreated and LPS-stimulated Raw 264.7 macrophages (**Fig. 18**).

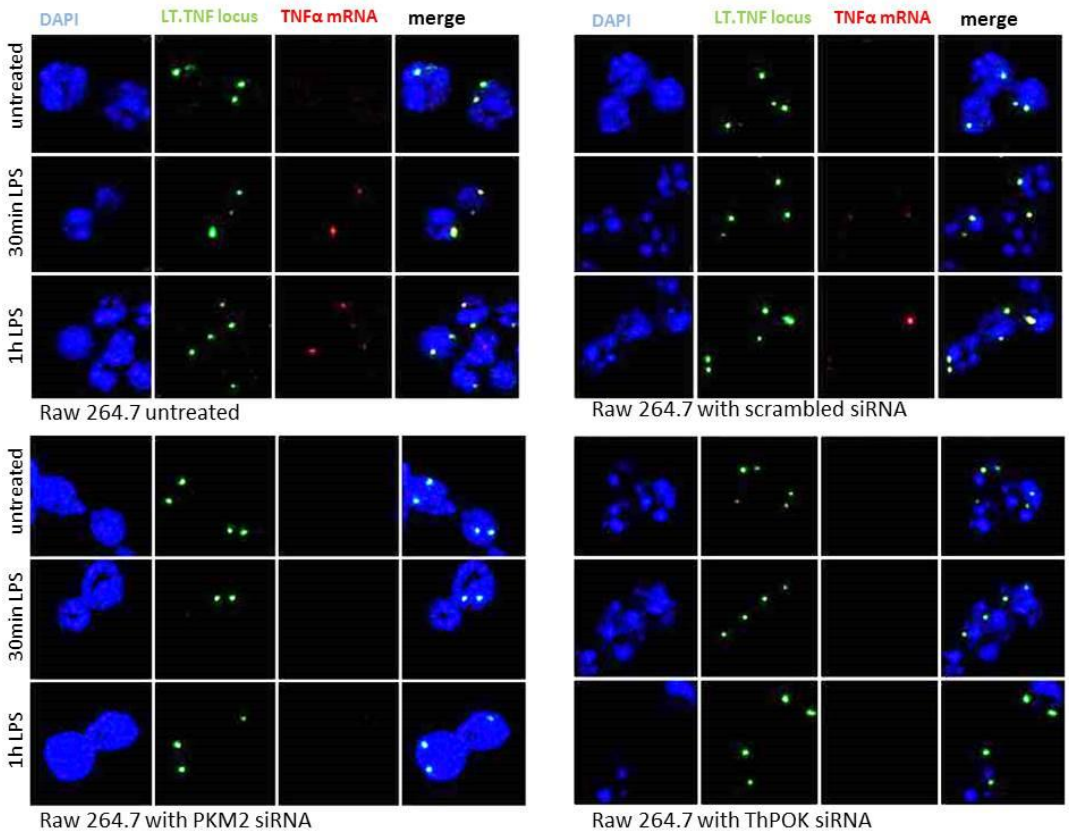

Figure 18. *Tnfα* expression before and after siRNA for PKM2 or ThPOK. Representative images from RNA-DNA FISH experiments showing *Tnfα* mRNA (red) in untreated cells (above left), cells treated with scrambled negative siRNA (above right), PKM2 siRNA (below left) and ThPOK siRNA (below right).

We observed that ThPOK knock-down decreased the levels of *Tnfα* expression, as portrayed by quantitative RT-PCR of RNA, extracted from untreated and siRNA-ThPOK treated stimulated macrophage cells (**Fig. 19**).

In addition, the percentage of cells with homologous pairing was decreased by 53.5% and ThPOK knock down also attenuated *Tnfα* expression, by blocking the mono- to bi-allelic switch (**Fig. 20**).

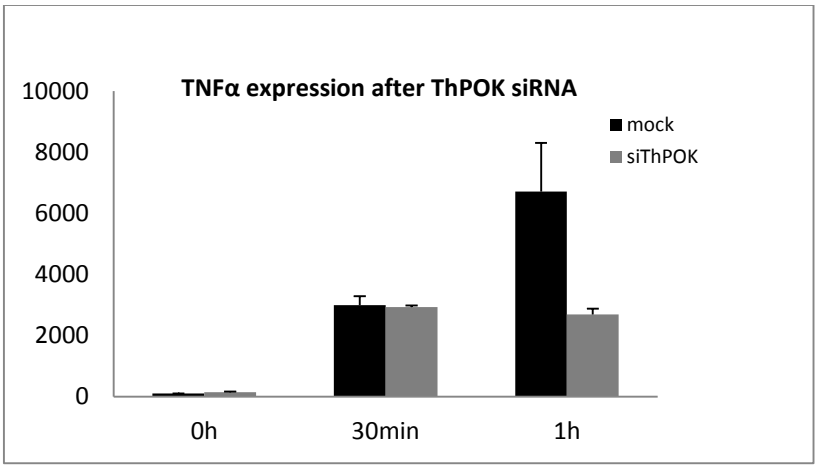

Figure 19. Quantitative RT-PCR of *Tnfα* mRNA before and after siRNA of ThPOK.

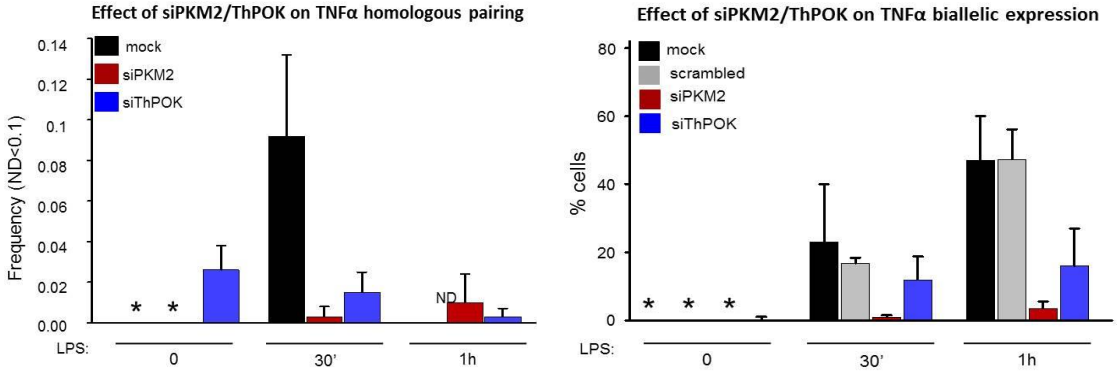

Figure 20. Left: The effect of PKM2 and ThPOK siRNA treatment on *Tnfα* homologous pairing. Right: The effect of PKM2 and ThPOK siRNA treatment on *Tnfα* bi-allelic expression.

Taken together, the above data show that *Tnfα* homologous pairing is mediated by PKM2 and ThPOK and that knocking down either of them disrupts the phenomenon and consequently blocks the switch from mono- to bi-allelic *Tnfα* expression.

Such an effect of a protein factor would require an activity with direct access to DNA, thus we performed Chromatin Immunoprecipitation (ChIP) experiments to investigate if both PKM2 and ThPOK bind the *Tnfα* proximal and distal promoters (**Fig, 21**). It was shown that both PKM2 and ThPOK occupy the *Tnfα* promoter. More specifically, the occupancy of the proximal *Tnfα* promoter (TNFprom1, **Fig. 21**) by PKM2 was increased upon the activation of the cells with LPS for 30min.

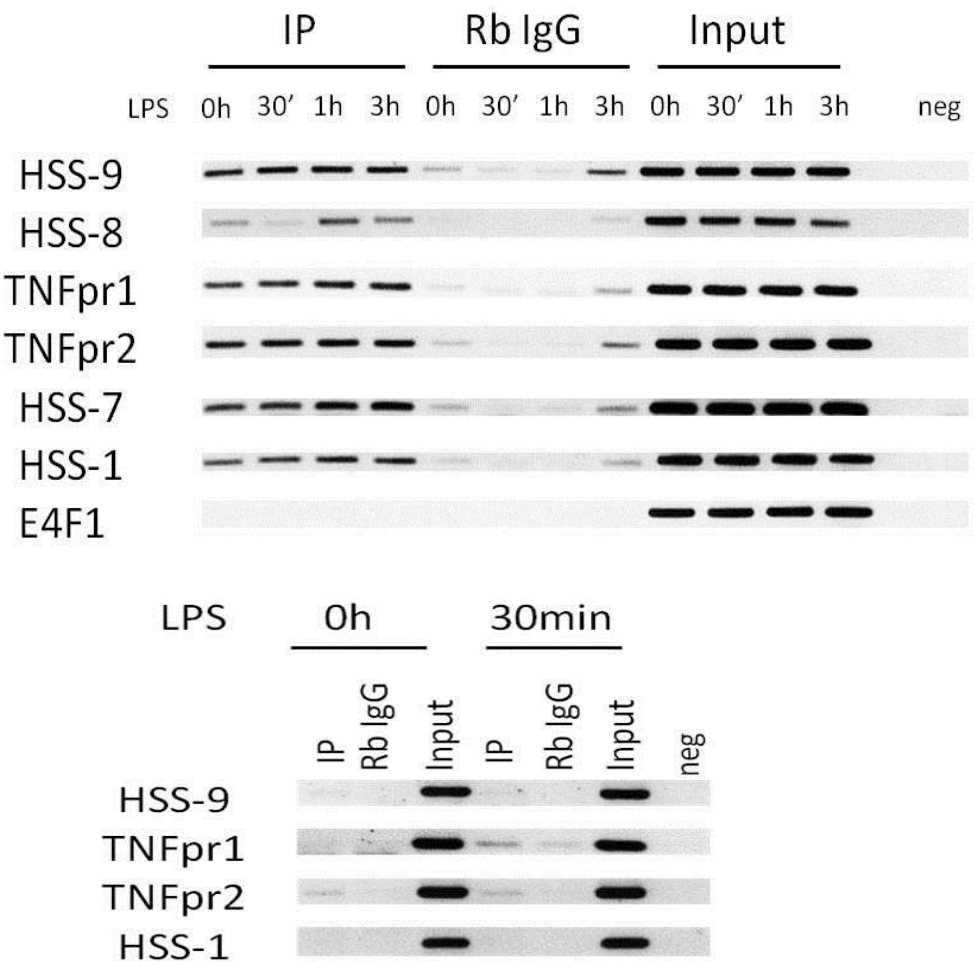

Figure 21. Chromatin Immunoprecipitation experiments portray binding of ThPOK (above) and PKM2 (below) on the *Tnfα* promoter. HSS9, 8, 7, and 1 are DNase I hypersensitive sites in the *LT/TNF* locus (see Fig. 43), TNFpr1 and TNFpr2 refer to the *Tnfα* proximal and distal promoters respectively and E4F1 is a region on the *E4f1* gene used as negative control.

Nevertheless, PKM2 does not evidently contain a DNA binding domain, thus it would be safe to assume that DNA occupancy emanates via a protein-protein interaction. To this end, we performed co-immunoprecipitation experiments with an anti-ThPOK antibody in both, whole cell and nuclear protein extracts of untreated and LPS-induced macrophages (30min) and detected the eluted proteins with an anti-PKM2 antibody, in order to investigate whether PKM2 and ThPOK physically interact (**Fig. 22**).

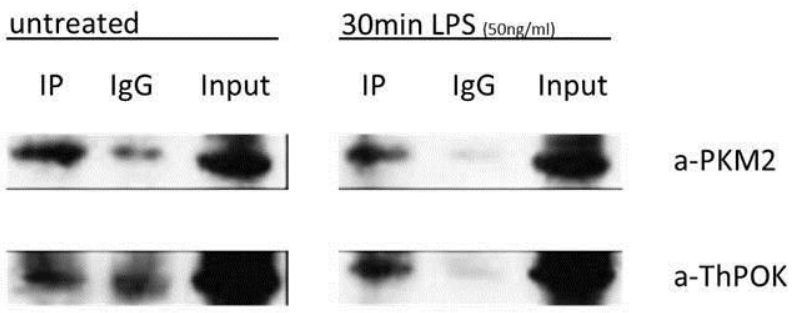

Figure 22. Co-immunoprecipitation of PKM2 and ThPOK from untreated and 30min-LPS stimulated Raw 264.7 nuclear extracts. anti-ThPOK was used to bind ThPOK in nuclear protein extracts and the ThPOK-PKM2 interaction was confirmed with anti-PKM2.

We observed that ThPOK interacted with PKM2 and that, indeed, this interaction was enhanced in 30min-LPS-stimulated macrophages. In summary, we conclude that a PKM2-ThPOK interaction takes place on the *Tnfα* promoter after the activation of macrophages with LPS. In addition, this interaction takes place at the same time as the occurrence of the homologous pairing of the *Tnfα* alleles (30min upon LPS activation). Since the knock-down of either one of the two proteins disrupted this homologous association, we suggest that the interaction of the proteins mediates the homologous pairing phenomenon and thus, controls the gene's allelic expression profile.

5.6 Long non-coding RNA transcripts

The various functions of long non-coding RNAs, that have already been discussed (e.g. the role of RNA in paramutation in plants), as well as the long transcripts involved in the well-studied phenomenon of homologous pairing between the two X chromosomes in X inactivation, directed us to examine whether there is evidence of such long transcripts in the *LT/TNF* locus. To this end, total RNA was extracted from untreated and 1h LPS-stimulated Raw 264.7 macrophages, cDNA was synthesized with random hexamers and specific-primer PCR was performed at 11 different sites of the *LT/TNF* locus (**Fig. 23**). When intergenic transcription was confirmed for sites 1 through 9, specific-primer reverse transcription was performed to examine the continuity of the transcripts. Reverse transcription primed at site 1, followed by PCR primed at site 9 and vice versa, confirmed

the existence of two complementary long transcripts, encompassing the sequences between sites 1 and 9.

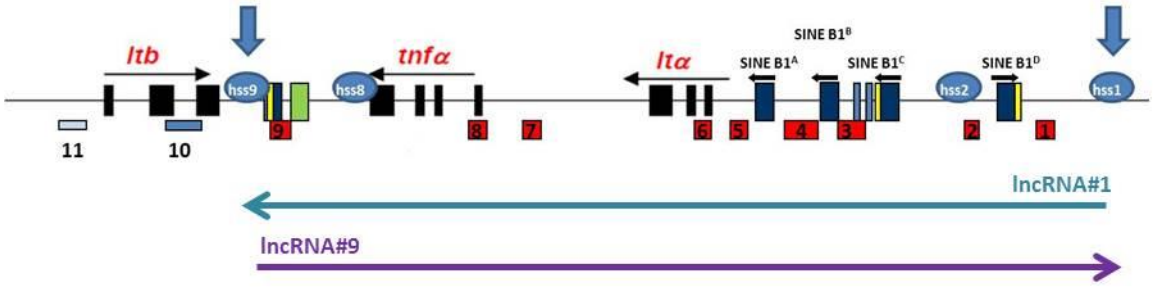

Figure 43. Long non-coding transcripts at the *LT/TNF* locus.

Then, Rapid Amplification of cDNA Ends (RACE) was employed, to identify the transcripts' 5' and 3' ends. DNA sequencing confirmed the two ends for each long non-coding RNA detected in the locus, which we name lncRNA#1 and lncRNA#9.

Mapping of DNase I hypersensitive (HS) sites in a gene locus has been a valuable tool for the identification of active gene regulatory elements. We employed this approach on the two highly conserved among primates, *LT/TNF* locus sequences flanking the 5' and 3' ends of the transcripts (**Fig. 24** and **25**).

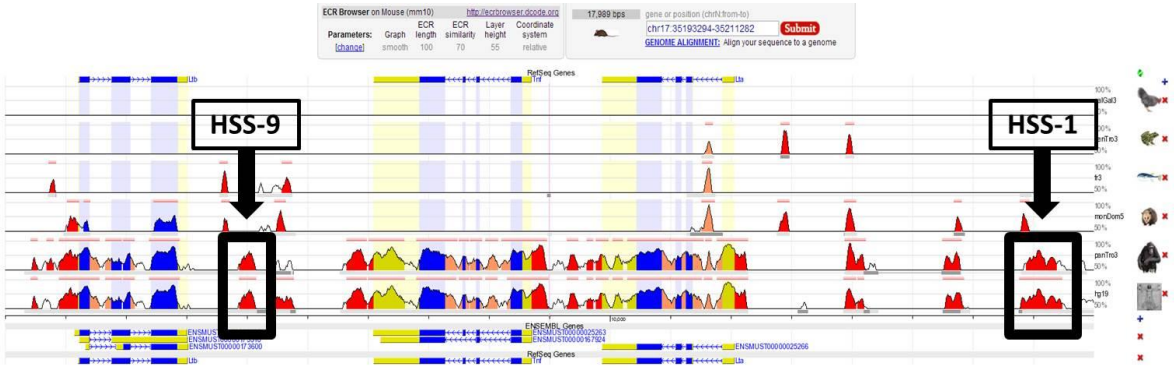

Figure 24. Cross-species conservation of DNA sequences on the 5'end of each lncRNA in the *Tnfα* locus, designated as #1 and #9.[138]

Two DNase I hypersensitive sites, HSS1 and HSS9, were uncovered and upon cloning of these conserved sequences, luciferase reporter assays were performed to measure their potential promoter activity (**Fig. 25**). We found that both sequences with DNase I hypersensitivity were capable in activating transcription and that this activity was LPS-induced.

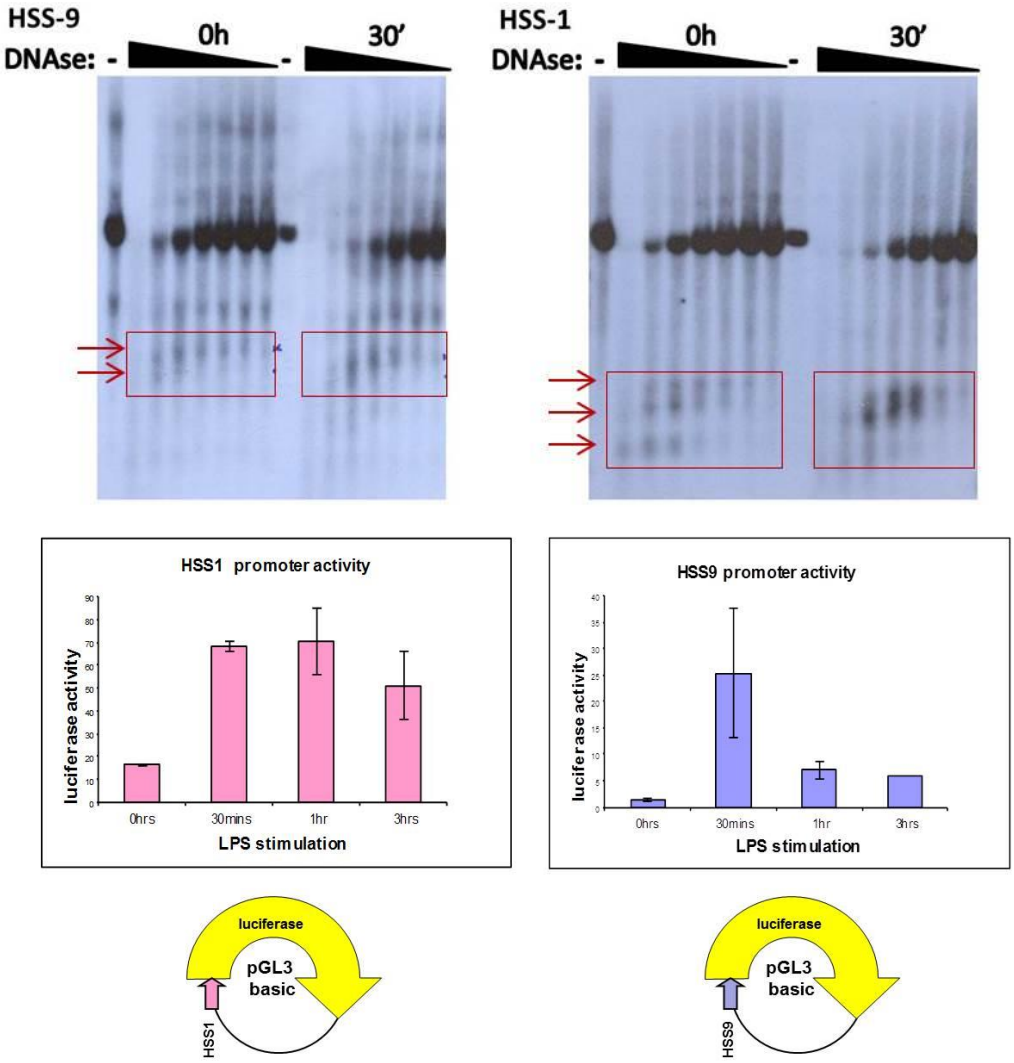

Figure 25. Above: DNase I Hypersensitivity mapping on the conserved DNA sequences directly 5' of the long transcripts on the *LT/TNF* locus. Two LPS-induced sites emerge for the sequence upstream and three for the sequence downstream the *Tnfα* gene (see Fig. 44). Below: Luciferase assays with the two DNA sequences show that HSS-1 and HSS-9 have LPS-inducible transcription activation capabilities.

The two lncRNAs' expression pattern was investigated with quantitative RT-PCR and biotinylated strand-specific riboprobes were used in RNA-DNA FISH experiments to detect each nascent lncRNA separately (**Fig. 26** and unpublished data).

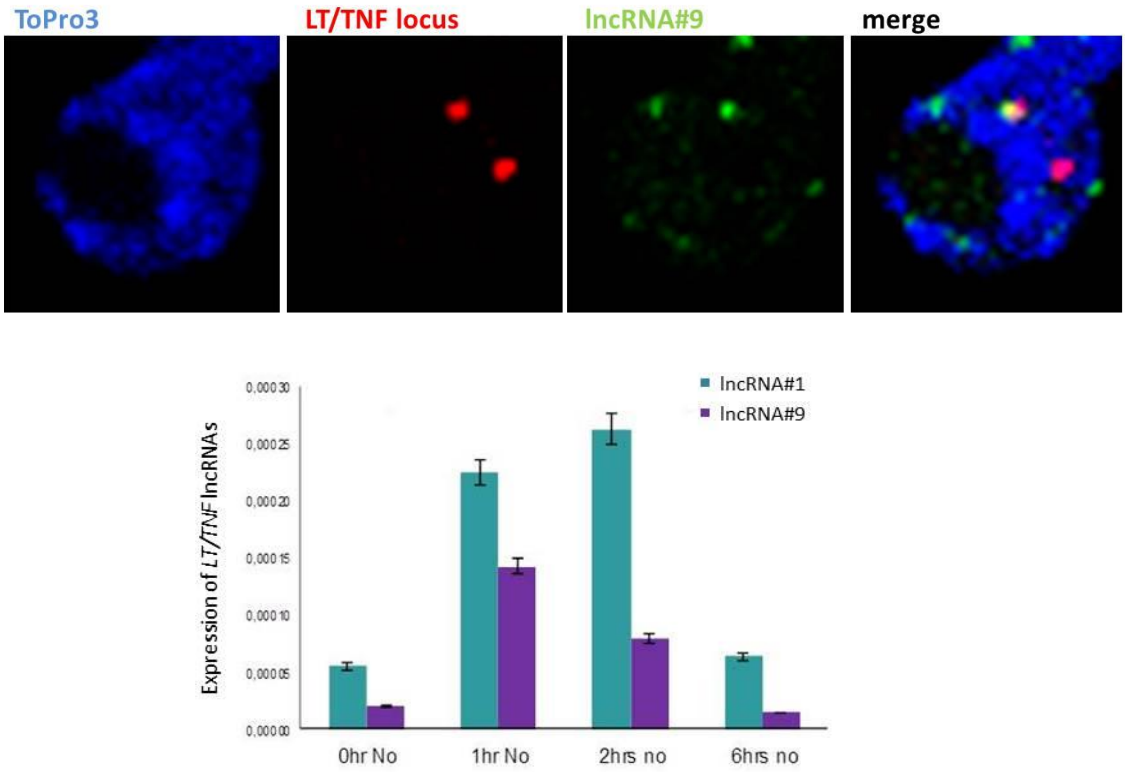

Figure 26. Above: RNA-DNA FISH representative images showing lncRNA#9 expressed in LPS-stimulated Raw 264.7 macrophages. Below: Expression of lncRNA#1 and lncRNA#9 in Raw 264.7 macrophages untreated or stimulated for 1h, 2h and 6h with LPS.

Long non-coding RNAs play a major role in gene regulation and the regulation of epigenetic events, and, more specifically, the long transcripts involved in X-chromosome inactivation have been associated with the homologous pairing that takes place at the onset of XCI. Thus, we hypothesized that these two lncRNAs might play a role in the association of the *Tnfα* alleles. To explore their involvement in the *Tnfα* homologous pairing we employed RNA-DNA FISH experiments after the treatment with LNAs (Locked Nucleic Acids) for each transcript separately, and measured their effect on *Tnfα* NDs and allelic expression. Interestingly, the two lncRNAs had distinctly different roles in the *Tnfα* homologous pairing and expression. Knock-down of lncRNA#1 using locked nucleic acid technology rendered *Tnfα* transcription bi-allelic, before and after the anticipated activation time (**Fig. 27**).

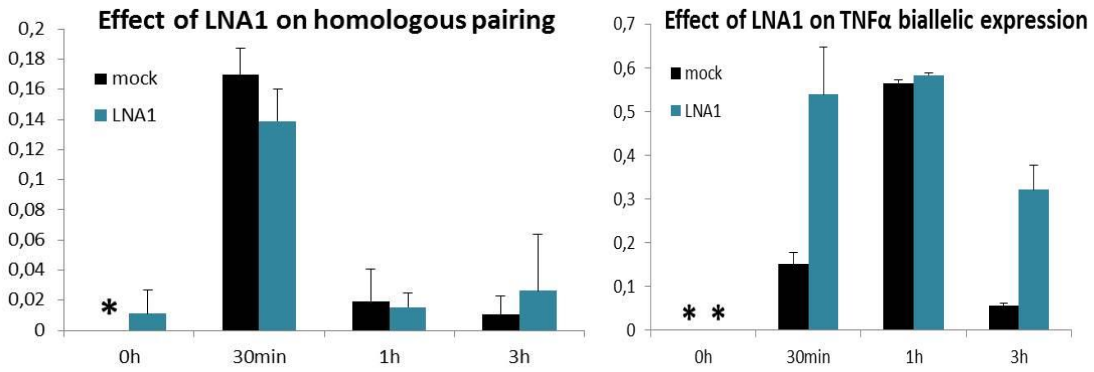

Figure 27. Effect of lncRNA#1 knock-down on *Tnfα* homologous pairing and bi-allelic gene expression.

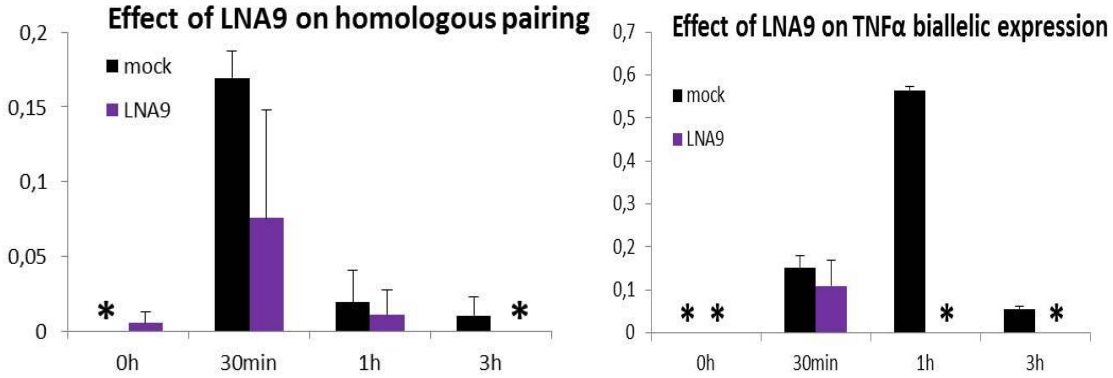

Figure 28. Effect of lncRNA#9 knock-down on *Tnfα* homologous pairing and bi-allelic gene expression.

On the other hand, knock-down of lncRNA#9 impaired both *Tnfα* locus homologous pairing and its bi-allelic gene expression (**Fig. 28**).

To summarize, we have identified two LPS-inducible DNase I hypersensitive sites in the *LT/TNF* locus in murine macrophages. HSS-1 acts as the promoter that drives the expression of lncRNA#1, necessary for preventing both *Tnfα* alleles from expressing *Tnfα* mRNA. HSS-9 can act as the promoter of lncRNA#9, complementary to lncRNA#1, the knock-down of which blocks the switch from mono- to bi-allelic *Tnfα* mRNA expression from the *Tnfα* gene.

5.7 Potential mechanism for allelic expression regulation

Summarizing our results, we investigated the subnuclear localization of the *Tnfα* alleles in LPS-stimulated Raw 264.7 murine macrophage cells. Fluorescence *in situ* hybridization (FISH) experiments provided evidence on the existence and kinetics of homologous pairing of the *Tnfα* alleles. We found that the maximal proximity of *Tnfα* alleles occurs 30 minutes upon LPS stimulation of macrophages at which time the gene was monoallelically expressed while upon homologous association, the maximal expression levels of *Tnfα* were detected in one hour upon stimulation where the *Tnfα* gene was biallelically expressed. This pairing was specific to the *Tnfα* locus, it was LPS-induced and actin-mediated. TNFα stimulation, in contrast to LPS induction, failed to activate the pairing phenomenon and, as a result *Tnfα* bi-allelic expression was reduced. By blocking actin polymerization with Latrunculin A (LTA), *Tnfα* homologous pairing did not occur and bi-allelic expression was impeded.

Moreover, we showed that *Tnfα* bi-allelic expression depends on homologous pairing, disruption of which also renders *Tnfα* expression solely mono-allelic (**Fig. 29**).

In addition, ThPOK and PKM2 proteins mediated *Tnfα* homologous pairing. ThPOK (T-helper-inducing POZ-Kruppel-like factor) was *in silico* predicted to be the mammalian homolog of the *Drosophila* GAGA factor and we showed that it regulates *Tnfα* homologous pairing and bi-allelic expression, by binding on *Tnfα* promoter. Electrophoretic Mobility Shift Assays (EMSA), SouthWestern blotting, Yeast One Hybrid assays and DNA Affinity Chromatography coupled to Mass Spectrometry (LC-ESI-MS/MS) were all employed to detect and identify protein complexes that bind on GA repeats and activate transcription. PKM2 (pyruvate kinase isoform M2), which was recently shown to directly regulate transcription as a protein kinase, was identified to bind GA repeat DNA elements in the *Tnfα* promoter and control homologous pairing, as well as *Tnfα* bi-allelic transcription. Lastly, a ThPOK-PKM2 interaction on the *LT/TNF* locus was also detected.

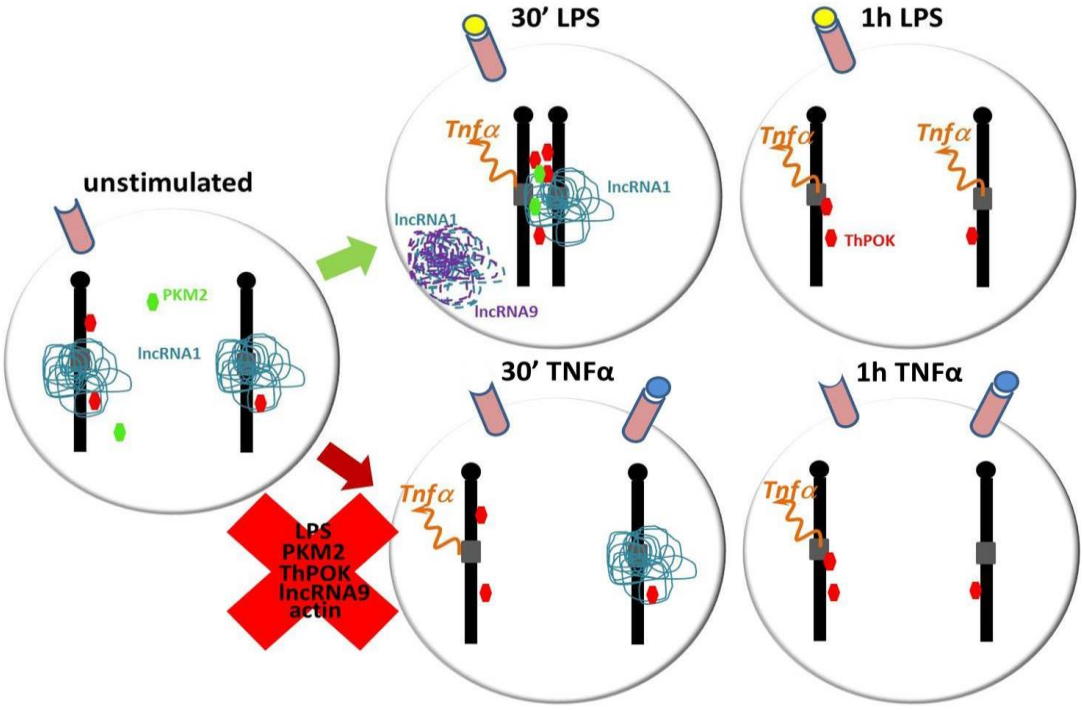

Figure 29. Potential mechanism for the *Tnfα* allelic expression regulation. Effect of TNFα stimulation, actin polymerization disruption, PKM2, ThPOK and lncRNA#9 knock down on *Tnfα* homologous pairing and allelic expression.

We confirmed that two complementary long non-coding RNA transcripts are expressed in the *LT/TNF* locus. RACE (Rapid Amplification of cDNA Ends) was employed to verify the transcripts' start sites and ends and qRT-PCR confirmed their expression profile. DNase I Hypersensitivity assays were performed upstream the transcription start sites of the two transcripts and the promoter activity of two DNA sequence regions with DNase I hypersensitivity (HSS1 and HSS9) was measured by luciferase reporter gene assays. LNA-mediated knock down of lncRNA#1 (downstream of HSS-1) rendered *Tnfα* gene transcription solely bi-allelic. On the other hand, knock down of lncRNA#9 (downstream of HSS-9) impaired the *Tnfα* homologous pairing and consequently, its bi-allelic expression (**Fig. 29** and **30**).

6. DISCUSSION

Our data revealed an LPS-induced, actin-mediated homologous pairing phenomenon that takes place between the two *Tnfα* alleles and regulates the mono- to bi-allelic switch in *Tnfα* gene expression in murine macrophages.

Although evidence of regional pairing of homologous chromosomes has increased over recent years, it still remains unclear how the two alleles find each other and what mediates and/or sustains these associations. It has been speculated to be either due to the properties of a larger region of the chromosome or due to the specific settings provided by distinct genomic elements.

Homologous pairing has been documented in several studies, the most prominent of which is the establishment of mono-allelic silencing of the X-chromosome. In X inactivation, the two chromosomes pair, *Tsix* is transiently downregulated, to allow the mono-allelic expression of *Xist* to reach levels sufficient for the coating and silencing of the inactive X chromosome [23]. Pairing is also found to occur between the immunoglobulin loci. In this case, one of the two alleles undergoes recombination-dependent cleavage, while the other is heterochromatinized [196]. In imprinted loci it is easier to differentiate between the two loci as they are differentially pre-marked. Homologous pairing in the cases of Prader-Willi/Angelman region in humans or the *Kcnq1* cluster has been extensively studied and in these cases too, the result of the association was mono-allelic expression [84, 85]. All these examples are associated with allelic exclusion, and it has been suggested that homologous pairing is a feature of regions in which one allele is silenced and mono-allelic expression is maintained. However, there are also examples of somatic homologous pairing, which are not associated with maintenance of mono-allelic expression.

Moreover, homologous pairing has also been associated with DNA repair of double strand breaks (DSBs). Although non-homologous end joining (NHEJ) is more commonly used in mammals for the repair of such DNA damage, homologous recombination – predominantly used in yeast – is also found in mammals in the case of replication induced

breaks [197, 198].

Krueger *et al.* recently showed that homologous pairing is not dependent on imprinting or allelic exclusion, in fact, loss of imprinting did not change pairing frequency. Instead, they found that somatic homologous pairing, although rare, depends on chromosomal position and transcriptional activity [199].

Our data are in line with these findings, since we describe an allelic association which is (1) transient and quickly established, thus independent of imprinting status and (2) does not occur to maintain allelic exclusion, but, instead, activates the expression of *Tnfα* from the second allele as well. Either used as a counting mechanism, as in X inactivation, or as a way of *information* exchange *in trans*, *Tnfα* homologous pairing ensures the production of maximal *Tnfα* mRNA levels necessary for macrophage immune response.

There have been recent studies in a case of allelic switch in expression, involving the *Nanog* locus, which undergoes reprogramming to biallelically express the gene during the transition towards ground-state pluripotency in the blastocyst's epiblast. It was confirmed that the starting mono-allelic expression of *Nanog* in 2-, 4- and 8-cell-stage embryos was random and not affected by imprinting. Specifically it was established that asynchronous replication, a characteristic trait of monoallelically expressed genes, was dynamically altered to synchronous replication in the case of *Nanog*, when its expression switched from mono- to bi-allelic [200, 201, 202]. It is in line with our finding that dose dependent regulation can be established through allelic switching.

We have also implicated a protein-protein interaction on the *Tnfα* promoter, between a protein kinase with transactivation potential and a transcription factor considered to be the mammalian homolog of the Drosophila GAGA factor in transvection. PKM2, a kinase involved in glycolysis and in cancer metabolism, is surprisingly capable of functioning as a protein kinase in the nucleus. It has been involved in several phosphorylation and transactivation events and has been found to bind on DNA, either indirectly or directly. It is intriguing, however, how a glycolytic enzyme is able to simultaneously function as a protein kinase. Studies of PKM2 in tumor cells, where it is predominantly found in its dimeric form, unable to convert PEP to pyruvate [203], give a possible answer to this question. Tetrameric PKM2 in the cytoplasm interacts with several

glycolytic enzymes or oncoproteins, which are able to stimulate the conversion of PKM2 to a dimer [204]. In addition, the binding of phosphorylated tyrosine peptides to PKM2 decreases its enzymatic activity [168]. This was found to be caused possibly by the exposure of a hydrophobic part of the dimeric protein, able to bind a protein substrate, in contrast to the tetrameric form, where this site would be inaccessible [205, 206]. Thus, even without a prominent DNA binding-domain, it is possible that LPS stimulation induces this switch to dimeric PKM2, via an interaction in the cytoplasm, facilitating PKM2 to bind ThPOK, as well as the *Tnfα* promoter. Although a phosphorylation event may be occurring during the binding of PKM2 to ThPOK, altering the function of the latter (ThPOK contains tyrosine residues predicted to be phosphorylated by protein kinases), we have proven that both proteins are functionally necessary for the establishment of *Tnfα* homologous pairing, as well as the switch in allelic expression.

There are several issues that still need to be addressed, though. The study of macrophage activation and *Tnfα* expression has returned conflicting evidence. The elucidation of the regulatory regions and transcription factors involved in *Tnfα* gene transcription is of critical importance, since deregulation of TNFα is associated with multiple disease states. As discussed above, NF-κB was believed to play a role in *Tnfα* transcription in LPS-stimulated macrophages, due to κB sites on the gene's promoter. It was later shown, however, that these sites are neither conserved in humans, nor do they function as true inducible NF-κB sites when fused to a heterologous promoter. In addition, it has been concluded that the proximal promoter of *Tnfα* is sufficient to activate expression at maximal levels and that NF-κB binding to the distal promoter may only contribute to the maintenance of *Tnfα* expression following induction of the gene [156]. This post-induction role of NF-κB in *Tnfα* expression was further strengthened by the finding that LPS induces an oscillatory behaviour of NF-κB [207, 208], which has two phases [209]: in the early phase (within 1 hour of macrophage activation) *Tnfα* is expressed via the activation of TLR4 and MyD88, whereas in the second, later phase, the already produced TNFα, acts in an autocrine fashion to activate NF-κB via the TNFR, MyD88-independent signaling pathway [121]. Although we did not directly address the role of NF-κB in the homologous paring of the *Tnfα* alleles, it is evident that the mono-allelic expression observed as soon as 10min upon LPS stimulation, the homologous association itself, as

well as the allelic switch in transcription, are part of the early phase of LPS induction. In 2007, Tsytsykova *et al*. concluded that NF-κB is not sufficient for the induction of *Tnfα* transcription. In line with this, we present here an LPS-specific, post-induction mechanism that activates a switch towards bi-allelic expression of *Tnfα*, allowing the cell to reach the necessary maximal mRNA levels.

Furthermore, we have implicated two long complementary transcripts, expressed by the *LT/TNF* locus, in the control of the switch in allelic expression of the *Tnfα* gene. The two lncRNAs involved seem to counteract one another by means of transcript quantity and localization. Unpublished preliminary data show that lncRNA#1 is expressed (and possibly stored within the nucleus) and is gathered around the locus (visualized by means of an increase in intensity of RNA FISH signals on the *LT/TNF* locus, unaccounted for by quantitative RT-PCR) only after LPS-induction of the macrophages.

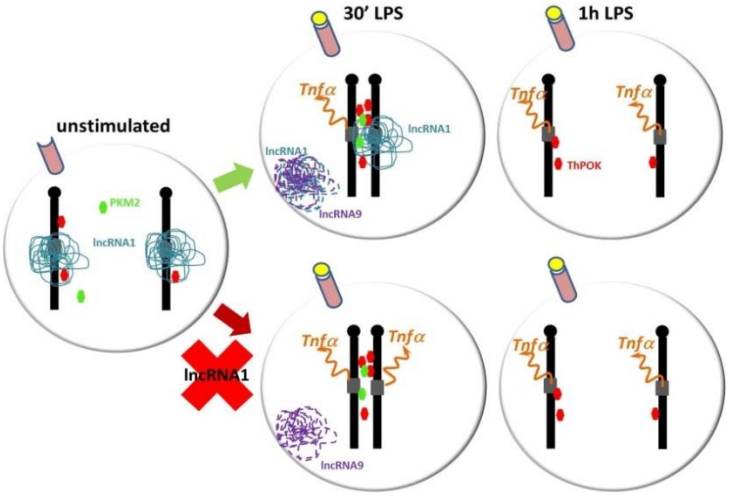

Figure 30. Potential mechanism for the *Tnfα* allelic expression regulation. Effect of lncRNA#1 knock down on *Tnfα* homologous pairing and allelic expression.

In correspondence to the function of *Xist* in X inactivation, we may suggest that lncRNA#1 blocks *Tnfα* transcription from the second allele by coating the locus 30min upon LPS stimulation (**Fig. 30**), supported by the fact that LNA-mediated knock-down of this transcript allows both alleles to express *Tnfα.*

At the same time, lncRNA#9 seems to function oppositely by displacing its complementary lncRNA#1 upon 1h of LPS stimulation (RNA-DNA FISH experiments show lncRNA#1 to be dispersed around the locus after 30min of LPS stimulation), allowing the switch to bi-allelic expression. LNA-knock-down of lncRNA#9 can both

disrupt homologous pairing, as well as render *Tnfα* expression mono-allelic, possibly by allowing lncRNA#1 to coat the locus. In addition, ChIP experiments with a-ThPOK antibodies showed that ThPOK binds on both promoters of the two long transcripts, HSS-1 and HSS-9. It would thus be of interest to investigate whether ThPOK mediates transcription from these promoters.

We should keep in mind that DNA is not randomly distributed within the nuclear space. The nucleus includes several sub-compartments (nucleolus, speckles, transcription factories, PML bodies, chromosomal territories, Cajal bodies, etc), in any of which inter-chromosomal interactions could take place. Besides transcription, genomic organization is correlated with the coordination of replication and recombination of DNA, based on which it is widely accepted that the architectural organization of DNA in the nucleus is closely associated with genomic function. For example, the inactive X chromosome is continuously targeted to a perinucleolar compartment to maintain its epigenetic state after homologous pairing of the two chromosomes[210]. In the case of *Tnfα* it is difficult to differentiate between the two alleles in the macrophage cell. However by measuring the total number of *Tnfα* alleles that are found adjacent to the nucleolus upon LPS induction of Raw 264.7, we observed that 54% of all alleles were adjacent to the nucleolus (alleles inside or touching the periphery of the nucleolus were only counted) 1h upon LPS stimulation, compared to the 27% found adjacent in untreated cells. However, we did not observe a relationship between the perinucleolar positioning of the *Tnfα* alleles and their expression state or homologous pairing.

Since the regulatory elements of the *Tnfα* alleles (HSS-1, HSS-9, *Tnfα* proximal and distal promoters) are highly conserved, and the proteins shown to be involved in the homologous pairing also exist in human macrophages, we would also expect a conservation of the phenomenon as well. Although the expression kinetics of *Tnfα* in human THP-1 monocytes (differentiated into macrophages with PMA) has been found to be similar with those of murine Raw 264.7 macrophages, we were unable to study the subnuclear localization of the *Tnfα* alleles, because THP-1 cells are stably triploid for the *LT/TNF* locus.

Further investigation in the mechanisms involved in the induction and maintenance of *Tnfα* maximal levels is of great importance for both basic research and

clinical practice. Firstly because a mechanism controlling allelic expression may be occurring in a wide range of inducible systems which have not been noticed and secondly because the identification of ways to exploit such a phenomenon could be used in the future to study and possibly resolve the deregulation of *Tnfα* gene expression in disease models.

7. REFERENCES

1. Li Q PK, Fang X, Stamatoyannopoulos G. Locus control regions. *Blood* 2002, **9**(100)**:** 3077-3086.

2. Maston GA ES, Green MR. Transcriptional regulatory elements in the human genome. *Annu Rev Genomics Hum Genet* 2006(7)**:** 29-59.

3. Ogbourne S, Antalis TM. Transcriptional control and the role of silencers in transcriptional regulation in eukaryotes. *The Biochemical journal* 1998, **331 (Pt 1):** 1-14.

4. Henikoff S, Comai L. Trans-sensing effects: the ups and downs of being together. *Cell* 1998, **93**(3)**:** 329-332.

5. Selker JTIaEU. Gene silencing in filamentous fungi: RIP, MIP and quelling. *J Genet* 1996, **75:** 313-324.

6. Rossignol JL, Faugeron G. Gene inactivation triggered by recognition between DNA repeats. *Experientia* 1994, **50**(3)**:** 307-317.

7. Galagan JE, Selker EU. RIP: the evolutionary cost of genome defense. *Trends in genetics : TIG* 2004, **20**(9)**:** 417-423.

8. Wu CT. Transvection, nuclear structure, and chromatin proteins. *The Journal of cell biology* 1993, **120**(3)**:** 587-590.

9. Duncan IW. Transvection effects in Drosophila. *Annual review of genetics* 2002, **36:** 521-556.

10. Gelbart ME, Kuroda MI. Drosophila dosage compensation: a complex voyage to the X chromosome. *Development* 2009, **136**(9)**:** 1399-1410.

11. Mank JE. The W, X, Y and Z of sex-chromosome dosage compensation. *Trends in genetics : TIG* 2009, **25**(5)**:** 226-233.

12. Dementyeva EV, Shevchenko AI, Zakian SM. X-chromosome upregulation and inactivation: two sides of the dosage compensation mechanism in mammals. *BioEssays : news and reviews in molecular, cellular and developmental biology* 2009, **31**(1)**:** 21-28.

13. Chandler VL. Paramutation: from maize to mice. *Cell* 2007, **128**(4)**:** 641-645.

14. Chandler VL, Stam M. Chromatin conversations: mechanisms and implications of paramutation. *Nature reviews* 2004, **5**(7)**:** 532-544.

15. Miele A, Dekker J. Long-range chromosomal interactions and gene regulation. *Molecular bioSystems* 2008, **4**(11)**:** 1046-1057.

16. Higgs DR, Wood WG. Long-range regulation of alpha globin gene expression during erythropoiesis. *Current opinion in hematology* 2008, **15**(3)**:** 176-183.

17. Palstra RJ, de Laat W, Grosveld F. Beta-globin regulation and long-range interactions. *Advances in genetics* 2008, **61:** 107-142.

18. Krueger C, Osborne CS. Raising the curtains on interchromosomal interactions. *Trends in genetics : TIG* 2006, **22**(12)**:** 637-639.

19. Ideraabdullah FY, Vigneau S, Bartolomei MS. Genomic imprinting mechanisms in mammals. *Mutation research* 2008, **647**(1-2)**:** 77-85.

20. Ling JQ, Li T, Hu JF, Vu TH, Chen HL, Qiu XW*, et al.* CTCF mediates interchromosomal colocalization between Igf2/H19 and Wsb1/Nf1. *Science* 2006, **312**(5771)**:** 269-272.

21. Xu N, Tsai CL, Lee JT. Transient homologous chromosome pairing marks the onset of X inactivation. *Science* 2006, **311**(5764)**:** 1149-1152.

22. Phillips JE, Corces VG. CTCF: master weaver of the genome. *Cell* 2009, **137**(7)**:** 1194-1211.

23. Anguera MC, Sun BK, Xu N, Lee JT. X-chromosome kiss and tell: how the Xs go their separate ways. *Cold Spring Harbor symposia on quantitative biology* 2006, **71:** 429-437.

24. Augui S, Filion GJ, Huart S, Nora E, Guggiari M, Maresca M*, et al.* Sensing X chromosome pairs before X inactivation via a novel X-pairing region of the Xic. *Science* 2007, **318**(5856)**:** 1632-1636.

25. Lomvardas S, Barnea G, Pisapia DJ, Mendelsohn M, Kirkland J, Axel R. Interchromosomal interactions and olfactory receptor choice. *Cell* 2006, **126**(2)**:** 403-413.

26. Fuss SH, Omura M, Mombaerts P. Local and cis effects of the H element on expression of odorant receptor genes in mouse. *Cell* 2007, **130**(2)**:** 373-384.

27. Spilianakis CG, Lalioti MD, Town T, Lee GR, Flavell RA. Interchromosomal associations between alternatively expressed loci. *Nature* 2005, **435**(7042)**:** 637-645.

28. Lee GR, Kim ST, Spilianakis CG, Fields PE, Flavell RA. T helper cell differentiation: regulation by cis elements and epigenetics. *Immunity* 2006, **24**(4)**:** 369-379.

29. Consortium EP, Dunham I, Kundaje A, Aldred SF, Collins PJ, Davis CA*, et al.* An integrated encyclopedia of DNA elements in the human genome. *Nature* 2012, **489**(7414)**:** 57-74.

30. Gerstein MB, Kundaje A, Hariharan M, Landt SG, Yan KK, Cheng C*, et al.* Architecture of the human regulatory network derived from ENCODE data. *Nature* 2012, **489**(7414)**:** 91-100.

31. Sanyal A, Lajoie BR, Jain G, Dekker J. The long-range interaction landscape of gene promoters. *Nature* 2012, **489**(7414)**:** 109-113.

32. Thurman RE, Rynes E, Humbert R, Vierstra J, Maurano MT, Haugen E*, et al.* The accessible chromatin landscape of the human genome. *Nature* 2012, **489**(7414)**:** 75-82.

33. Khrameeva EE, Mironov AA, Fedonin GG, Khaitovich P, Gelfand MS. Spatial proximity and similarity of the epigenetic state of genome domains. *PloS one* 2012, **7**(4)**:** e33947.

34. Granok H, Leibovitch BA, Shaffer CD, Elgin SC. Chromatin. Ga-ga over GAGA factor. *Current biology : CB* 1995, **5**(3)**:** 238-241.

35. Mahmoudi T, Katsani KR, Verrijzer CP. GAGA can mediate enhancer function in trans by linking two separate DNA molecules. *The EMBO journal* 2002, **21**(7)**:** 1775-1781.

36. Lehmann M. Anything else but GAGA: a nonhistone protein complex reshapes chromatin structure. *Trends in genetics : TIG* 2004, **20**(1)**:** 15-22.

37. Adkins NL, Hagerman TA, Georgel P. GAGA protein: a multi-faceted transcription factor.

Biochemistry and cell biology = Biochimie et biologie cellulaire 2006, **84**(4)**:** 559-567.

38. Zaratiegui M, Irvine DV, Martienssen RA. Noncoding RNAs and gene silencing. *Cell* 2007, **128**(4)**:** 763-776.

39. Avner P, Heard E. X-chromosome inactivation: counting, choice and initiation. *Nature reviews Genetics* 2001, **2**(1)**:** 59-67.

40. Nora EP, Heard E. X chromosome inactivation: when dosage counts. *Cell* 2009, **139**(5)**:** 865-867.

41. McKee BD. Homologous pairing and chromosome dynamics in meiosis and mitosis. *Biochimica et biophysica acta* 2004, **1677**(1-3)**:** 165-180.

42. Kelly WG, Aramayo R. Meiotic silencing and the epigenetics of sex. *Chromosome research : an international journal on the molecular, supramolecular and evolutionary aspects of chromosome biology* 2007, **15**(5)**:** 633-651.

43. Nakayashiki H. RNA silencing in fungi: mechanisms and applications. *FEBS letters* 2005, **579**(26)**:** 5950-5957.

44. Cambareri EB, Singer MJ, Selker EU. Recurrence of repeat-induced point mutation (RIP) in Neurospora crassa. *Genetics* 1991, **127**(4)**:** 699-710.

45. Watters MK, Randall TA, Margolin BS, Selker EU, Stadler DR. Action of repeat-induced point mutation on both strands of a duplex and on tandem duplications of various sizes in Neurospora. *Genetics* 1999, **153**(2)**:** 705-714.

46. Grayburn WS, Selker EU. A natural case of RIP: degeneration of the DNA sequence in an ancestral tandem duplication. *Molecular and cellular biology* 1989, **9**(10)**:** 4416-4421.

47. Freitag M, Williams RL, Kothe GO, Selker EU. A cytosine methyltransferase homologue is essential for repeat-induced point mutation in Neurospora crassa. *Proceedings of the National Academy of Sciences of the United States of America* 2002, **99**(13)**:** 8802-8807.

48. Selker EU, Tountas NA, Cross SH, Margolin BS, Murphy JG, Bird AP*, et al.* The methylated component of the Neurospora crassa genome. *Nature* 2003, **422**(6934)**:** 893-897.

49. Singer MJ, Marcotte BA, Selker EU. DNA methylation associated with repeat-induced

point mutation in Neurospora crassa. *Molecular and cellular biology* 1995, **15**(10)**:** 5586-5597.

50. Chandler VL, Eggleston WB, Dorweiler JE. Paramutation in maize. *Plant molecular biology* 2000, **43**(2-3)**:** 121-145.

51. Coe EH. The properties, origin, and mechanism of conversion-type inheritance at the B locus in maize. *Genetics* 1966, **53**(6)**:** 1035-1063.

52. Stam M, Belele C, Ramakrishna W, Dorweiler JE, Bennetzen JL, Chandler VL. The regulatory regions required for B' paramutation and expression are located far upstream of the maize b1 transcribed sequences. *Genetics* 2002, **162**(2)**:** 917-930.

53. Alleman M, Sidorenko L, McGinnis K, Seshadri V, Dorweiler JE, White J*, et al.* An RNA-dependent RNA polymerase is required for paramutation in maize. *Nature* 2006, **442**(7100)**:** 295-298.

54. Erhard KF, Jr., Stonaker JL, Parkinson SE, Lim JP, Hale CJ, Hollick JB. RNA polymerase IV functions in paramutation in Zea mays. *Science* 2009, **323**(5918)**:** 1201-1205.

55. Woodhouse MR, Freeling M, Lisch D. The mop1 (mediator of paramutation1) mutant progressively reactivates one of the two genes encoded by the MuDR transposon in maize. *Genetics* 2006, **172**(1)**:** 579-592.

56. Dorweiler JE, Carey CC, Kubo KM, Hollick JB, Kermicle JL, Chandler VL. mediator of paramutation1 is required for establishment and maintenance of paramutation at multiple maize loci. *The Plant cell* 2000, **12**(11)**:** 2101-2118.

57. Martienssen R. Epigenetic phenomena: paramutation and gene silencing in plants. *Current biology : CB* 1996, **6**(7)**:** 810-813.

58. Rassoulzadegan M, Grandjean V, Gounon P, Vincent S, Gillot I, Cuzin F. RNA-mediated non-mendelian inheritance of an epigenetic change in the mouse. *Nature* 2006, **441**(7092)**:** 469-474.

59. Geyer PK, Green MM, Corces VG. Tissue-specific transcriptional enhancers may act in trans on the gene located in the homologous chromosome: the molecular basis of transvection in Drosophila. *The EMBO journal* 1990, **9**(7)**:** 2247-2256.

60. Lindsley DL, Sandler L, Baker BS, Carpenter AT, Denell RE, Hall JC*, et al.* Segmental

aneuploidy and the genetic gross structure of the Drosophila genome. *Genetics* 1972, **71**(1)**:** 157-184.

61. Georgiev PG, Corces VG. The su(Hw) protein bound to gypsy sequences in one chromosome can repress enhancer-promoter interactions in the paired gene located in the other homolog. *Proceedings of the National Academy of Sciences of the United States of America* 1995, **92**(11)**:** 5184-5188.

62. Morris JR, Chen JL, Geyer PK, Wu CT. Two modes of transvection: enhancer action in trans and bypass of a chromatin insulator in cis. *Proceedings of the National Academy of Sciences of the United States of America* 1998, **95**(18)**:** 10740-10745.

63. Morris JR, Chen J, Filandrinos ST, Dunn RC, Fisk R, Geyer PK*, et al.* An analysis of transvection at the yellow locus of Drosophila melanogaster. *Genetics* 1999, **151**(2)**:** 633-651.

64. http://genepath.med.harvard.edu/WuLab/research.php.

65. Pirrotta V. The genetics and molecular biology of zeste in Drosophila melanogaster. *Advances in genetics* 1991, **29:** 301-348.

66. Wu CT, Goldberg ML. The Drosophila zeste gene and transvection. *Trends in genetics : TIG* 1989, **5**(6)**:** 189-194.

67. Gubb D, Ashburner M, Roote J, Davis T. A novel transvection phenomenon affecting the white gene of Drosophila melanogaster. *Genetics* 1990, **126**(1)**:** 167-176.

68. Biggin MD, Tjian R. Transcription factors that activate the Ultrabithorax promoter in developmentally staged extracts. *Cell* 1988, **53**(5)**:** 699-711.

69. Gilmour DS, Thomas GH, Elgin SC. Drosophila nuclear proteins bind to regions of alternating C and T residues in gene promoters. *Science* 1989, **245**(4925)**:** 1487-1490.

70. Lee H, Kraus KW, Wolfner MF, Lis JT. DNA sequence requirements for generating paused polymerase at the start of hsp70. *Genes & development* 1992, **6**(2)**:** 284-295.

71. Soeller WC, Poole SJ, Kornberg T. In vitro transcription of the Drosophila engrailed gene. *Genes & development* 1988, **2**(1)**:** 68-81.

72. Tsukiyama T, Becker PB, Wu C. ATP-dependent nucleosome disruption at a heat-shock promoter mediated by binding of GAGA transcription factor. *Nature* 1994, **367**(6463)**:** 525-532.

73. Horard B, Tatout C, Poux S, Pirrotta V. Structure of a polycomb response element and in vitro binding of polycomb group complexes containing GAGA factor. *Molecular and cellular biology* 2000, **20**(9)**:** 3187-3197.

74. Strutt H, Cavalli G, Paro R. Co-localization of Polycomb protein and GAGA factor on regulatory elements responsible for the maintenance of homeotic gene expression. *The EMBO journal* 1997, **16**(12)**:** 3621-3632.

75. Bardwell VJ, Treisman R. The POZ domain: a conserved protein-protein interaction motif. *Genes & development* 1994, **8**(14)**:** 1664-1677.

76. Greenberg AJ, Schedl P. GAGA factor isoforms have distinct but overlapping functions in vivo. *Molecular and cellular biology* 2001, **21**(24)**:** 8565-8574.

77. Omichinski JG, Pedone PV, Felsenfeld G, Gronenborn AM, Clore GM. The solution structure of a specific GAGA factor-DNA complex reveals a modular binding mode. *Nature structural biology* 1997, **4**(2)**:** 122-132.

78. Wilkins RC, Lis JT. DNA distortion and multimerization: novel functions of the glutamine-rich domain of GAGA factor. *Journal of molecular biology* 1999, **285**(2)**:** 515-525.

79. Nakayama T, Nishioka K, Dong YX, Shimojima T, Hirose S. Drosophila GAGA factor directs histone H3.3 replacement that prevents the heterochromatin spreading. *Genes & development* 2007, **21**(5)**:** 552-561.

80. Raff JW, Kellum R, Alberts B. The Drosophila GAGA transcription factor is associated with specific regions of heterochromatin throughout the cell cycle. *The EMBO journal* 1994, **13**(24)**:** 5977-5983.

81. Arnoldus EP, Noordermeer IA, Peters AC, Raap AK, Van der Ploeg M. Interphase cytogenetics reveals somatic pairing of chromosome 17 centromeres in normal human brain tissue, but no trisomy 7 or sex-chromosome loss. *Cytogenetics and cell genetics* 1991, **56**(3-4)**:** 214-216.

82. Arnoldus EP, Peters AC, Bots GT, Raap AK, van der Ploeg M. Somatic pairing of chromosome 1 centromeres in interphase nuclei of human cerebellum. *Human genetics*

1989, **83**(3)**:** 231-234.

83. Monajembashi S, Rapp A, Schmitt E, Dittmar H, Greulich KO, Hausmann M. Spatial association of homologous pericentric regions in human lymphocyte nuclei during repair. *Biophysical journal* 2005, **88**(3)**:** 2309-2322.

84. LaSalle JM, Lalande M. Homologous association of oppositely imprinted chromosomal domains. *Science* 1996, **272**(5262)**:** 725-728.

85. Thatcher KN, Peddada S, Yasui DH, Lasalle JM. Homologous pairing of 15q11-13 imprinted domains in brain is developmentally regulated but deficient in Rett and autism samples. *Human molecular genetics* 2005, **14**(6)**:** 785-797.

86. Clerc P, Avner P. Multiple elements within the Xic regulate random X inactivation in mice. *Seminars in cell & developmental biology* 2003, **14**(1)**:** 85-92.

87. Mukherjee BB, Sinha AK. Single-Active-X Hypothesis: Cytological Evidence for Random Inactivation of X-Chromosomes in a Female Mule Complement. *Proceedings of the National Academy of Sciences of the United States of America* 1964, **51:** 252-259.

88. Jeon Y, Sarma K, Lee JT. New and Xisting regulatory mechanisms of X chromosome inactivation. *Current opinion in genetics & development* 2012, **22**(2)**:** 62-71.

89. Kay GF, Barton SC, Surani MA, Rastan S. Imprinting and X chromosome counting mechanisms determine Xist expression in early mouse development. *Cell* 1994, **77**(5)**:** 639-650.

90. Migeon BR, Jeppesen P, Torchia BS, Fu S, Dunn MA, Axelman J*, et al.* Lack of X inactivation associated with maternal X isodisomy: evidence for a counting mechanism prior to X inactivation during human embryogenesis. *American journal of human genetics* 1996, **58**(1)**:** 161-170.

91. Lee JT, Jaenisch R. Long-range cis effects of ectopic X-inactivation centres on a mouse autosome. *Nature* 1997, **386**(6622)**:** 275-279.

92. Lee JT, Strauss WM, Dausman JA, Jaenisch R. A 450 kb transgene displays properties of the mammalian X-inactivation center. *Cell* 1996, **86**(1)**:** 83-94.

93. Marahrens Y. X-inactivation by chromosomal pairing events. *Genes & development* 1999, **13**(20)**:** 2624-2632.

94. Orkin SH. Regulation of globin gene expression in erythroid cells. *European journal of biochemistry / FEBS* 1995, **231**(2)**:** 271-281.

95. Grosveld F, van Assendelft GB, Greaves DR, Kollias G. Position-independent, high-level expression of the human beta-globin gene in transgenic mice. *Cell* 1987, **51**(6)**:** 975-985.

96. Ashe HL, Monks J, Wijgerde M, Fraser P, Proudfoot NJ. Intergenic transcription and transinduction of the human beta-globin locus. *Genes & development* 1997, **11**(19)**:** 2494-2509.

97. Mosser DM, Edwards JP. Exploring the full spectrum of macrophage activation. *Nature reviews Immunology* 2008, **8**(12)**:** 958-969.

98. Verschoor CP, Puchta A, Bowdish DM. The macrophage. *Methods in molecular biology* 2012, **844:** 139-156.

99. O'Shea JJ, Murray PJ. Cytokine signaling modules in inflammatory responses. *Immunity* 2008, **28**(4)**:** 477-487.

100. Lawrence T, Natoli G. Transcriptional regulation of macrophage polarization: enabling diversity with identity. *Nature reviews Immunology* 2011, **11**(11)**:** 750-761.

101. Bauer S, Muller T, Hamm S. Pattern recognition by Toll-like receptors. *Advances in experimental medicine and biology* 2009, **653:** 15-34.

102. Schwartz Y, Svistelnik AV. Functional phenotypes of macrophages and the M1-M2 polarization concept. Part I. Proinflammatory phenotype. *Biochemistry Biokhimiia* 2012, **77**(3)**:** 246-260.

103. Brandt E, Woerly G, Younes AB, Loiseau S, Capron M. IL-4 production by human polymorphonuclear neutrophils. *Journal of leukocyte biology* 2000, **68**(1)**:** 125-130.

104. Kreider T, Anthony RM, Urban JF, Jr., Gause WC. Alternatively activated macrophages in helminth infections. *Current opinion in immunology* 2007, **19**(4)**:** 448-453.

105. Alber A, Howie SE, Wallace WA, Hirani N. The role of macrophages in healing the wounded lung. *International journal of experimental pathology* 2012, **93**(4)**:** 243-251.

106. D'Angelo F, Bernasconi E, Schafer M, Moyat M, Michetti P, Maillard MH*, et al.* Macrophages promote epithelial repair through hepatocyte growth factor secretion. *Clinical and experimental immunology* 2013.

107. Li S, Li B, Jiang H, Wang Y, Qu M, Duan H*, et al.* Macrophage depletion impairs corneal wound healing after autologous transplantation in mice. *PloS one* 2013, **8**(4)**:** e61799.

108. Mantovani A, Biswas SK, Galdiero MR, Sica A, Locati M. Macrophage plasticity and polarization in tissue repair and remodelling. *The Journal of pathology* 2013, **229**(2)**:** 176-185.

109. Sternberg EM. Neural regulation of innate immunity: a coordinated nonspecific host response to pathogens. *Nature reviews Immunology* 2006, **6**(4)**:** 318-328.

110. Hayashi A, Sato T, Kamada N, Mikami Y, Matsuoka K, Hisamatsu T*, et al.* A Single Strain of Clostridium butyricum Induces Intestinal IL-10-Producing Macrophages to Suppress Acute Experimental Colitis in Mice. *Cell host & microbe* 2013, **13**(6)**:** 711-722.

111. Marie Melief S, Schrama CL, M HB, Tiemessen MM, Johannes Hoogduijn M, Fibbe WE*, et al.* Multipotent Stromal Cells Induce Human Regulatory T Cells through a Novel Pathway Involving Skewing of Monocytes towards Anti- Inflammatory Macrophages. *Stem cells* 2013.

112. Zizzo G, Cohen PL. IL-17 stimulates differentiation of human anti-inflammatory macrophages and phagocytosis of apoptotic neutrophils in response to IL-10 and glucocorticoids. *Journal of immunology* 2013, **190**(10)**:** 5237-5246.

113. Balkwill FR, Mantovani A. Cancer-related inflammation: common themes and therapeutic opportunities. *Seminars in cancer biology* 2012, **22**(1)**:** 33-40.

114. Van der Meide PH, Schellekens H. Cytokines and the immune response. *Biotherapy* 1996, **8**(3-4)**:** 243-249.

115. Carswell EA, Old LJ, Kassel RL, Green S, Fiore N, Williamson B. An endotoxin-induced serum factor that causes necrosis of tumors. *Proceedings of the National Academy of Sciences of the United States of America* 1975, **72**(9)**:** 3666-3670.

116. Vassalli P. The pathophysiology of tumor necrosis factors. *Annual review of immunology* 1992, **10:** 411-452.

117. Black RA, Rauch CT, Kozlosky CJ, Peschon JJ, Slack JL, Wolfson MF*, et al.* A metalloproteinase disintegrin that releases tumour-necrosis factor-alpha from cells. *Nature* 1997, **385**(6618)**:** 729-733.

118. Meldrum DR. Tumor necrosis factor in the heart. *The American journal of physiology* 1998, **274**(3 Pt 2)**:** R577-595.

119. Vandenabeele P, Declercq W, Beyaert R, Fiers W. Two tumour necrosis factor receptors: structure and function. *Trends in cell biology* 1995, **5**(10)**:** 392-399.

120. Grell M, Douni E, Wajant H, Lohden M, Clauss M, Maxeiner B*, et al.* The transmembrane form of tumor necrosis factor is the prime activating ligand of the 80 kDa tumor necrosis factor receptor. *Cell* 1995, **83**(5)**:** 793-802.

121. Covert MW, Leung TH, Gaston JE, Baltimore D. Achieving stability of lipopolysaccharide-induced NF-kappaB activation. *Science* 2005, **309**(5742)**:** 1854-1857.

122. Pobezinskaya YL, Liu Z. The role of TRADD in death receptor signaling. *Cell cycle* 2012, **11**(5)**:** 871-876.

123. Takada H, Chen NJ, Mirtsos C, Suzuki S, Suzuki N, Wakeham A*, et al.* Role of SODD in regulation of tumor necrosis factor responses. *Molecular and cellular biology* 2003, **23**(11)**:** 4026-4033.

124. http://commons.wikimedia.org/wiki/File:TNF_signaling.jpg.

125. Ha H, Han D, Choi Y. TRAF-mediated TNFR-family signaling. *Current protocols in immunology / edited by John E Coligan [et al]* 2009, **Chapter 11:** Unit11 19D.

126. Wang Y, Zhang P, Liu Y, Cheng G. TRAF-mediated regulation of immune and inflammatory responses. *Science China Life sciences* 2010, **53**(2)**:** 159-168.

127. Chen G, Goeddel DV. TNF-R1 signaling: a beautiful pathway. *Science* 2002, **296**(5573)**:** 1634-1635.

128. Kolb WP, Granger GA. Lymphocyte in vitro cytotoxicity: characterization of mouse lymphotoxin. *Cellular immunology* 1970, **1**(1)**:** 122-132.

129. Locksley RM, Killeen N, Lenardo MJ. The TNF and TNF receptor superfamilies: integrating

mammalian biology. *Cell* 2001, **104**(4)**:** 487-501.

130. Wajant H, Pfizenmaier K, Scheurich P. Tumor necrosis factor signaling. *Cell death and differentiation* 2003, **10**(1)**:** 45-65.

131. Park SM, Schickel R, Peter ME. Nonapoptotic functions of FADD-binding death receptors and their signaling molecules. *Current opinion in cell biology* 2005, **17**(6)**:** 610-616.

132. Pennarun B, Meijer A, de Vries EG, Kleibeuker JH, Kruyt F, de Jong S. Playing the DISC: turning on TRAIL death receptor-mediated apoptosis in cancer. *Biochimica et biophysica acta* 2010, **1805**(2)**:** 123-140.

133. Verweij CL. Tumour necrosis factor gene polymorphisms as severity markers in rheumatoid arthritis. *Annals of the rheumatic diseases* 1999, **58 Suppl 1:** I20-26.

134. Akassoglou K, Probert L, Kontogeorgos G, Kollias G. Astrocyte-specific but not neuron-specific transmembrane TNF triggers inflammation and degeneration in the central nervous system of transgenic mice. *Journal of immunology* 1997, **158**(1)**:** 438-445.

135. Grewal IS, Grewal KD, Wong FS, Picarella DE, Janeway CA, Jr., Flavell RA. Local expression of transgene encoded TNF alpha in islets prevents autoimmune diabetes in nonobese diabetic (NOD) mice by preventing the development of auto-reactive islet-specific T cells. *The Journal of experimental medicine* 1996, **184**(5)**:** 1963-1974.

136. McDermott MF, Aksentijevich I, Galon J, McDermott EM, Ogunkolade BW, Centola M*, et al.* Germline mutations in the extracellular domains of the 55 kDa TNF receptor, TNFR1, define a family of dominantly inherited autoinflammatory syndromes. *Cell* 1999, **97**(1)**:** 133-144.

137. Xanthoulea S, Pasparakis M, Kousteni S, Brakebusch C, Wallach D, Bauer J*, et al.* Tumor necrosis factor (TNF) receptor shedding controls thresholds of innate immune activation that balance opposing TNF functions in infectious and inflammatory diseases. *The Journal of experimental medicine* 2004, **200**(3)**:** 367-376.

138. http://ecrbrowser.dcode.org/xB.php?db=mm10&location=chr17:35194507-35196305.

139. Pasparakis M, Alexopoulou L, Episkopou V, Kollias G. Immune and inflammatory responses in TNF alpha-deficient mice: a critical requirement for TNF alpha in the formation of primary B cell follicles, follicular dendritic cell networks and germinal centers, and in the maturation of the humoral immune response. *The Journal of*

experimental medicine 1996, **184**(4)**:** 1397-1411.

140. Pasparakis M, Kousteni S, Peschon J, Kollias G. Tumor necrosis factor and the p55TNF receptor are required for optimal development of the marginal sinus and for migration of follicular dendritic cell precursors into splenic follicles. *Cellular immunology* 2000, **201**(1)**:** 33-41.

141. Pfeffer K, Matsuyama T, Kundig TM, Wakeham A, Kishihara K, Shahinian A*, et al.* Mice deficient for the 55 kd tumor necrosis factor receptor are resistant to endotoxic shock, yet succumb to L. monocytogenes infection. *Cell* 1993, **73**(3)**:** 457-467.

142. Rothe J, Lesslauer W, Lotscher H, Lang Y, Koebel P, Kontgen F*, et al.* Mice lacking the tumour necrosis factor receptor 1 are resistant to TNF-mediated toxicity but highly susceptible to infection by Listeria monocytogenes. *Nature* 1993, **364**(6440)**:** 798-802.

143. Aderka D. The potential biological and clinical significance of the soluble tumor necrosis factor receptors. *Cytokine & growth factor reviews* 1996, **7**(3)**:** 231-240.

144. Vallabhapurapu S, Karin M. Regulation and function of NF-kappaB transcription factors in the immune system. *Annual review of immunology* 2009, **27:** 693-733.

145. Verstrepen L, Bekaert T, Chau TL, Tavernier J, Chariot A, Beyaert R. TLR-4, IL-1R and TNF-R signaling to NF-kappaB: variations on a common theme. *Cellular and molecular life sciences : CMLS* 2008, **65**(19)**:** 2964-2978.

146. Mogensen TH. Pathogen recognition and inflammatory signaling in innate immune defenses. *Clinical microbiology reviews* 2009, **22**(2)**:** 240-273, Table of Contents.

147. Colonna M. TLR pathways and IFN-regulatory factors: to each its own. *European journal of immunology* 2007, **37**(2)**:** 306-309.

148. Arnett HA, Mason J, Marino M, Suzuki K, Matsushima GK, Ting JP. TNF alpha promotes proliferation of oligodendrocyte progenitors and remyelination. *Nature neuroscience* 2001, **4**(11)**:** 1116-1122.

149. Grell M, Becke FM, Wajant H, Mannel DN, Scheurich P. TNF receptor type 2 mediates thymocyte proliferation independently of TNF receptor type 1. *European journal of immunology* 1998, **28**(1)**:** 257-263.

150. Holloway AF, Rao S, Shannon MF. Regulation of cytokine gene transcription in the

immune system. *Molecular immunology* 2002, **38**(8)**:** 567-580.

151. Collart MA, Baeuerle P, Vassalli P. Regulation of tumor necrosis factor alpha transcription in macrophages: involvement of four kappa B-like motifs and of constitutive and inducible forms of NF-kappa B. *Molecular and cellular biology* 1990, **10**(4)**:** 1498-1506.

152. Kuprash DV, Udalova IA, Turetskaya RL, Kwiatkowski D, Rice NR, Nedospasov SA. Similarities and differences between human and murine TNF promoters in their response to lipopolysaccharide. *Journal of immunology* 1999, **162**(7)**:** 4045-4052.

153. Udalova IA, Knight JC, Vidal V, Nedospasov SA, Kwiatkowski D. Complex NF-kappaB interactions at the distal tumor necrosis factor promoter region in human monocytes. *The Journal of biological chemistry* 1998, **273**(33)**:** 21178-21186.

154. Drouet C, Shakhov AN, Jongeneel CV. Enhancers and transcription factors controlling the inducibility of the tumor necrosis factor-alpha promoter in primary macrophages. *Journal of immunology* 1991, **147**(5)**:** 1694-1700.

155. Goldfeld AE, Doyle C, Maniatis T. Human tumor necrosis factor alpha gene regulation by virus and lipopolysaccharide. *Proceedings of the National Academy of Sciences of the United States of America* 1990, **87**(24)**:** 9769-9773.

156. Tsytsykova AV, Falvo JV, Schmidt-Supprian M, Courtois G, Thanos D, Goldfeld AE. Post-induction, stimulus-specific regulation of tumor necrosis factor mRNA expression. *The Journal of biological chemistry* 2007, **282**(16)**:** 11629-11638.

157. Falvo JV, Jasenosky LD, Kruidenier L, Goldfeld AE. Epigenetic Control of Cytokine Gene Expression: Regulation of the TNF/LT Locus and T Helper Cell Differentiation. *Advances in immunology* 2013, **118:** 37-128.

158. Sandoval J, Pereda J, Rodriguez JL, Escobar J, Hidalgo J, Joosten LA*, et al.* Ordered transcriptional factor recruitment and epigenetic regulation of tnf-alpha in necrotizing acute pancreatitis. *Cellular and molecular life sciences : CMLS* 2010, **67**(10)**:** 1687-1697.

159. Sullivan KE, Reddy AB, Dietzmann K, Suriano AR, Kocieda VP, Stewart M*, et al.* Epigenetic regulation of tumor necrosis factor alpha. *Molecular and cellular biology* 2007, **27**(14)**:** 5147-5160.

160. Falvo JV, Tsytsykova AV, Goldfeld AE. Transcriptional control of the TNF gene. *Current directions in autoimmunity* 2010, **11:** 27-60.

161. Tsytsykova AV, Rajsbaum R, Falvo JV, Ligeiro F, Neely SR, Goldfeld AE. Activation-dependent intrachromosomal interactions formed by the TNF gene promoter and two distal enhancers. *Proceedings of the National Academy of Sciences of the United States of America* 2007, **104**(43)**:** 16850-16855.

162. Ferguson EC, Rathmell JC. New roles for pyruvate kinase M2: working out the Warburg effect. *Trends in biochemical sciences* 2008, **33**(8)**:** 359-362.

163. Gupta V, Bamezai RN. Human pyruvate kinase M2: a multifunctional protein. *Protein science : a publication of the Protein Society* 2010, **19**(11)**:** 2031-2044.

164. Harris I, McCracken S, Mak TW. PKM2: a gatekeeper between growth and survival. *Cell research* 2012, **22**(3)**:** 447-449.

165. Chen M, David CJ, Manley JL. Concentration-dependent control of pyruvate kinase M mutually exclusive splicing by hnRNP proteins. *Nature structural & molecular biology* 2012, **19**(3)**:** 346-354.

166. David CJ, Chen M, Assanah M, Canoll P, Manley JL. HnRNP proteins controlled by c-Myc deregulate pyruvate kinase mRNA splicing in cancer. *Nature* 2010, **463**(7279)**:** 364-368.

167. http://atlasgeneticsoncology.org/Genes/PKM2ID41728ch15q22.html.

168. Christofk HR, Vander Heiden MG, Wu N, Asara JM, Cantley LC. Pyruvate kinase M2 is a phosphotyrosine-binding protein. *Nature* 2008, **452**(7184)**:** 181-186.

169. Anastasiou D, Yu Y, Israelsen WJ, Jiang JK, Boxer MB, Hong BS*, et al.* Pyruvate kinase M2 activators promote tetramer formation and suppress tumorigenesis. *Nature chemical biology* 2012, **8**(10)**:** 839-847.

170. Yang W, Lu Z. Regulation and function of pyruvate kinase M2 in cancer. *Cancer letters* 2013.

171. Gao X, Wang H, Yang JJ, Liu X, Liu ZR. Pyruvate kinase M2 regulates gene transcription by acting as a protein kinase. *Molecular cell* 2012, **45**(5)**:** 598-609.

172. Semenova G, Chernoff J. PKM2 enters the morpheein academy. *Molecular cell* 2012, **45**(5)**:** 583-584.

173. Yang W, Xia Y, Hawke D, Li X, Liang J, Xing D*, et al.* PKM2 phosphorylates histone H3 and promotes gene transcription and tumorigenesis. *Cell* 2012, **150**(4)**:** 685-696.

174. Hoshino A, Hirst JA, Fujii H. Regulation of cell proliferation by interleukin-3-induced nuclear translocation of pyruvate kinase. *The Journal of biological chemistry* 2007, **282**(24)**:** 17706-17711.

175. Sajad M, Zargan J, Zargar MA, Sharma J, Umar S, Arora R*, et al.* Quercetin prevents protein nitration and glycolytic block of proliferation in hydrogen peroxide insulted cultured neuronal precursor cells (NPCs): Implications on CNS regeneration. *Neurotoxicology* 2013, **36:** 24-33.

176. Stetak A, Veress R, Ovadi J, Csermely P, Keri G, Ullrich A. Nuclear translocation of the tumor marker pyruvate kinase M2 induces programmed cell death. *Cancer research* 2007, **67**(4)**:** 1602-1608.

177. Szokoloczi O, Schwab R, Petak I, Orfi L, Pap A, Eberle AN*, et al.* TT232, a novel signal transduction inhibitory compound in the therapy of cancer and inflammatory diseases. *Journal of receptor and signal transduction research* 2005, **25**(4-6)**:** 217-235.

178. Lee J, Kim HK, Han YM, Kim J. Pyruvate kinase isozyme type M2 (PKM2) interacts and cooperates with Oct-4 in regulating transcription. *The international journal of biochemistry & cell biology* 2008, **40**(5)**:** 1043-1054.

179. Luo W, Hu H, Chang R, Zhong J, Knabel M, O'Meally R*, et al.* Pyruvate kinase M2 is a PHD3-stimulated coactivator for hypoxia-inducible factor 1. *Cell* 2011, **145**(5)**:** 732-744.

180. Yang W, Xia Y, Ji H, Zheng Y, Liang J, Huang W*, et al.* Nuclear PKM2 regulates beta-catenin transactivation upon EGFR activation. *Nature* 2011, **480**(7375)**:** 118-122.

181. Ignacak J, Stachurska MB. The dual activity of pyruvate kinase type M2 from chromatin extracts of neoplastic cells. *Comparative biochemistry and physiology Part B, Biochemistry & molecular biology* 2003, **134**(3)**:** 425-433.

182. Ho IC, Tai TS, Pai SY. GATA3 and the T-cell lineage: essential functions before and after T-helper-2-cell differentiation. *Nature reviews Immunology* 2009, **9**(2)**:** 125-135.

183. Naito T, Tanaka H, Naoe Y, Taniuchi I. Transcriptional control of T-cell development. *International immunology* 2011, **23**(11)**:** 661-668.

184. Taniuchi I. Transcriptional regulation in helper versus cytotoxic-lineage decision. *Current opinion in immunology* 2009, **21**(2)**:** 127-132.

185. Matharu NK, Hussain T, Sankaranarayanan R, Mishra RK. Vertebrate homologue of Drosophila GAGA factor. *Journal of molecular biology* 2010, **400**(3)**:** 434-447.

186. Batista PJ, Chang HY. Long noncoding RNAs: cellular address codes in development and disease. *Cell* 2013, **152**(6)**:** 1298-1307.

187. Mercer TR, Mattick JS. Structure and function of long noncoding RNAs in epigenetic regulation. *Nature structural & molecular biology* 2013, **20**(3)**:** 300-307.

188. Kung JT, Colognori D, Lee JT. Long noncoding RNAs: past, present, and future. *Genetics* 2013, **193**(3)**:** 651-669.

189. Chisholm KM, Wan Y, Li R, Montgomery KD, Chang HY, West RB. Detection of long non-coding RNA in archival tissue: correlation with polycomb protein expression in primary and metastatic breast carcinoma. *PloS one* 2012, **7**(10)**:** e47998.

190. Burgess DJ. Non-coding RNA: HOTTIP goes the distance. *Nature reviews Genetics* 2011, **12**(5)**:** 300.

191. Wang KC, Yang YW, Liu B, Sanyal A, Corces-Zimmerman R, Chen Y*, et al.* A long noncoding RNA maintains active chromatin to coordinate homeotic gene expression. *Nature* 2011, **472**(7341)**:** 120-124.

192. Willingham AT, Orth AP, Batalov S, Peters EC, Wen BG, Aza-Blanc P*, et al.* A strategy for probing the function of noncoding RNAs finds a repressor of NFAT. *Science* 2005, **309**(5740)**:** 1570-1573.

193. Sunwoo H, Dinger ME, Wilusz JE, Amaral PP, Mattick JS, Spector DL. MEN epsilon/beta nuclear-retained non-coding RNAs are up-regulated upon muscle differentiation and are essential components of paraspeckles. *Genome research* 2009, **19**(3)**:** 347-359.

194. Scadden D. A NEAT way of regulating nuclear export of mRNAs. *Molecular cell* 2009, **35**(4)**:** 395-396.

195. Yaneva M, Tempst P. Isolation and mass spectrometry of specific DNA binding proteins. *Methods in molecular biology* 2006, **338:** 291-303.

196. Hewitt SL, Yin B, Ji Y, Chaumeil J, Marszalek K, Tenthorey J*, et al.* RAG-1 and ATM coordinate monoallelic recombination and nuclear positioning of immunoglobulin loci. *Nature immunology* 2009, **10**(6)**:** 655-664.

197. Dion V, Gasser SM. Chromatin movement in the maintenance of genome stability. *Cell* 2013, **152**(6)**:** 1355-1364.

198. Holthausen JT, Wyman C, Kanaar R. Regulation of DNA strand exchange in homologous recombination. *DNA repair* 2010, **9**(12)**:** 1264-1272.

199. Krueger C, King MR, Krueger F, Branco MR, Osborne CS, Niakan KK*, et al.* Pairing of homologous regions in the mouse genome is associated with transcription but not imprinting status. *PloS one* 2012, **7**(7)**:** e38983.

200. Miyanari Y, Torres-Padilla ME. Control of ground-state pluripotency by allelic regulation of Nanog. *Nature* 2012, **483**(7390)**:** 470-473.

201. Faddah DA, Wang H, Cheng AW, Katz Y, Buganim Y, Jaenisch R. Single-Cell Analysis Reveals that Expression of Nanog Is Biallelic and Equally Variable as that of Other Pluripotency Factors in Mouse ESCs. *Cell stem cell* 2013, **13**(1)**:** 23-29.

202. Filipczyk A, Gkatzis K, Fu J, Hoppe PS, Lickert H, Anastassiadis K*, et al.* Biallelic expression of nanog protein in mouse embryonic stem cells. *Cell stem cell* 2013, **13**(1)**:** 12-13.

203. Mazurek S, Boschek CB, Hugo F, Eigenbrodt E. Pyruvate kinase type M2 and its role in tumor growth and spreading. *Seminars in cancer biology* 2005, **15**(4)**:** 300-308.

204. Zwerschke W, Mazurek S, Massimi P, Banks L, Eigenbrodt E, Jansen-Durr P. Modulation of type M2 pyruvate kinase activity by the human papillomavirus type 16 E7 oncoprotein. *Proceedings of the National Academy of Sciences of the United States of America* 1999, **96**(4)**:** 1291-1296.

205. Dombrauckas JD, Santarsiero BD, Mesecar AD. Structural basis for tumor pyruvate kinase M2 allosteric regulation and catalysis. *Biochemistry* 2005, **44**(27)**:** 9417-9429.

206. Muirhead H, Clayden DA, Barford D, Lorimer CG, Fothergill-Gilmore LA, Schiltz E*, et al.* The structure of cat muscle pyruvate kinase. *The EMBO journal* 1986, **5**(3)**:** 475-481.

207. Gangstad SW, Feldager CW, Juul J, Trusina A. Noisy transcription factor NF-kappaB

oscillations stabilize and sensitize cytokine signaling in space. *Physical review E, Statistical, nonlinear, and soft matter physics* 2013, **87**(2)**:** 022702.

208. Wang Y, Paszek P, Horton CA, Kell DB, White MR, Broomhead DS*, et al.* Interactions among oscillatory pathways in NF-kappa B signaling. *BMC systems biology* 2011, **5:** 23.

209. Han SJ, Ko HM, Choi JH, Seo KH, Lee HS, Choi EK*, et al.* Molecular mechanisms for lipopolysaccharide-induced biphasic activation of nuclear factor-kappa B (NF-kappa B). *The Journal of biological chemistry* 2002, **277**(47)**:** 44715-44721.

210. Zhang LF, Huynh KD, Lee JT. Perinucleolar targeting of the inactive X during S phase: evidence for a role in the maintenance of silencing. *Cell* 2007, **129**(4)**:** 693-706.